

AD-A037 157

HERCULES INC MAGNA UTAH BACCHUS WORKS
SPACE SHUTTLE RESPONSE TO ACOUSTIC COMBUSTION INSTABILITY IN TH--ETC(U)
JUN 76 F R JENSEN

F/G 22/2

F04611-73-C-0025

UNCLASSIFIED

AFRPL-TR-76-62

NL

1 OF 1
AD
A037157



END

DATE
FILMED
4-77

ADA037157

AFRPL- TR-76-62

12

J

SPACE SHUTTLE RESPONSE TO ACOUSTIC COMBUSTION
INSTABILITY IN THE SOLID ROCKET BOOSTERS

Final Report

HERCULES INCORPORATED
SYSTEMS GROUP
WILMINGTON, DELAWARE 19899

AUTHOR: F. R. JENSEN

JUNE 1976

APPROVED FOR PUBLIC RELEASE
DISTRIBUTION UNLIMITED

AIR FORCE ROCKET PROPULSION LABORATORY
DIRECTOR OF SCIENCE AND TECHNOLOGY
AIR FORCE SYSTEMS COMMAND
EDWARDS, CALIFORNIA 93523

DDC
RECEIVED
MAR 18 1977
A

COPY AVAILABLE TO DDC DOES NOT
PERMIT FULLY LEGIBLE PRODUCTION

Copy available to DDC does not
permit fully legible reproduction

NOTICES

When U. S. Government drawings, specifications, or other data are used for any purpose other than a definitely related Government procurement operation, the Government thereby incurs no responsibility nor any obligation whatsoever, and the fact that the Government may have formulated, furnished, or in any way supplied the said drawings, specifications, or other data, is not to be regarded by implication or otherwise, or in any manner licensing the holder or any other person or corporation, or conveying any rights or permission to manufacture, use, or sell any patented invention that may in any way be related thereto.

FOREWORD

This report constitutes the final report for the Space Shuttle portion of the AFRPL Motor Component Vibration Study, Contract F04611-73-C-0025. The final report for the Component Vibration Study portion of this contract was issued previously. The work reported was accomplished at Hercules Incorporated, Bacchus Works, Magna, Utah

This report is submitted in accordance with data item B-004 of the referenced contract. Contract F04611-73-C-0025 was issued to Hercules by the Air Force Rocket Propulsion Laboratory, Edwards, CA, 93523. Mr. W. C. Andrepont, Chief, Combustion Section, was the project engineer.

Some of the analysis data used in this report was furnished by the North American Rockwell Space Division at Downey, CA, 90241. The data were gathered by Mr. S. Yahata and transmitted by Mr. R. P. Bergeron.

Additional data were supplied by the Marshall Space Flight Center at Huntsville, Alabama. Mr. F. Bugg was responsible for these data.

All of the acoustic mode and natural frequency data for the solid rocket motor were supplied by the Naval Weapons Center at China Lake, CA. The acoustic analyses were performed by Mr. C. Bicker under the direction of Dr. R. Derr.

Dr. D. Wang of Hercules assisted with the SRM NASTRAN analysis. Dr. F. R. Jensen was the Principal Investigator.

This report has been reviewed by the Information Office/DOZ and is releasable to the National Technical Information Service (NTIS). At NTIS it will be available to the general public, including foreign nations.

This technical report has been reviewed and is approved for publication.



W. C. ANDREPONT
Project Engineer



MARVIN R. BILSE, Major, USAF
Chief, Supporting Technology Branch

FOR THE COMMANDER



WILLIAM F. MORRIS, Colonel, USAF
Chief, Technology Division

UNCLASSIFIED

SECURITY CLASSIFICATION OF THIS PAGE (When Data Entered)

REPORT DOCUMENTATION PAGE		READ INSTRUCTIONS BEFORE COMPLETING FORM	
1. REPORT NUMBER 18 AFRPL-TR-76-62	2. GOVT ACCESSION NO.	3. RECIPIENT'S CATALOG NUMBER	
4. TITLE (and Subtitle) Space Shuttle Response to Acoustic Combustion Instability in the Solid Rocket Boosters		5. TYPE OF REPORT & PERIOD COVERED Final rept. June 1975 to June 1976	
7. AUTHOR(s) 10 F. R. Jensen		6. PERFORMING ORG. REPORT NUMBER	
9. PERFORMING ORGANIZATION NAME AND ADDRESS Hercules Incorporated Bacchus Works Magna UT 84044		8. CONTRACT OR GRANT NUMBER(s) 15 F04611-73-C-0025	
11. CONTROLLING OFFICE NAME AND ADDRESS Air Force Rocket Propulsion Laboratory (DYSC) Edwards AFB, CA 93523		10. PROGRAM ELEMENT, PROJECT, TASK AREA & WORK UNIT NUMBERS 62302F 16 573010BY 17 10	
14. MONITORING AGENCY NAME & ADDRESS (if different from Controlling Office)		12. REPORT DATE 12 June 1976	
		13. NUMBER OF PAGES 86 12 84201	
		15. SECURITY CLASS. (of this report) UNCLASSIFIED	
		15a. DECLASSIFICATION/DOWNGRADING SCHEDULE	
16. DISTRIBUTION STATEMENT (of this Report) Approved for Public Release, Distribution Unlimited			
17. DISTRIBUTION STATEMENT (of the abstract entered in Block 20, if different from Report)			
18. SUPPLEMENTARY NOTES			
19. KEY WORDS (Continue on reverse side if necessary and identify by block number) Space Shuttle, structural dynamics analyses, structural response to unstable acoustic oscillations in solid rocket motors, mechanical impedance applications			
20. ABSTRACT (Continue on reverse side if necessary and identify by block number) Response of the Space Shuttle vehicle to unstable acoustic pressure oscillations in the solid rocket boosters (SRB's) was calculated. The response was expressed in terms of forces and displacements at the attach points between the SRB's and the External Tank (ET), and between the ET and the Orbiter. The response calculations satisfied the objectives of the program.			

402250

672

20.

The NASTRAN computer program was used to analyze the various finite element shuttle models. Finite element models of the SRB, ET, and Orbiter were supplied by North American Rockwell, Space Division, at Downey, CA. A detailed finite element model of the solid rocket motor (SRM) was constructed for use with the cyclic symmetry option in NASTRAN. The models were analyzed separately and results were combined to represent the total structure by using a mechanical impedance-type approach. Some hand calculations were performed to estimate the axial connection point force and displacement. The good agreement between hand calculation and computer solution provided some confidence in the computer solution.

Due to limitations in time and budget, only the first longitudinal acoustic mode at 15.25 Hz was studied. Acoustic analyses were performed at the Naval Weapons Center (NWC) at China Lake, CA. The acoustic natural frequencies and mode shapes were transmitted to Hercules for use in this analysis program.

A maximum attach point load of 1600 lbs was calculated for a ± 1.0 psi pressure oscillation level. Therefore, maximum attach point loads of 16,000 to 32,000 lbs can be expected for maximum pressure oscillation levels of ± 10 to ± 20 psi. The attach point loads would be applied at a frequency of 15.25 Hz. Space shuttle engineers must determine the significance of such loads.

ACCESSION IS	
NTIS	WFO COPY <input checked="" type="checkbox"/>
DDC	DDC COPY <input type="checkbox"/>
USAMC/STP/STB	USAMC/STP/STB <input type="checkbox"/>
JUSTIFICATION	
BY	
DISTRIBUTION AVAILABILITY CODES	
DISC	AVAIL. AND/OR ORIGIN
A	

TABLE OF CONTENTS

<u>Section</u>	<u>Page</u>
DD Form 1473	2
List of Symbols	2
I INTRODUCTION	5
II GENERAL APPROACH	6
III DETAILED ANALYSIS METHOD	7
A. Frequency Response Analyses	7
B. Mechanical Impedance Techniques	10
C. Specific Shuttle Analysis Details	13
IV NASTRAN COMPUTER SOLUTION.	24
SRM Analysis Using the Cyclic Symmetry Model.	24
Calculation of $\{R_{SRB}\}$ and $\{U_0\}_{SRB}$	47
Analysis of the Rockwell ET and Orbiter Models.	47
Calculation of the Force and Displacement Response.	47
V DISCUSSION OF RESULTS.	70
Estimation of Longitudinal Mode Attach Forces by Hand Calculation	75
VI CONCLUSIONS AND RECOMMENDATIONS.	78
LIST OF REFERENCES	79

LIST OF SYMBOLS

A	Subscript indicating asymmetric boundary conditions
$[B]$	Viscous damping matrix
c	Subscript indicating response due only to interconnection forces for free body structure
$[D]$	Dynamic matrix
ET	Subscript indicating external tank portion of space shuttle
F	Subscript indicating response to internal forces at interconnection points between nose cone and SRM
$\{F\}$, $\{F(t)\}$	Applied load vector
f_j	Element in the j^{th} row in the load vector
g	A damping constant
i	Subscript used to indicate response of SRM model at the SRM/nose cone connection points
$[I]$	The identify matrix
INC	Subscript indicating degrees of freedom on the nose cone model at the attachment point between the nose cone and the SRM
$[K]$	Stiffness matrix
$[M]$	Mass matrix
N	Subscript indicating matrix partition for nose cone receptance matrix
NC	Subscript indicating nose cone, i.e., all SRB structure above the SRM
o	Subscript indicating response due only to internal acoustic pressure oscillations for free body structure, i.e., not attached at usual attach points
ORB	Subscript used to indicate orbiter
p	Subscript used to indicate response to acoustic pressure oscillation similar to subscript o

$\{R\}$	Receptance matrix
r	Radius
r_{ij}	Element in the i^{th} row and j^{th} column of the receptance matrix
RSS	Subscript indicating the remaining space shuttle structure after one SRB has been removed, i.e., the connected ET, orbiter, and second SRB
RX, RY, RZ	Subscripts indicating rotation about the X, Y, and Z axes, respectively
S	Subscript indicating matrix partition for SRM receptance matrix
s	Subscript indicating symmetric boundary conditions
SRB	Subscript indicating solid rocket booster
SRM	Subscript indicating solid rocket motor
T	Superscript indicating matrix transpose
T	Subscript indicating total response to two or more load sets
t	Time
$\{T\}$, $\{\bar{T}\}$	Transformation matrices
$\{U\}$	Displacement
$\{\dot{U}\}$	Velocity vector (first displacement derivative)
$\{\ddot{U}\}$	Acceleration vector (second displacement derivative)
x, y, z	Subscripts used to indicate vector components in the x, y, z rectangular (space shuttle) coordinate system
α	A matrix as defined in equation (25)
ϕ	Angle defining circumferential location of points around the NASTRAN motor model
ω	Circular frequency (rad/sec)

SECTION I

INTRODUCTION

Most solid propellant rocket motors exhibit some degree of combustion instability, which is characterized by chamber pressure oscillations. The hot combustion gasses in the combustion cavity can oscillate in various natural acoustic modes much the same way that the column of air in an organ pipe resonates. Special pressure transducers, that are designed to measure the alternating component of the chamber pressure, are used to measure the unstable pressure oscillations. The oscillations are considered to be unstable because a small perturbation can excite a particular mode which in turn increases in amplitude in an unstable ($e^{\alpha t}$ envelope) fashion until some limiting amplitude is reached. As burning in the motor continues, the conditions required to sustain oscillation in a particular mode change and the mode typically dies away before the end of motor operation. Motors that exhibit unstable pressure oscillations in more than one acoustic mode during motor operation time are common.

In the past, unstable acoustic pressure oscillations in upper stage motors on certain ballistic missiles have produced relatively high amplitude vibration levels on the motor case and attached components. Vibration levels as high as 300 g's have been measured during upper stage motor operation. This past experience with solid rocket motors has been cause for the concern with possible acoustic instabilities in the Space Shuttle Solid Rocket Booster (SRB) motors. The objective of the work covered in this final report is to analyze the Space Shuttle vehicle to determine structural response to possible acoustic combustion instability in the solid rocket boosters. The analysis is to provide an estimate of the forces to be expected at the attachment points between the Solid Rocket Boosters and the External Tank (ET).

Work to define the likelihood of any particular acoustic mode being unstable, to define the natural mode shapes, and to estimate limiting amplitudes of unstable modes is being carried on at the Naval Weapons Center (NWC) at China Lake, California under the direction of Dr. Ron Derr. For the work reported herein, a mode was assumed to be unstable and the response was calculated for a normalized (1.0 psi maximum) pressure mode shape. Since the solutions are linear, different pressure oscillation levels can be accounted for by direct multiplication of the 1.0 psi results; e.g., for 10 psi, multiply by 10. The acoustic natural modes and frequencies used in the present work were supplied by Mr. C. Bicker of NWC.

The second section of this report gives a general overview of the general approach used in the analyses. The third section contains a detailed discussion of the theory upon which the analysis is based and presents all applicable equations. Details associated with the NASTRAN computer solution are discussed in Section IV. The final two sections cover a discussion of results and conclusions. In Section V, it should be emphasized again that force and displacement values given in the text are for a pressure oscillation level of 1.0 psi unless otherwise stated. Since pressure oscillation levels of 10 to 20 psi or higher are conceivable, the values given in the text should be multiplied by 10 or 20 to obtain probable maximum values.

SECTION II
GENERAL APPROACH

The general approach consisted of following procedures used in a previous program¹. Finite element models were used to represent the entire space shuttle structure. Mass and stiffness matrices for half models of the orbiter and the external tank with both symmetric and antisymmetric boundary conditions were supplied by North American Rockwell Space Division at Downey, California. In addition, Rockwell furnished a model, (mass and stiffness matrices), for an SRB. A separate model of the SRB structure above the solid motor was provided by the Marshall Space Flight Center at Huntsville, Alabama. Hercules constructed a detailed finite element model of the solid motor as a part of the effort on this program.

The NASTRAN program on an IBM 370/155 computer was the basic analysis tool used in the program. Two versions of the NASTRAN program were used: (1) A NASA level 15.1 version, and (2) a MacNeal-Schwendler Company (MSC) program that is approximately equivalent to level 15.5. The MSC version contains a cyclic symmetry option in the Frequency Response Rigid Format, (R.F. 8). The cyclic symmetry capability in MSC NASTRAN was used to analyze the Hercules solid rocket motor (SRM) model.

Attaching the models together to obtain a single large model for the total shuttle vehicle would have violated the conditions that allow the use of a cyclic symmetry model. Therefore, a mechanical impedance type approach was used which allowed each model to be analyzed separately. Results from the separate analyses were then combined to obtain the response of the total assembled space shuttle vehicle. Details of the approach are given in the following section.

¹ F. R. Jensen, Analytical Prediction of Motor Component Vibrations Driven by Acoustic Combustion Instability, Final Report AFRPL-TR-76-11, Hercules Incorporated, for the Air Force Rocket Propulsion Laboratory, Edwards, CA, February 1976.

SECTION III

DETAILED ANALYSIS METHOD

The purpose of this section of the report is to provide details on how the analysis was performed. The various finite element models are described in detail, general application of mechanical impedance is discussed, and the equations and other details applicable to the shuttle analysis are provided.

A. FREQUENCY RESPONSE ANALYSES

For a finite element model with viscous damping, the equations of motion are:

$$[M]\{\ddot{U}\} + [B]\{\dot{U}\} + [K]\{U\} = \{F(t)\} \quad (1)$$

where: $[M]$ = the mass matrix
 $[B]$ = the viscous damping matrix
 $[K]$ = the stiffness matrix
 $\{U\}$ = the displacement vector
 $\{F(t)\}$ = the applied load vector

For a harmonic forcing function at a particular frequency, such as $\{F(t)\} = \{F\}e^{i\omega t}$, the equations representing the steady state motion² are:

$$(-\omega^2[M] + i\omega[B] + [K])\{U\} = \{F\} \quad (2)$$

A common method of handling the damping is to assume that elements in the damping matrix are proportional to corresponding elements in the stiffness matrix³

$$[B] = (g/\omega)[K]$$

Equation (2) then becomes

$$(-\omega^2[M] + (1 + ig)[K])\{U\} = \{F\} \quad (3)$$

²The NASTRAN Theoretical Manual, (Level 15), R. H. MacNeal, Ed., April 1972, NASA SP-221(01), NASA, Washington, D.C., page 12.1-3.

³Ibid., p9.3-8.

Equation (3) is solved by the NASTRAN program when analyses are performed using the frequency response rigid format⁴. Let

$$[D] = (-\omega^2[M] + (1 + i\eta)[K])$$

Then equation (3) can be written

$$[D]\{U\} = \{F\}$$

and the solution to equation (3) can be written

$$\{U\} = [D^{-1}]\{F\} \quad (4)$$

Let

$$[R] = [D^{-1}]$$

Then equation (4) can be written as

$$\{U\} = [R]\{F\} \quad (5)$$

Using the terminology suggested in Reference 5, [R] is called a receptance matrix.

Where a receptance matrix is desired for only a fraction of the degrees of freedom in the finite element model, the displacement vector can be partitioned

$$\begin{Bmatrix} U_1 \\ U_2 \end{Bmatrix} = \begin{bmatrix} R_{11} & R_{12} \\ R_{21} & R_{22} \end{bmatrix} \begin{Bmatrix} F_1 \\ F_2 \end{Bmatrix} \quad (6)$$

Solving for $\{U_1\}$ with $\{F_2\} = 0$:

$$\{U_1\} = [R_{11}]\{F_1\} \quad (7)$$

This method of obtaining a reduced receptance matrix is not efficient because the large D matrix must be inverted to obtain the R matrix.

⁴The NASTRAN User's Manual, (Level 15), C. W. McCormick, Ed., June 1972, NASA SP-222(01), NASA, Washington, D.C., p3.9-11.

⁵Bishop, R. E. D., and Johnson, D. C., The Mechanics of Vibration, Cambridge at the University Press, 1960, London, England.

A more efficient way to obtain a reduced R matrix is to apply unit loads at each of the coordinates in F_1 and solve for U_1 , using the regular NASTRAN R.F.-8 solution. To clarify this approach, equation (7) can be written as follows:

$$\begin{pmatrix} U_1 \\ U_2 \\ U_3 \\ \vdots \\ U_n \end{pmatrix} = \begin{bmatrix} r_{11} & r_{12} & r_{13} & \dots & r_{1n} \\ r_{21} & r_{22} & r_{23} & \dots & r_{2n} \\ r_{31} & r_{32} & r_{33} & \dots & r_{3n} \\ \vdots & \vdots & \vdots & \ddots & \vdots \\ r_{n1} & r_{n2} & r_{n3} & \dots & r_{nn} \end{bmatrix} \begin{pmatrix} f_1 \\ f_2 \\ f_3 \\ \vdots \\ f_n \end{pmatrix}$$

or:

$$\begin{aligned} U_1 &= r_{11}f_1 + r_{12}f_2 + r_{13}f_3 + \dots + r_{1n}f_n \\ U_2 &= r_{21}f_1 + r_{22}f_2 + r_{23}f_3 + \dots + r_{2n}f_n \\ U_3 &= r_{31}f_1 + r_{32}f_2 + r_{33}f_3 + \dots + r_{3n}f_n \\ &\vdots \\ U_n &= r_{n1}f_1 + r_{n2}f_2 + r_{n3}f_3 + \dots + r_{nn}f_n \end{aligned}$$

In the above equations, when $f_1 = 1.0$ and $f_i = 0$, $i \neq 1$, the solution for the (U_i) 's gives the first column in the desired reduced receptance matrix:

$$\begin{aligned} r_{11} &= U_1 \\ r_{21} &= U_2 \\ r_{31} &= U_3 \\ &\dots \\ r_{n1} &= U_n \end{aligned}$$

The other columns in the receptance matrix can be determined by solving for other force terms of unit value. For example, a solution with $f_2 = 1.0$ and all other $f_i = 0$ would provide the second column in the receptance matrix.

A DMAP ALTER must be used to save the displacements calculated by NASTRAN:

```
ALTER 141
OUTPUT2 UDVF,,,,/C,N,-1/C,N,17/C,N,UDVFTP$
END ALTER
```

When the above ALTER is used in the executive control deck, the displacement matrix UDVF is written on tape unit 17 and can be saved for later use. In the same computer run or in another run, UDVF can be partitioned to obtain the R matrix.

In the space shuttle analysis, the receptance matrix at the inter-connection coordinates was required for each model. The appropriate receptance matrices were obtained by applying unit forces at each connection coordinate for each finite element model.

B. MECHANICAL IMPEDANCE TECHNIQUES

"Impedance" and "admittance" are terms generally associated with electrical circuits. The terms "mechanical impedance" and "mechanical admittance" are normally used to indicate that an analogy is being made between an electrical circuit and a mechanical system. The literature on mechanical vibration analysis contains a large amount of information on mechanical impedance-type approaches. For example, the Shock and Vibration Bulletin contains many papers on application of mechanical impedance techniques.⁶

Mechanical impedance is a ratio of force to velocity. Mechanical admittance, commonly called "mobility," is the inverse of mechanical impedance, i.e., a ratio of velocity to force. A basic discussion on mechanical impedance and mobility can be found in Reference 7. The term "receptance" is used to denote the ratio of displacement to force. The concept of receptance is discussed in References 7, 8, and 9. Additional discussion on electromechanical analogies are contained in References 10 and 11.

The term "immittance" has been used to represent impedance or admittance. Mechanical immittance and transmission matrix concepts are discussed in References 12, 13, and 14.

⁶ Index to the Shock and Vibration Bulletins, February 1968, The Shock and Vibration Information Center, Naval Research Laboratory, Washington, D.C.

⁷ Harris, C. M., and Crede, C. E., Shock and Vibration Handbook, Vol. 1, Chapter 10, McGraw-Hill Book Co., New York, 1961.

⁸ Bishop, R. E. D., Gladwell, G. M. L., and Michaelson, S., The Matrix Analysis of Vibration, Section 5.5, Cambridge at the University Press, London, 1965.

⁹ Bishop, R. E. D., and Johnson, D. C., The Mechanics of Vibration, Cambridge at the University Press, London, 1960.

¹⁰ Crafton, P. A., Shock and Vibration in Linear Systems, Harper and Brothers, New York, 1961.

¹¹ MacNeal, R. H., Electric Circuit Analogies for Elastic Structures, Vol 2, John Wiley and Sons, New York, 1962.

¹² Rubin, S., Review of Mechanical Immittance and Transmission Concepts, Presented at the 71st Meeting of the Acoustical Society of America, Boston, Mass., June 1966.

¹³ Rubin, S., Class Notes distributed at UCLA Short Course on Structural Dynamics Analysis, Los Angeles, California, 1967.

¹⁴ Rubin, S., On the Use of Eight-Pole Parameters for Analysis of Beam Systems, Soc. of Automotive Engineers, Reprint 925F, October 1964.

When a sinusoidal force drives a linear system, the steady state response displacements, velocities, and accelerations are sinusoidal at the frequency of the driving force. For a damped system, the response is out-of-phase with the driving force. The relationship between driving force and response can be expressed by algebraic equations involving complex numbers, (such as equation 5). The analysis of such a system is called a "frequency response analysis." The use of frequency response-type analyses is implied when mechanical impedance is discussed.

The concept of impedance or receptance of the space shuttle structure at a set of points was used to allow the individual shuttle models to be analyzed separately. The results from the individual analyses were combined to obtain solutions that represent the total structure.

Equation (7) represents a linear system. Since the system is linear, the response for two different load sets applied simultaneously can be determined by applying each load set separately and summing the results. Consider one SRB undergoing acoustic pressure oscillations. The SRB would be subjected to two separate loading systems:

- (1) The acoustic natural mode would load the solid motor by means of a certain pressure distribution in the motor combustion cavity.
- (2) The remainder of the space shuttle vehicle would apply loads to the SRB at the SRB attach points as the total vehicle vibrates in response to the pressure oscillations.

The objective of this work is to calculate the second load set.

In the NASTRAN finite element models, a certain set of displacement coordinates represents the SRB attach coordinates. The SRB is attached to the ET at nodes 303, 310, and 311. The node locations and x, y, z coordinate directions are defined in a later section of this report. The attach point displacement coordinates are:

$$\{U\} = \begin{Bmatrix} U_{303x} \\ U_{303y} \\ U_{303z} \\ U_{310y} \\ U_{310z} \\ U_{311y} \end{Bmatrix} \quad (8)$$

For this linear system, the total response at the attach points, $\{U_T\}$, can be obtained by summing the responses due to the two separate load sets discussed above

$$\{U_T\} = \{U_o\}_{SRB} + \{U_c\} \quad (9)$$

where: $\{U_o\}_{SRB}$ = the response at the attach coordinates due only to the acoustic pressure mode

$\{U_c\}$ = the response at the attach coordinates due to the attach loads applied by the remaining shuttle structure, i.e. the total shuttle less one SRB.

The displacement response $\{U_o\}$ can be calculated directly by using a NASTRAN model of an SRB. To obtain $\{U_o\}$, a cyclic symmetry model of an SRM was analyzed to determine response to the first acoustic natural mode at 15.25 Hz. Details of the $\{U_o\}$ calculation are discussed in a following section.

If the receptance of the SRB at the attach points is denoted $[R_{SRB}]$, then $\{U_c\}$ can be expressed as

$$\{U_c\} = [R_{SRB}]\{F_c\} \quad (10)$$

where: $\{F_c\}$ = the set of forces applied to the SRB at the SRB attach points

By way of further explanation of $\{F_c\}$, the set of forces $\{F_c\}$ are internal forces that occur at the attach points between the SRB and the ET due to pressure oscillations in the SRM. Cutting the structure at the attach points to show free body diagrams would yield a diagram showing internal forces $\{F_c\}$ applied to the SRB and equal, but opposite, forces, $\{-F_c\}$, applied to the ET.

An equation similar to equation (10) can be written for the remainder of the space shuttle vehicle. When one SRB has been removed, the remaining structure consists of the ET, the orbiter, and the other SRB. If the receptance of the remaining structure at the attach points is denoted $[R_{RSS}]$, then the forces applied result in $\{U_T\}$ displacements

$$\{U_T\} = [R_{RSS}]\{-F_c\} \quad (11)$$

For this analysis, the only forces applied to the remaining shuttle structure are the forces $\{-F_c\}$; therefore, the displacements in equation (11) are the total displacements, $\{U_T\}$, rather than the displacements due to connection forces, $\{U_c\}$, as in equation (10). Equation (11) can be solved for connection forces $\{F_c\}$ and the result substituted into equation (10) to eliminate the unknown forces

$$\{U_c\} = -[R_{SRB}][R_{RSS}]^{-1}\{U_T\} \quad (12)$$

When equation (12) is substituted into equation (9), then the total displacements are found to be

$$\{U_T\} = ([I] + [R_{SRB}][R_{RSS}]^{-1})^{-1}\{U_o\}_{SRB} \quad (13)$$

The solution to equation (13) represents the desired response of the shuttle to acoustic oscillations. The connection forces can be recovered by using the solution of equation (11)

$$\{F_c\} = -[R_{RSS}^{-1}]\{U_T\} \quad (14)$$

An equation similar to that of equation (13) was used in the component vibration program. The Component Vibration Final Report¹⁵ contains a simple example showing that the technique of equation (13) is applicable.

C. SPECIFIC SHUTTLE ANALYSIS DETAILS

To obtain the desired solution to equation (13) the matrices $[R_{SRB}]$, $[R_{RSS}]$, and $\{U_o\}_{SRB}$ must be available. The calculation of these three matrices is discussed below. The calculation of each of the three matrices is somewhat complicated by the fact that each depends on solutions from two different finite element models. Two different models were used to represent the SRB, a cyclic symmetry model of the SRM and a model of the nose section above the SRM. Models of the ET and the orbiter with symmetric and antisymmetric boundary conditions are used to represent the remaining shuttle structure for calculation of $[R_{RSS}]$.

Locations of the nodes that represent the attach points are indicated in Figure 1. The figure also shows the basic X, Y, Z coordinate system used throughout this report. The coordinate system shown in Figure 1 was adopted because it coincides with the coordinate system used for definition of the ET, orbiter, and SRB models furnished by North American Rockwell. The actual mass and stiffness matrices involved were transmitted to Hercules on a computer tape.

The calculation of $[R_{SRB}]$ is discussed first. Figure 2 shows a sketch of one SRB divided into two parts, an SRM and the structure above the SRM. For purposes of discussion, the structure above the SRM is referred to as the nose cone. This use of "nose cone" is not in agreement with official NASA nomenclature. The SRM was represented by a cyclic symmetry NASTRAN model. Since 10 degree sections were used in the cyclic symmetry model, there are 36 nodes around the circumference of the model as shown in Figure 3. The cyclic symmetry SRM is described in a later section.

A NASTRAN cylindrical local coordinate system, R, θ , Z, was used to define node locations and displacement components in the cyclic symmetry model. The Z axis of the local system is parallel to the X axis of the global (Rockwell) coordinate system. The relationship between the local R, θ and the Global Y, Z axes is indicated in Figure 3. Attach nodes 310 and 311 are located circumferentially as shown in Figure 3. The transformation below was written to relate the displacements in the two coordinate systems.

¹⁵ Analytical Prediction of Motor Component Vibrations Driven by Acoustic Combustion Instability, op. cit.

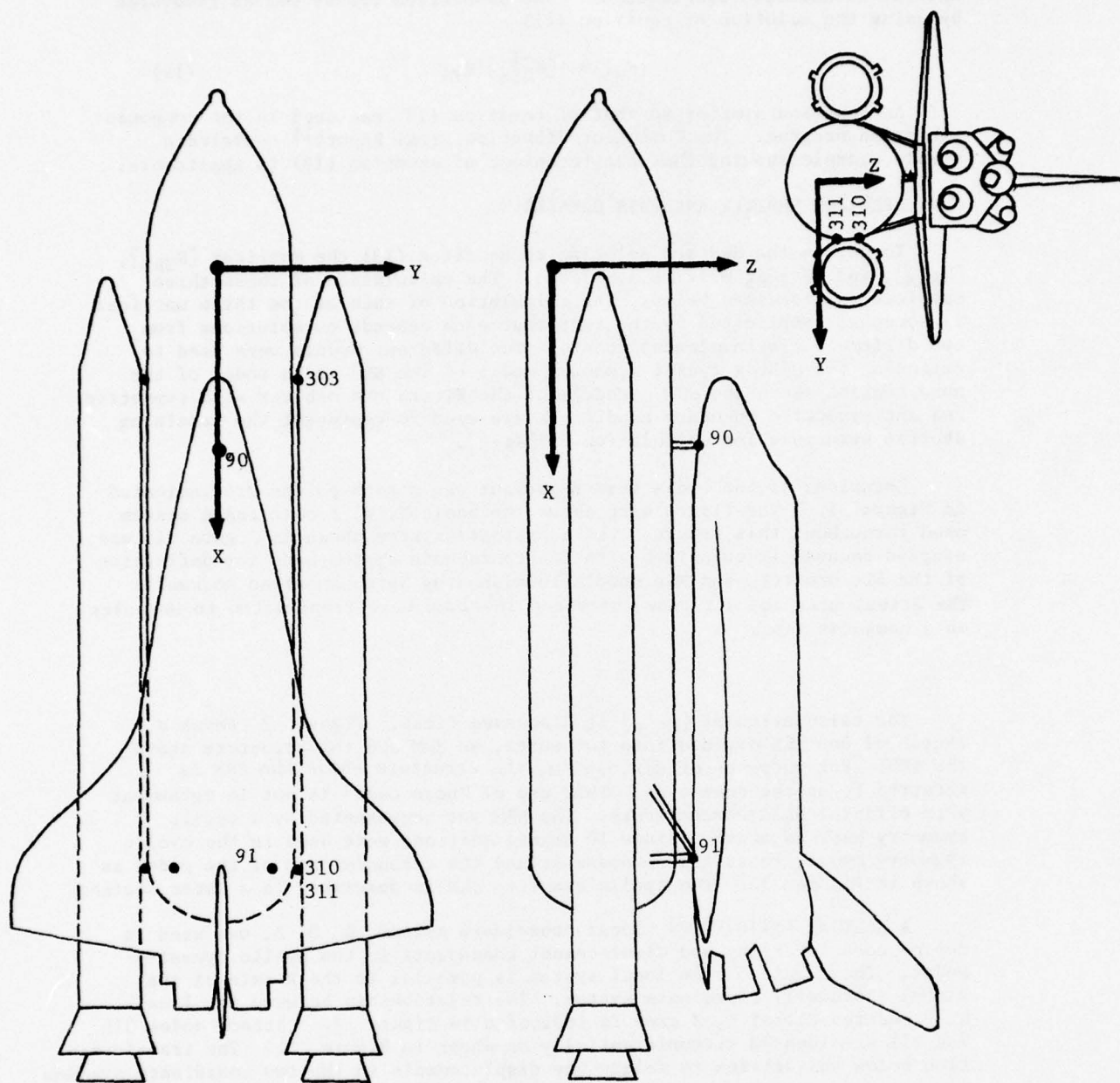


Figure 1. Sketch of the Space Shuttle Vehicle Showing SRB and Orbiter Attach Points and Showing Location of the X, Y, Z Coordinate System

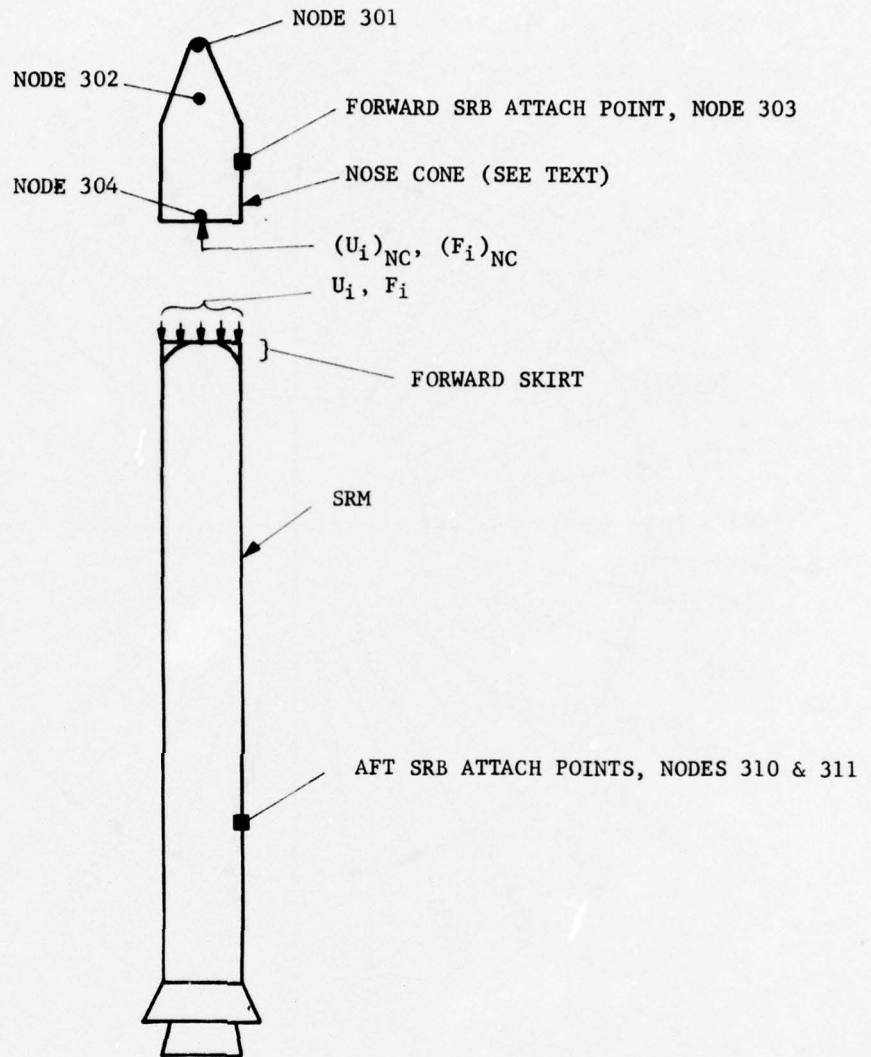


Figure 2. Sketch of the SRB Showing the Division into SRM and Nose Cone Models

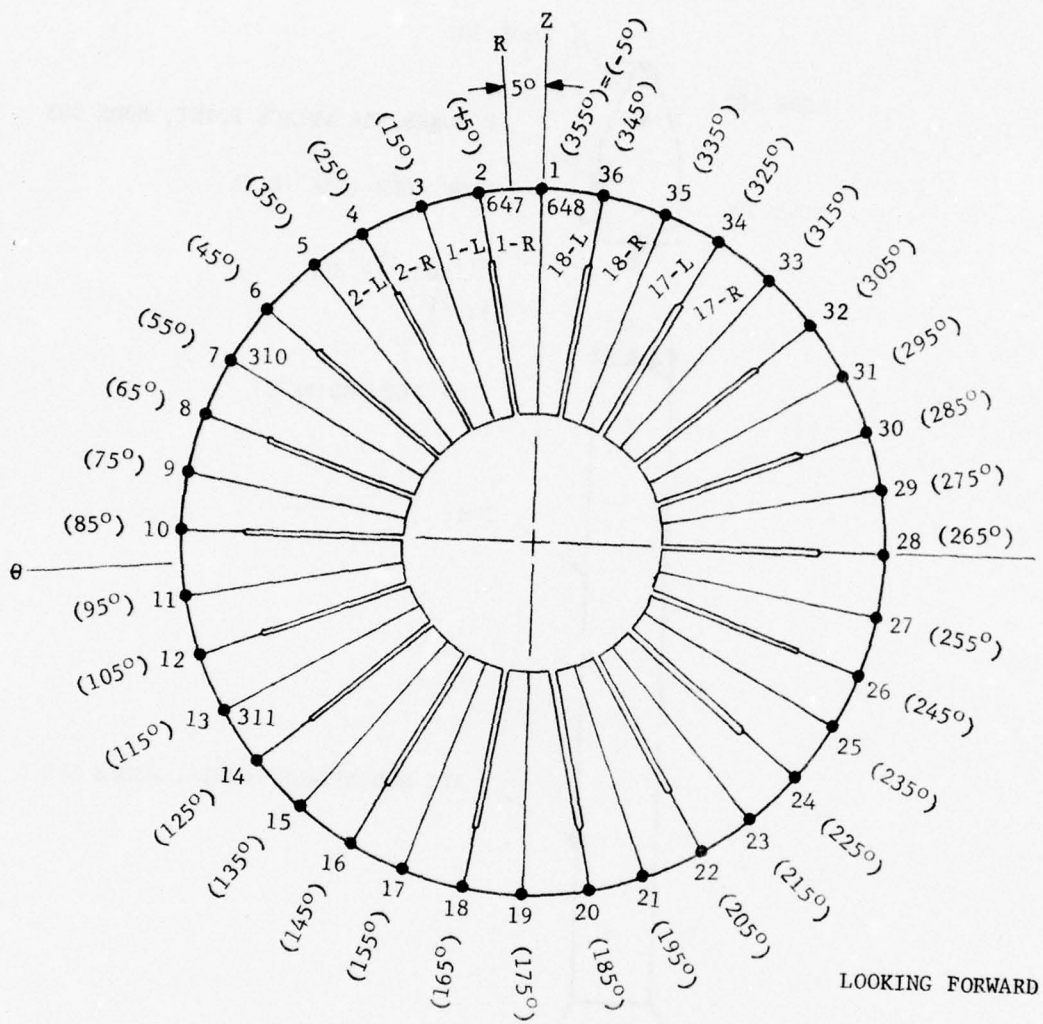


Figure 3. Nodes Around Forward Skirt Showing Difference Between Local R- θ and Global Y-Z Coordinates

The receptance matrix from the SRM analysis was partitioned in equation (16) to separate the U_i displacements from the attach point displacements. Equation (16) can be expanded as follows

$$U_i = R_{S11} F_i + R_{S12} F'_{310, 11} \quad (17a)$$

$$U'_{310, 11} = R_{S21} F_i + R_{S22} F'_{310, 11} \quad (17b)$$

The transformation of equation (15) also holds when forces are substituted for displacements

$$\{F'_{310, 11}\} = [\bar{T}]\{F_{310, 11}\} \quad (18)$$

Substituting equations (15) and (18) into equations (17a) and (17b) gives

$$U_i = R_{S11} F_i + (R_{S12} \bar{T}) F_{310, 11} \quad (19a)$$

$$\bar{T} U_{310, 11} = R_{S21} F_i + R_{S22} \bar{T} F_{310, 11} \quad (19b)$$

Since multiplying (\bar{T}^T) by (\bar{T}) gives the identity matrix, equation (19b) can be rewritten as

$$U_{310, 11} = (\bar{T}^T R_{S21}) F_i + (\bar{T}^T R_{S22} \bar{T}) F_{310, 11} \quad (19c)$$

The nose cone model only contains four nodes as shown in Figure 2. Details on how the nose cone model was obtained are given in a later section. Unit forces were applied at nodes 303 and 304 to obtain the nose cone receptance matrix:

$$\begin{Bmatrix} U_{303X} \\ U_{303Y} \\ U_{303Z} \\ \dots \\ U_{304X} \\ U_{304Y} \\ U_{304Z} \\ U_{304RX} \\ U_{304RY} \\ U_{304RZ} \end{Bmatrix} = \begin{bmatrix} r_{11} & r_{12} & \dots & \vdots \\ r_{21} & r_{22} & \dots & \vdots \\ \dots & \dots & \dots & \vdots \\ \vdots & \vdots & \vdots & \vdots \end{bmatrix} \begin{Bmatrix} F_{303X} \\ F_{303Y} \\ F_{303Z} \\ \dots \\ F_{304X} \\ F_{304Y} \\ F_{304Z} \\ F_{304RX} \\ F_{304RY} \\ F_{304RZ} \end{Bmatrix}$$

In compact form:

$$\begin{Bmatrix} U_{303} \\ \dots \\ U_{iNC} \end{Bmatrix} = \begin{bmatrix} R_{N11} & R_{N12} \\ \dots & \dots \\ R_{N21} & R_{N22} \end{bmatrix} \begin{Bmatrix} F_{303} \\ \dots \\ F_{iNC} \end{Bmatrix} \quad (20)$$

Again, the receptance matrix is partitioned to separate the ET/SRB attach degrees of freedom from the SRM/nose cone interface degrees of freedom. Equation (20) can be expanded as follows:

$$U_{303} = R_{N11} F_{303} + R_{N12} F_{iNC} \quad (21a)$$

$$U_{iNC} = R_{N21} F_{303} + R_{N22} F_{iNC} \quad (21b)$$

At this point, another transformation equation is needed to relate the U_i displacements at 36 nodes on the SRM to the U_{iNC} displacements at the single node (304) on the nose cone. The angle φ_i is measured counterclockwise from the R axis as shown in Figure 3. The required transformation for the i^{th} node of the 36 SRM interconnection nodes is then

$$\begin{Bmatrix} U_{iR} \\ U_{i\theta} \\ U_{iZ} \end{Bmatrix} = \begin{bmatrix} 0 & -\sin(\varphi_i+5) & \cos(\varphi_i+5) & 0 & 0 & 0 \\ 0 & -\cos(\varphi_i+5) & -\sin(\varphi_i+5) & r & 0 & 0 \\ 1 & 0 & 0 & 0 & r\cos(\varphi_i+5) & r\sin(\varphi_i+5) \end{bmatrix} \begin{Bmatrix} U_{304X} \\ U_{304Y} \\ U_{304Z} \\ U_{304RX} \\ U_{304RY} \\ U_{304RZ} \end{Bmatrix}$$

When the above equation is written to include all 36 nodes, the following compact expression is used

$$\{U_i\} = [T]\{U_{iNC}\} \quad (22)$$

The internal forces applied to the SRM are equal in magnitude but opposite in direction from those applied to the Nose Cone. Therefore, the force transformation corresponding to equation (22) is:

$$\{F_i\} = -[T]\{F_{iNC}\} \quad (23)$$

Substituting equations (22) and (23) into equations (19a) and (19c) gives

$$T U_{iNC} = -R_{S11} T F_{iNC} + R_{S12} \bar{T} F_{310, 11} \quad (24a)$$

$$U_{310, 11} = -\bar{T}^T R_{S21} T F_{iNC} + \bar{T}^T R_{S22} \bar{T} F_{310, 11} \quad (24b)$$

Substituting equation (21b) into equation (24a) and rearranging gives

$$(T R_{N22} + R_{S11} T) F_{iNC} = R_{S12} \bar{T} F_{310, 11} - T R_{N21} F_{303}$$

Premultiply by the transpose of T

$$T^T (T R_{N22} + R_{S11} T) F_{iNC} = T^T R_{S12} \bar{T} F_{310, 11} - T^T T R_{N21} F_{303}$$

Let

$$\alpha = T^T (T R_{N22} + R_{S11} T) \quad (25)$$

Then

$$F_{iNC} = \alpha^{-1} T^T R_{S12} \bar{T} F_{310, 11} - \alpha^{-1} T^T T R_{N21} F_{303} \quad (26)$$

Equation (26) can be used to eliminate F_{iNC} from equations (21a) and (24b)

$$U_{303} = (R_{N11} - R_{N12} \alpha^{-1} T^T T R_{N21}) F_{303} + R_{N12} \alpha^{-1} T^T R_{S12} \bar{T} F_{310, 11} \quad (27a)$$

$$U_{310, 11} = \bar{T}^T R_{S21} T \alpha^{-1} T^T T R_{N21} F_{303} + (\bar{T}^T R_{S22} \bar{T} - \bar{T}^T R_{S21} T \alpha^{-1} T^T R_{S12} \bar{T}) F_{310, 11} \quad (27b)$$

Equations (27a) and (27b) can be combined to give an expression for the SRB receptance matrix

$$\begin{Bmatrix} U_{303} \\ U_{310, 11} \end{Bmatrix} = \begin{bmatrix} (R_{N11} - R_{N12} \alpha^{-1} T^T T R_{N21}) & (R_{N12} \alpha^{-1} T^T R_{S12} \bar{T}) \\ (\bar{T}^T R_{S21} T \alpha^{-1} T^T T R_{N21}) & (\bar{T}^T R_{S22} \bar{T} - \bar{T}^T R_{S21} T \alpha^{-1} T^T R_{S12} \bar{T}) \end{bmatrix} \begin{Bmatrix} F_{303} \\ F_{310, 11} \end{Bmatrix} \quad (28)$$

The square matrix in equation (28) is the receptance matrix for one SRB, $[R_{SRB}]$.

The calculation of $\{U_o\}_{SRB}$ is discussed below. $\{U_o\}_{SRB}$ is the response of the SRB at the attach points to a particular acoustic natural mode. The calculation of $\{U_o\}_{SRB}$ is similar to the calculation of $[R_{SRM}]$ discussed above. The response cannot be determined by direct analysis because one attach point is on the nose cone while the other two attach points are on the SRM.

Considering the SRM to be isolated from the nose cone, the response at the SRM attach points, nodes 310 and 311, is obtained by adding the response due to acoustic mode (p) forces to the response due to internal (F_i) forces at the SRM/nose cone interface

$$\{U_{310, 11}\}_T = \{U_{310, 11}\}_p + \{U_{310, 11}\}_F \quad (29)$$

The response at the SRM/nose cone interface is expressed in a similar manner:

$$\{U_i\}_T = \{U_i\}_p + \{U_i\}_F \quad (30)$$

The response of the SRM to the acoustic mode is obtained directly by applying loads that represent the acoustic mode pressure distribution to the NASTRAN cyclic symmetry model. Therefore, $\{U_{310, 11}\}_p$ and $\{U_i\}_p$ are obtained by partitioning the UDVF displacement matrix from a NASTRAN solution. Note that equations (29) and (30) are similar to equation (9).

The terms $\{U_{310, 11}\}_F$ and $\{U_i\}_F$ represent the response of the SRM to the interface forces, F_i . Using equations (19a) and (19c) with $F_{310, 11} = 0$, the following expressions are obtained

$$(U_i)_F = R_{S11} F_i \quad (31a)$$

$$(U_{310, 11})_F = (\bar{T}^T R_{S21}) F_i \quad (31b)$$

Substituting (31a) and (31b) into equations (29) and (30) gives:

$$(U_{310, 11})_T = (U_{310, 11})_p + (\bar{T}^T R_{S21}) F_i \quad (32a)$$

$$(U_i)_T = (U_i)_p + R_{S11} F_i \quad (32b)$$

Substituting equation (23) into (32a) and substituting equations (22) and (23) into equation (32b) results in

$$(U_{310, 11})_T = (U_{310, 11})_p - (\bar{T}^T R_{S21})^T F_{iNC} \quad (33a)$$

$$T(U_{iNC})_T = (U_i)_p - R_{S11} T F_{iNC} \quad (33b)$$

For the nose cone, only the response to interface forces $\{F_{iNC}\}$ is required. Using equations (21a) and (21b) with F_{303} equal to zero gives

$$(U_{303})_T = R_{N12} F_{iNC} \quad (34a)$$

$$(U_{iNC})_T = R_{N22} F_{iNC} \quad (34b)$$

Substituting equations (34b) into equation (33b) premultiplying by T^T and rearranging gives

$$T^T(R_{S11} T + T R_{N22}) F_{iNC} = T^T (U_i)_p$$

The coefficient of F_{iNC} in the last equation can be recognized as α , as defined in equation (25).

Therefore,

$$F_{iNC} = \alpha^{-1} T^T (U_i)_p \quad (35)$$

Substituting equation (35) into equations (33a) and (34a) gives

$$(U_{310, 11})_T = (U_{310, 11})_p - (\bar{T}^T R_{S21})^T \alpha^{-1} T^T (U_i)_p \quad (36a)$$

$$(U_{303})_T = R_{N12} \alpha^{-1} T^T (U_i)_p \quad (36b)$$

In equation (36a), equation (15a) is substituted to obtain the result in the primed system that corresponds to direct NASTRAN output:

$$(U_{310, 11})_T = \bar{T}^T (U'_{310, 11})_p - (\bar{T}^T R_{S21})^T \alpha^{-1} T^T (U_i)_p \quad (36c)$$

Using equations (36b) and (36c), an expression can be written for $\{U_o\}_{SRB}$

$$\{U_o\}_{SRB} = \begin{Bmatrix} (U_{303})_T \\ \hline (U_{310, 11})_T \end{Bmatrix} = \begin{bmatrix} (RN12 \alpha^{-1} T^T) & \vdots & 0 \\ \hline (-T^T R_{S21T} \alpha^{-1} T^T) & \vdots & T^T \end{bmatrix} \begin{Bmatrix} (U_i)_p \\ \hline (U'_{310, 11})_p \end{Bmatrix} \quad (37)$$

The remainder of the discussion in this section is concerned with the calculation of $[R_{RSS}]$. Equation (11) defines the displacement and force vectors that are associated with receptance matrix $[R_{RSS}]$. The $\{U_T\}$ vector in equation (11) has individual components as defined in equation (8).

NASTRAN finite element models of the ET and the orbiter were supplied by the North American Rockwell Company, Space Division, at Downey, California. The furnished models represent only one-half of the structure and separate models were supplied for symmetric and asymmetric boundary conditions. The X-Z plane as shown in Figure 1 was taken as the plane of symmetry for the models. When the models with symmetry boundary conditions are analyzed, the results should represent a symmetric structure subjected to symmetric loads. Therefore, a solution for a particular acoustic mode using the models with symmetric boundary conditions should represent the condition where both solid rocket motors are being subjected to unstable acoustic oscillations that are in-phase. Use of the models with asymmetric boundary conditions would represent the condition where both SRM's were oscillating out-of-phase with one another. The difference between the symmetric and asymmetric solutions should give results for the situation where only one SRM is undergoing unstable acoustic oscillations.

The receptance equation for the ET is as follows

$$\{U_{ET}\} = \begin{Bmatrix} U \\ \hline \bar{U} \end{Bmatrix} = \begin{bmatrix} R_{11} & \vdots & R_{12} \\ \hline R_{21} & \vdots & R_{22} \end{bmatrix} \begin{Bmatrix} F \\ \hline \bar{F} \end{Bmatrix} \quad (38)$$

The $\{U\}$ vector in equation (38) has components as defined in equation (8) for both symmetric and asymmetric solutions. The $\{\bar{U}\}$ vector of equation (38) has different components for the symmetric and asymmetric models as follows

$$\{\bar{U}\}_S = \begin{Bmatrix} U_{90x} \\ U_{90z} \\ U_{91x} \\ U_{91y} \\ U_{91z} \end{Bmatrix} \quad (39a)$$

$$\{\bar{U}\}_A = \begin{Bmatrix} U_{90y} \\ U_{91x} \\ U_{91y} \\ U_{91z} \end{Bmatrix} \quad (39b)$$

In equation (38), $\{\bar{F}\}$ is defined as the interface force vector applied to the ET. Equal and opposite forces $\{-\bar{F}\}$ are applied to the orbiter. Therefore, the displacements at the ET/orbiter attach points are

$$\{\bar{U}\} = [R_{ORB}]\{-\bar{F}\} \quad (40)$$

The ET and Orbiter receptance matrices defined in equations (38) and (40) were both calculated by applying unit loads at the frequency of interest as explained in a previous section.

Equation (38) can be expanded as follows

$$U = R_{11} F + R_{12} \bar{F} \quad (41a)$$

$$\bar{U} = R_{21} F + R_{22} \bar{F} \quad (41b)$$

Equation (40) can be solved for the unknown forces, $\{\bar{F}\}$

$$\{\bar{F}\} = -[R_{ORB}^{-1}]\{\bar{U}\} \quad (42)$$

Substituting (42) into equations (41a) and (41b)

$$U = R_{11} F - R_{12} R_{ORB}^{-1} \bar{U} \quad (43a)$$

$$\bar{U} = (I + R_{22} R_{ORB}^{-1})^{-1} R_{21} F \quad (43b)$$

The desired receptance equation can be obtained by substituting equation (43b) into equation (43a)

$$\{U\} = [R_{11} - R_{12} R_{ORB}^{-1} (I + R_{22} R_{ORB}^{-1})^{-1} R_{21}]\{F\} \quad (44)$$

Therefore, the desired receptance matrix is

$$[R_{RSS}] = [R_{11} - R_{12} R_{ORB}^{-1} (I + R_{22} R_{ORB}^{-1})^{-1} R_{21}] \quad (45)$$

SECTION IV

NASTRAN COMPUTER SOLUTION

The preceding section (Section III) contains a discussion of the theory upon which this analysis is based. In this section, application of the theory is discussed. The NASTRAN computer program was used as the basic analysis tool. The cyclic symmetry analysis of the SRM model and the DMAP program analysis of the Rockwell furnished models are furnished under separate headings.

SRM Analysis Using the Cyclic Symmetry Model

Recent versions of NASTRAN (i.e. Level 15.5 and Level 16.0) contain the capability to analyze cyclic symmetric structures using the static analysis (R.F.-1) or real eigenvalue analysis (R.F.-3) rigid formats. Corresponding NASTRAN documentation¹⁶ contains a description of cyclic symmetry; the description will not be repeated here.

A special version of NASTRAN was used for the cyclic symmetry analysis of the SRM model. The Mac Neal-Schwendler Company (MSC), working under contract with Hercules Incorporated, added the cyclic symmetry capability to the frequency response rigid format, (R.F.-8), in NASTRAN. The work was sponsored by the Air Force Rocket Propulsion Laboratory at Edwards AFB under contract F04611-73-C-0025 with Hercules. The MSC version of NASTRAN can be obtained from the Mac Neal-Schwendler Corporation at 7442 No. Figueroa Street, Los Angeles, California (90041), or it can be used on some of the large computer systems that lease it from MSC; e.g., the CDC Cybernet system.

The cyclic symmetry analysis capability in NASTRAN allows an efficient general three-dimensional analysis to be performed on a structure that is cyclic symmetric by modeling only a portion of the structure. For a rocket motor with the usual slotted grain design, a radial-axial plane passed through the center of each slot divides the motor into sections which repeat around the circumference of the motor. Since each such section is also symmetric about a radial-axial plane that would bisect it, NASTRAN requires a model of only one-half of a section. The SRM has 11 slots in the grain design. A half section model would therefore cover 1/22 of the circumference or about 16.4 degrees. Previous work¹⁷ has indicated that a grid slice somewhat less than 15 degrees is desirable because of the better approximation of curved surfaces that a narrow slice would offer. To obtain a slice narrower than 16.4 degrees two different approaches could be used: 1.) The 16.4 degree motor section could be modeled with a grid containing two 8.2 degree slices, or 2.) a model could be constructed for a motor with a greater number of slots. Option 1.) results in a grid with more degrees of freedom and a stiffness matrix with a larger bandwidth. A significantly larger run time would result from the use of option 1.).

¹⁶ NASTRAN Theoretical Manual, op. cit.

¹⁷ "Analytical Prediction of Motor Component Vibrations...", op. cit.

In an effort to maintain reasonable run times on the computer, option 2.) was adopted. A motor model with 18 slots was used to represent the actual motor which has 11 slots. The slot shape in a radial-axial plane was not changed and slot width was adjusted to keep the volume of propellant in the slotted area of the motor approximately constant between the 18 slot and 11 slot configurations. The 18 slot model should provide a good representation of the 11 slot motor in the most important longitudinal fundamental mode since the major structural effect the slots have is to reduce the hoop stiffness of the propellant grain in the slotted area. Hercules has obtained good results from a 2-D axisymmetric finite element computer program that utilizes slot approximation elements that have no hoop stiffness.

The grid layout in a radial-axial plane is shown in Figure 4. A projected view of the grid is shown in Figure 5. In both Figures 4 and 5, the actual grid has been rotated 180 degrees about the motor axis and plotted at both the 0 and 180 degree locations to show the motor outline. The grid is quite coarse compared with the usual solid rocket motor finite-element grid. The coarse grid is a result of efforts to model a very large structure with an adequate model and still maintain reasonable computer run times. Based on past experience, the grid should provide adequate results for low frequency analyses but would have questionable accuracy at higher frequencies. More discussion on grid refinement is contained in the Component Vibration Program Final Report¹⁸.

To avoid a lengthy description of the model geometry, material properties, etc., a copy of the NASTRAN bulk data deck is included as Table I. The corresponding case control deck is shown (abridged) in Table II. Only the first and last pages of the case control deck are shown in Table II because intermediate subcase cards are very repetitious. The corresponding executive control deck listing is shown in Table III. The alter statements, with the exception of the OUTPUT2 statement, were required to use the cyclic symmetry option in MSC NASTRAN. The OUTPUT2 alter was used to write the displacement solutions on a computer tape that could be saved for later use.

The NASTRAN solution represented by the data of Tables I, II, and III was run to obtain data for the SRM receptance matrix. A total of 10 unit loads were applied to the SRM model to determine the receptance matrix. Four unit loads were applied at the attach points, (load set F_{310,11}), and six unit loads were applied at the SRM/Nose Cone interconnection points. Unit loads were applied at points 1 and 2 as shown in Fig. 3. Points 1 and 2 represent the only types of unique points among the 36 different interface nodes of Fig. 3. Node 1 represents nodes that are half way between slots and node 2 represents nodes that are in line with slot tips. The computer solution represented by Tables I, II, and III was run on the IBM 370/155 with 1000K of core. The CPU time for the run was 7.07 hours and the total run time (CPU plus wait) was 8.07 hours. The problem had 1832 degrees of freedom in the analysis set. The 1/36 section grid therefore represents an equivalent full 360 degree equivalent model with $18 \times 1832 = 32,976$ degrees of freedom. Results from the analysis were the displacements at all nodes for each of the 10 different loads. All displacements are in data block UDVF which was written on an OUTPUT2 tape.

¹⁸ Op. Cit.

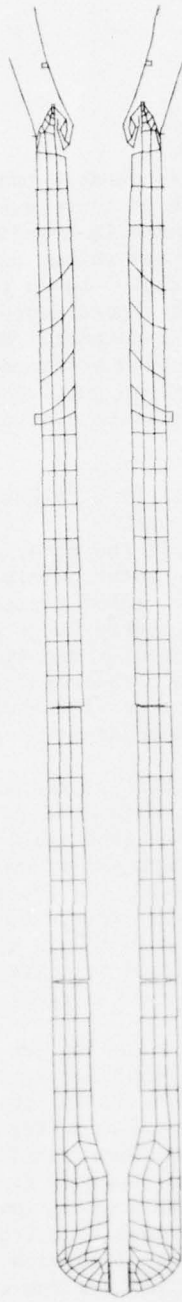


Figure 4. Outline of SRM Grid Used in Cyclic Symmetry Analysis

NOCTILE GRID PROFILE (7/11/ 3/78)
UNDESIGNED SHAPE

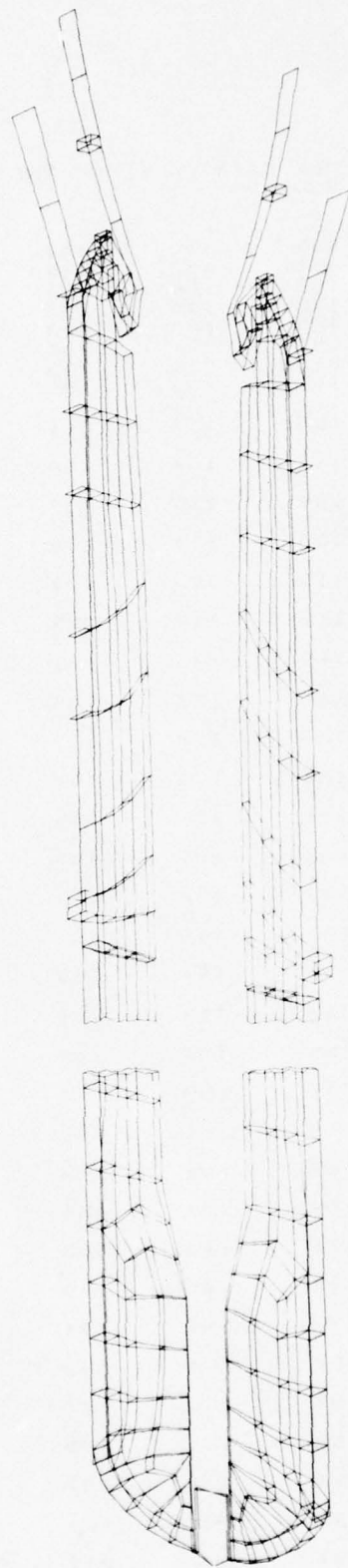


Figure 5. Computer Plot of SRM Grid Used in Cyclic Symmetry Analysis

TABLE I - NASTRAN BULK DATA DECK FOR THE SRM CYCLIC SYMMETRY MODEL

***	***	***	***	***	***	***	***	***	***	***
CBAR	501	501	139	140	141					2
CBAR	502	502	151	152	149					2
CBAR	503	502	163	164	161					2
CBAR	504	502	175	176	173					2
CBAR	505	502	185	186	183					2
CBAR	506	502	203	204	201					2
CBAR	507	503	215	216	213					2
CHEXA2	101	300	101	103	105	33	102	104	+H101	
+H101	106	34								
CHEXA2	102	300	103	109	111	105	104	110	+H102	
+H102	112	106								
CHEXA2	103	300	101	107	109	103	102	108	+H103	
+H103	110	104								
CHEXA2	104	300	109	115	117	111	110	116	+H104	
+H104	118	112								
CHEXA2	105	300	107	113	115	109	108	114	+H105	
+H105	116	116								
CHEXA2	106	300	115	123	121	117	116	124	+H106	
+H106	122	118								
CHEXA2	107	300	113	119	123	115	114	120	+H107	
+H107	124	116								
CHEXA2	108	300	119	125	127	123	120	126	+H108	
+H108	128	124								
CHEXA2	109	300	121	123	135	133	122	124	+H109	
+H109	136	134								
CHEXA2	110	300	123	127	137	135	124	128	+H110	
+H110	138	136								
CHEXA2	111	300	125	129	137	127	126	130	+H111	
+H111	138	128								
CHEXA2	112	300	131	133	145	143	132	134	+H112	
+H112	146	144								
CHEXA2	113	300	133	135	147	145	134	136	+H113	
+H113	146	146								
CHEXA2	114	300	135	137	149	147	136	138	+H114	
+H114	150	148								
CHEXA2	115	300	143	145	157	155	144	146	+H115	
+H115	158	156								
CHEXA2	116	300	145	147	159	157	146	148	+H116	
+H116	160	158								
CHEXA2	117	300	147	149	161	159	148	150	+H117	
+H117	162	160								
CHEXA2	118	300	155	157	169	167	156	158	+H118	
+H118	170	168								
CHEXA2	119	300	157	159	171	169	158	160	+H119	
+H119	172	170								
CHEXA2	120	300	159	161	173	171	160	162	+H120	
+H120	174	172								
CHEXA2	121	300	167	169	179	177	168	170	+H121	
+H121	180	178								
CHEXA2	122	300	169	171	181	179	170	172	+H122	
+H122	182	180								
CHEXA2	123	300	171	173	183	181	172	174	+H123	
+H123	184	182								
CHEXA2	124	300	177	179	189	187	178	180	+H124	
+H124	190	188								
CHEXA2	125	300	179	181	191	189	180	182	+H125	
+H125	192	190								
CHEXA2	126	300	181	183	193	191	182	184	+H126	
+H126	194	192								
CHEXA2	127	300	187	189	197	195	188	190	+H127	
+H127	198	196								
CHEXA2	128	300	189	191	199	197	190	192	+H128	
+H128	200	198								
CHEXA2	129	300	191	193	201	199	192	194	+H129	
+H129	202	200								
CHEXA2	130	300	195	197	209	207	196	198	+H130	
+H130	210	208								
CHEXA2	131	300	197	199	211	209	198	200	+H131	
+H131	212	210								

Table I (Continued)

CHEXA2	132	300	199	201	213	211	200	202	+H132
+H132	214	212							
CHEXA2	133	300	207	209	219	217	208	210	+H133
+H133	220	218							
CHEXA2	134	300	209	211	221	219	210	212	+H134
+H134	222	220							
CHEXA2	135	300	211	213	223	221	212	214	+H135
+H135	224	222							
CHEXA2	136	300	307	305	313	315	308	306	+H136
+H136	314	312							
CHEXA2	137	300	305	303	311	313	306	304	+H137
+H137	312	314							
CHEXA2	138	300	303	223	309	311	304	224	+H138
+H138	310	312							
CHEXA2	139	300	315	313	321	323	316	314	+H139
+H139	322	324							
CHEXA2	140	300	313	311	319	321	314	312	+H140
+H140	320	322							
CHEXA2	141	300	311	309	317	319	312	310	+H141
+H141	318	320							
CHEXA2	142	300	323	321	329	331	324	322	+H142
+H142	330	332							
CHEXA2	143	300	321	319	327	329	322	320	+H143
+H143	328	330							
CHEXA2	144	300	319	317	325	327	320	318	+H144
+H144	326	328							
CHEXA2	145	300	331	329	337	339	332	330	+H145
+H145	338	340							
CHEXA2	146	300	329	327	335	337	330	328	+H146
+H146	336	338							
CHEXA2	147	300	327	325	333	335	328	326	+H147
+H147	334	336							
CHEXA2	148	300	339	337	345	347	340	338	+H148
+H148	346	348							
CHEXA2	149	300	337	335	343	345	338	336	+H149
+H149	344	346							
CHEXA2	150	300	335	333	341	343	336	334	+H150
+H150	342	344							
CHEXA2	151	300	347	345	353	355	348	346	+H151
+H151	354	356							
CHEXA2	152	300	345	343	351	353	346	344	+H152
+H152	352	354							
CHEXA2	153	300	343	341	349	351	344	342	+H153
+H153	350	352							
CHEXA2	154	300	355	353	361	363	356	354	+H154
+H154	362	364							
CHEXA2	155	300	353	351	359	361	354	352	+H155
+H155	360	362							
CHEXA2	156	300	351	349	357	359	352	350	+H156
+H156	358	360							
CHEXA2	157	300	363	361	369	371	364	362	+H157
+H157	370	372							
CHEXA2	158	300	361	359	367	369	362	360	+H158
+H158	368	370							
CHEXA2	159	300	359	357	365	367	360	358	+H159
+H159	366	368							
CHEXA2	160	300	407	405	413	415	408	406	+H160
+H160	414	416							
CHEXA2	161	300	405	403	411	413	406	404	+H161
+H161	412	414							
CHEXA2	162	300	403	365	409	411	404	366	+H162
+H162	410	412							
CHEXA2	163	300	415	413	421	423	416	414	+H163
+H163	422	424							
CHEXA2	164	300	413	411	419	421	414	412	+H164
+H164	420	422							
CHEXA2	165	300	411	409	417	419	412	410	+H165
+H165	418	420							
CHEXA2	166	300	423	421	429	431	424	422	+H166
+H166	430	432							
CHEXA2	167	300	421	419	427	429	422	420	+H167
+H167	428	430							
CHEXA2	168	300	419	417	425	427	420	418	+H168
+H168	426	428							
CHEXA2	169	300	431	429	437	439	432	430	+H169
+H169	438	440							
CHEXA2	170	300	429	427	435	437	430	428	+H170

Table I (Continued)

+H170	436	438								
CHEXA2	171	300	427	425	433	435	428	426	+H171	
+H171	434	436								
CHEXA2	172	300	439	437	445	447	440	436	+H172	
+H172	446	448								
CHEXA2	173	300	437	435	443	445	438	436	+H173	
+H173	444	446								
CHEXA2	174	300	435	433	441	443	436	434	+H174	
+H174	442	444								
CHEXA2	175	300	447	445	453	455	448	446	+H175	
+H175	454	456								
CHEXA2	176	300	445	443	451	453	446	444	+H176	
+H176	452	454								
CHEXA2	177	300	443	441	449	451	444	442	+H177	
+H177	450	452								
CHEXA2	178	300	455	453	461	463	456	454	+H178	
+H178	462	464								
CHEXA2	179	300	453	451	459	461	454	452	+H179	
+H179	460	462								
CHEXA2	180	300	451	449	457	459	452	450	+H180	
+H180	458	460								
CHEXA2	181	300	463	461	469	471	464	462	+H181	
+H181	470	472								
CHEXA2	182	300	461	459	467	469	462	460	+H182	
+H182	468	470								
CHEXA2	183	300	459	457	465	467	460	458	+H183	
+H183	466	468								
CHEXA2	184	300	507	505	513	515	508	506	+H184	
+H184	514	516								
CHEXA2	185	300	505	503	511	513	506	504	+H185	
+H185	512	514								
CHEXA2	186	300	503	460	509	511	504	466	+H186	
+H186	510	512								
CHEXA2	187	300	515	513	521	523	516	514	+H187	
+H187	522	524								
CHEXA2	188	300	513	511	519	521	514	512	+H188	
+H188	520	522								
CHEXA2	189	300	511	509	517	519	512	510	+H189	
+H189	518	520								
CHEXA2	190	300	523	521	529	531	524	522	+H190	
+H190	530	532								
CHEXA2	191	300	521	519	527	529	522	520	+H191	
+H191	528	530								
CHEXA2	192	300	519	517	525	527	520	518	+H192	
+H192	526	528								
CHEXA2	193	300	531	529	537	539	532	530	+H193	
+H193	538	540								
CHEXA2	194	300	529	527	535	537	530	528	+H194	
+H194	536	538								
CHEXA2	195	300	527	525	533	535	528	526	+H195	
+H195	534	536								
CHEXA2	196	300	539	537	545	543	540	538	+H196	
+H196	542	544								
CHEXA2	197	300	537	535	547	541	538	536	+H197	
+H197	548	542								
CHEXA2	198	300	535	533	545	547	536	534	+H198	
+H198	546	548								
CHEXA2	199	300	543	541	551	553	544	542	+H199	
+H199	552	554								
CHEXA2	200	300	541	547	549	551	542	546	+H200	
+H200	550	552								
CHEXA2	201	300	553	551	561	563	554	552	+H201	
+H201	562	564								
CHEXA2	202	300	551	549	559	561	552	550	+H202	
+H202	560	562								
CHEXA2	203	300	549	547	557	559	550	548	+H203	
+H203	558	560								
CHEXA2	204	300	547	545	555	557	548	546	+H204	
+H204	556	558								
CHEXA2	205	300	563	561	571	573	564	562	+H205	
+H205	572	574								
CHEXA2	206	300	561	559	569	571	562	560	+H206	
+H206	570	572								
CHEXA2	207	300	559	557	567	569	560	558	+H207	
+H207	568	570								
CHEXA2	208	300	557	555	565	567	558	556	+H208	
+H208	566	568								

Table I (Continued)

CHEXA2	209	300	573	571	581	583	574	572	+H209
+H209	582	584							
CHEXA2	210	300	571	569	579	581	572	570	+H210
+H210	580	582							
CHEXA2	211	300	569	567	577	579	570	568	+H211
+H211	578	580							
CHEXA2	212	300	567	565	575	577	568	566	+H212
+H212	576	578							
CHEXA2	213	300	583	581	591	593	584	582	+H213
+H213	592	594							
CHEXA2	214	300	581	579	589	591	582	580	+H214
+H214	590	592							
CHEXA2	215	300	579	577	587	589	580	578	+H215
+H215	588	590							
CHEXA2	216	300	577	575	585	587	578	576	+H216
+H216	586	588							
CHEXA2	217	300	593	591	603	605	594	592	+H217
+H217	604	606							
CHEXA2	218	300	591	589	601	603	592	590	+H218
+H218	602	604							
CHEXA2	219	300	589	587	597	601	590	588	+H219
+H219	598	602							
CHEXA2	220	300	587	585	595	597	588	586	+H220
+H220	596	598							
CHEXA2	221	300	597	595	599	601	592	590	+H221
+H221	600	602							
CHEXA2	222	300	605	603	615	617	606	604	+H222
+H222	616	618							
CHEXA2	223	300	603	601	613	615	604	602	+H223
+H223	614	616							
CHEXA2	224	300	601	599	611	613	602	600	+H224
+H224	612	614							
CHEXA2	225	300	605	617	619	607	606	618	+H225
+H225	620	622							
CHEXA2	226	300	617	625	629	619	618	626	+H226
+H226	630	620							
CHEXA2	227	300	615	613	625	617	616	614	+H227
+H227	626	616							
CHEXA2	228	300	613	611	623	625	614	612	+H228
+H228	624	626							
CHEXA2	229	300	625	613	627	629	626	624	+H229
+H229	628	630							
CHEXA2	230	300	607	619	621	609	608	620	+H230
+H230	622	610							
CHEXA2	231	300	619	629	633	621	626	630	+H231
+H231	634	622							
CHEXA2	232	300	629	627	631	633	630	628	+H232
+H232	632	634							
CHEXA2	233	300	609	621	633	635	610	622	+H233
+H233	634	636							
CHEXA2	234	300	633	621	637	635	634	632	+H234
+H234	638	636							
CHEXA2	301	400	29	25	19	23	30	26	+H301
+H301	20	24							
CHEXA2	401	200	35	37	101	33	36	38	+H401
+H401	102	34							
CORDP2C	1		0.0	0.0	0.0	0.0	0.0	1.0	+BC
+BC	1.0	0.0	0.0						
CQUAD2	1	10	1	2	4	3		0.0	
CQUAD2	2	10	3	4	6	5		0.0	
CQUAD2	3	40	5	6	8	7		0.0	
CQUAD2	4	40	7	8	12	11		0.0	
CQUAD2	5	40	11	12	10	9		0.0	
CQUAD2	6	10	5	6	10	9		0.0	
CQUAD2	7	10	9	10	14	13		0.0	
CQUAD2	8	10	13	14	16	15		0.0	
CQUAD2	9	10	15	16	18	17		0.0	
CQUAL2	10	39	17	18	22	21		0.0	
CQUAD2	11	39	21	22	28	27		0.0	
CQUAD2	12	39	27	28	32	31		0.0	
CQUAD2	13	42	17	18	20	19		0.0	
CQUAD2	14	42	19	20	26	25		0.0	
CQUAD2	16	43	23	24	30	29		0.0	
CQUAD2	15	42	25	26	28	27		0.0	
CQUAD2	17	44	25	26	34	33		0.0	
CQUAD2	18	45	33	34	36	35		0.0	
CQUAD2	19	45	35	36	38	37		0.0	

Table I (Continued)

CQUAD2	26	46	101	102	108	107	0.0		
CQUAD2	27	47	107	108	114	113	0.0		
CQUAD2	28	47	113	114	120	119	0.0		
CQUAD2	29	47	119	120	126	125	0.0		
CQUAD2	30	60	125	126	130	129	0.0		
CQUAD2	31	46	129	130	142	141	0.0		
CQUAD2	32	49	141	142	140	139	0.0		
CQUAD2	33	50	141	142	154	153	0.0		
CQUAD2	34	50	153	154	166	165	0.0		
CQUAD2	35	52	129	130	138	137	0.0		
CQUAD2	36	52	137	138	150	149	0.0		
CQUAD2	37	54	149	150	152	151	0.0		
CQUAD2	38	52	149	150	162	161	0.0		
CQUAD2	39	54	161	162	164	163	0.0		
CQUAD2	40	52	161	162	174	173	0.0		
CQUAD2	41	54	173	174	176	175	0.0		
CQUAD2	42	52	173	174	184	183	0.0		
CQUAD2	43	54	183	184	186	185	0.0		
CQUAD2	44	52	183	184	194	193	0.0		
CQUAD2	45	52	193	194	202	201	0.0		
CQUAD2	46	52 1	201	202	214	213	0.0		
CQUAD2	47	56	201	202	204	203	0.0		
CQUAD2	48	58	203	204	206	205	0.0		
CQUAD2	49	58	205	206	216	215	0.0		
CQUAD2	50	56	213	214	216	215	0.0		
CQUAD2	51	52	213	214	224	223	0.0		
CQUAD2	52	60	223	224	310	309	0.0		
CQUAD2	53	60	309	310	318	317	0.0		
CQUAD2	54	60	317	318	326	325	0.0		
CQUAD2	55	60	325	326	334	333	0.0		
CQUAD2	56	60	333	334	342	341	0.0		
CQUAD2	57	60	341	342	350	349	0.0		
CQUAD2	58	60	349	350	358	357	0.0		
CQUAD2	59	60	357	358	366	365	0.0		
CQUAD2	60	60	365	366	410	409	0.0		
CQUAD2	61	60	409	410	418	417	0.0		
CQUAD2	62	60	417	418	426	425	0.0		
CQUAD2	63	60	425	426	434	433	0.0		
CQUAD2	64	60	433	434	442	441	0.0		
CQUAD2	65	60	441	442	450	449	0.0		
CQUAD2	66	60	449	450	458	457	0.0		
CQUAD2	67	60	457	458	466	465	0.0		
CQUAD2	68	62	465	466	510	509	0.0		
CQUAD2	69	62	509	510	518	517	0.0		
CQUAD2	70	62	517	518	526	525	0.0		
CQUAD2	71	62	525	526	534	533	0.0		
CQUAD2	72	62	533	534	546	545	0.0		
CQUAD2	73	62	545	546	556	555	0.0		
CQUAD2	74	62	555	556	566	565	0.0		
CQUAD2	75	62	565	566	576	575	0.0		
CQUAD2	76	62	575	576	586	585	0.0		
CQUAD2	77	62	585	586	648	647	0.0		
CQUAD2	78	63	585	586	596	595	0.0		
CQUAD2	79	64	595	596	600	599	0.0		
CQUAD2	80	65	599	600	612	611	0.0		
CQUAD2	81	66	611	612	624	623	0.0		
CQUAD2	82	67	623	624	628	627	0.0		
CQUAD2	83	68	627	628	632	631	0.0		
CQUAD2	84	69	631	632	638	637	0.0		
CQUAD2	85	70	637	638	640	639	0.0		
CQUAD2	86	71	639	640	642	641	0.0		
CQUAD2	87	72	639	640	644	643	0.0		
CQUAD2	88	73	643	644	646	645	0.0		
CYJOIN	1	C	2	4	6	8	10	12	+CY1
+CY1	14	16	18	20	22	24	26	28	+CY2
+CY2	30	32	34	36	38	40	42	44	+CY3
+CY3	108	110	112	114	116	118	120	122	+CY4
+CY4	124	126	128	130	132	134	136	138	+CY5
+CY5	140	142	144	146	148	150	152	154	+CY6
+CY6	156	158	160	162	164	166	168	170	+CY7
+CY7	172	174	176	178	180	182	184	186	+CY8
+CY8	186	190	192	194	196	198	200	202	+CY9
+CY9	204	206	208	210	212	214	216	218	+CY10
+CY10	220	222	224	304	306	308	310	312	+CY11
+CY11	314	316	318	320	322	324	326	328	+CY12
+CY12	330	332	334	336	338	340	342	344	+CY13
+CY13	346	348	350	352	354	356	358	360	+CY14

Table I (Continued)

+CY14	362	364	366	368	370	372	404	406	+CY15
+CY15	408	410	412	414	416	418	420	422	+CY16
+CY16	424	426	428	430	432	434	436	438	+CY17
+CY17	440	442	444	446	448	450	452	454	+CY18
+CY18	456	458	460	462	464	466	468	470	+CY19
+CY19	472	504	506	508	510	512	514	516	+CY20
+CY20	518	520	522	524	526	528	530	532	+CY21
+CY21	534	536	538	540	542	544	546	548	+CY22
+CY22	550	552	554	556	558	560	562	564	+CY23
+CY23	566	568	570	572	574	576	578	580	+CY24
+CY24	582	584	586	588	590	592	594	596	+CY25
+CY25	598	600	602	604	606	608	610	612	+CY26
+CY26	614	616	618	620	622	624	626	628	+CY27
+CY27	630	632	634	636	638	640	642	644	+CY28
+CY28	646	648							+CY29
CYJUN	7	8	9	10	11	12	13	14	+CY30
+CY29	15	16	17	18	19	20	21	22	+CY31
+CY30	23	24	25	26	27	28	29	30	+CY32
+CY31	107	109	111	113	115	117	119	121	+CY33
+CY32	123	125	127	129	131	133	135	137	+CY34
+CY33	139	141	143	145	147	149	151	153	+CY35
+CY34	155	157	159	161	163	165	167	169	+CY36
+CY35	171	173	175	177	179	181	183	185	+CY37
+CY36	187	189	191	193	195	197	199	201	+CY38
+CY37	203	205	207	209	211	213	215	217	+CY39
+CY38	219	221	223	225	227	229	231	233	+CY40
+CY39	315	317	319	321	323	325	327	329	+CY41
+CY40	329	331	333	335	337	339	341	343	+CY42
+CY41	345	347	349	351	353	355	357	359	+CY43
+CY42	361	363	365	367	369	371	373	375	+CY44
+CY43	407	409	411	413	415	417	419	421	+CY45
+CY44	423	425	427	429	431	433	435	437	+CY46
+CY45	439	441	443	445	447	449	451	453	+CY47
+CY46	455	457	459	461	463	465	467	469	+CY48
+CY47	471	473	475	477	479	481	483	485	+CY49
+CY48	517	519	521	523	525	527	529	531	+CY50
+CY49	533	535	537	539	541	543	545	547	+CY51
+CY50	565	567	569	571	573	575	577	579	+CY52
+CY51	599	601	603	605	607	609	611	613	+CY53
+CY52	631	633	635	637	639	641	643	645	
+CY53	647								
DAREA	801	648	1	1.0					
DAREA	802	648	2	1.0					
DAREA	803	648	3	1.0					
DAREA	804	647	1	1.0					
DAREA	805	647	2	1.0					
DAREA	806	647	3	1.0					
DAREA	807	200	1	1.0					
DAREA	808	200	2	1.0					
DAREA	809	200	1	1.0					
DAREA	810	200	2	1.0					
FREQ	1	15.2450							
\$									
GRID	1	1	73.50	5.0	1990.00	1			
GRID	2	1	73.50	-5.0	1990.00	1			
GRID	3	1	66.75	5.0	1957.20	1			
GRID	4	1	66.75	-5.0	1957.20	1			
GRID	5	1	58.25	5.0	1925.50	1			
GRID	6	1	58.25	-5.0	1925.50	1			
GRID	7	1	64.25	5.0	1925.50	1			
GRID	8	1	64.25	-5.0	1925.50	1			
GRID	9	1	56.75	5.0	1920.20	1			
GRID	10	1	56.75	-5.0	1920.20	1			
GRID	11	1	64.25	5.0	1920.20	1			
GRID	12	1	64.25	-5.0	1920.20	1			
GRID	13	1	44.50	5.0	1884.59	1			
GRID	14	1	44.50	-5.0	1884.59	1			
GRID	15	1	30.00	5.0	1851.00	1			
GRID	16	1	30.00	-5.0	1851.00	1			
GRID	17	1	33.80	5.0	1829.75	1			
GRID	18	1	33.80	-5.0	1829.75	1			
GRID	19	1	39.50	5.0	1835.00	1			
GRID	20	1	39.50	-5.0	1835.00	1			
GRID	21	1	41.25	5.0	1824.00	1			
GRID	22	1	41.25	-5.0	1824.00	1			
GRID	23	1	36.00	5.0	1847.75	1			
GRID	24	1	36.00	-5.0	1847.75	1			

Table I (Continued)

GRID	25	1	45.00	5.0	1845.90	1				
GRID	26	1	45.00	-5.0	1845.90	1				
GRID	27	1	47.25	5.0	1846.00	1				
GRID	28	1	47.25	-5.0	1846.00	1				
GRID	29	1	37.75	5.0	1857.70	1				
GRID	30	1	37.75	-5.0	1857.70	1				
GRID	31	1	47.25	5.0	1859.30	1				
GRID	32	1	47.25	-5.0	1859.30	1				
GRID	33	1	51.00	5.0	1873.00	1				
GRID	34	1	51.00	-5.0	1873.00	1				
GRID	35	1	51.00	5.0	1876.10	1				
GRID	36	1	51.00	-5.0	1876.10	1				
GRID	37	1	54.70	5.0	1876.10	1				
GRID	38	1	54.70	-5.0	1876.10	1				
\$	GRID	POINTS	101	THRU	299	ARE	FOR	THE	AFT	SECTION
GRID	101	1	54.40	5.0	1873.00	1				
GRID	102	1	54.40	-5.0	1873.00	1				
GRID	103	1	54.00	5.0	1865.75	1				
GRID	104	1	54.00	-5.0	1865.75	1				
GRID	105	1	50.70	5.0	1865.50	1				
GRID	106	1	50.70	-5.0	1865.50	1				
GRID	107	1	59.55	5.0	1866.15	1				
GRID	108	1	59.55	-5.0	1866.15	1				
GRID	109	1	56.75	5.0	1861.20	1				
GRID	110	1	56.75	-5.0	1861.20	1				
GRID	111	1	50.60	5.0	1859.60	1				
GRID	112	1	50.60	-5.0	1859.60	1				
GRID	113	1	63.60	5.0	1859.85	1				
GRID	114	1	63.60	-5.0	1859.85	1				
GRID	115	1	58.20	5.0	1853.50	1				
GRID	116	1	58.20	-5.0	1853.50	1				
GRID	117	1	50.50	5.0	1851.00	1				
GRID	118	1	50.50	-5.0	1851.00	1				
GRID	119	1	66.75	5.0	1853.15	1				
GRID	120	1	66.75	-5.0	1853.15	1				
GRID	121	1	50.45	5.0	1842.00	1				
GRID	122	1	50.45	-5.0	1842.00	1				
GRID	123	1	62.50	5.0	1845.00	1				
GRID	124	1	62.50	-5.0	1845.00	1				
GRID	125	1	69.75	5.0	1845.05	1				
GRID	126	1	69.75	-5.0	1845.05	1				
GRID	127	1	67.50	5.0	1843.00	1				
GRID	128	1	67.50	-5.0	1843.00	1				
GRID	129	1	72.60	5.0	1834.25	1				
GRID	130	1	72.60	-5.0	1834.25	1				
GRID	131	1	38.75	5.0	1814.30	1				
GRID	132	1	38.75	-5.0	1814.30	1				
GRID	133	1	50.15	5.0	1818.30	1				
GRID	134	1	50.15	-5.0	1818.30	1				
GRID	135	1	61.50	5.0	1819.50	1				
GRID	136	1	61.50	-5.0	1819.50	1				
GRID	137	1	72.75	5.0	1821.00	1				
GRID	138	1	72.75	-5.0	1821.00	1				
GRID	139	1	78.50	5.0	1839.70	1				
GRID	140	1	78.50	-5.0	1839.70	1				
GRID	141	1	72.75	5.0	1839.70	1				
GRID	142	1	72.75	-5.0	1839.70	1				
GRID	143	1	37.00	5.0	1777.80	1				
GRID	144	1	37.00	-5.0	1777.80	1				
GRID	145	1	50.00	5.0	1777.80	1				
GRID	146	1	50.00	-5.0	1777.80	1				
GRID	147	1	61.50	5.0	1777.80	1				
GRID	148	1	61.50	-5.0	1777.80	1				
GRID	149	1	72.75	5.0	1777.80	1				
GRID	150	1	72.75	-5.0	1777.80	1				
GRID	151	1	76.80	5.0	1777.80	1				
GRID	152	1	76.80	-5.0	1777.80	1				
GRID	153	1	87.85	5.0	1884.59	1				
GRID	154	1	87.85	-5.0	1884.59	1				
GRID	155	1	35.01	5.0	1733.75	1				
GRID	156	1	35.01	-5.0	1733.75	1				
GRID	157	1	50.00	5.0	1733.75	1				
GRID	158	1	50.00	-5.0	1733.75	1				
GRID	159	1	61.50	5.0	1733.75	1				
GRID	160	1	61.50	-5.0	1733.75	1				
GRID	161	1	72.75	5.0	1733.75	1				
GRID	162	1	72.75	-5.0	1733.75	1				

Table I (Continued)

GRID	163	1	76.80	5.0	1733.75	1
GRID	164	1	76.80	-5.0	1733.75	1
GRID	165	1	103.75	5.0	1930.70	1
GRID	166	1	103.75	-5.0	1930.70	1
GRID	167	1	33.30	5.0	1692.5	1
GRID	168	1	33.30	-5.0	1692.5	1
GRID	169	1	46.80	5.0	1676.25	1
GRID	170	1	46.80	-5.0	1676.25	1
GRID	171	1	59.40	5.0	1665.80	1
GRID	172	1	59.40	-5.0	1665.80	1
GRID	173	1	72.75	5.0	1657.70	1
GRID	174	1	72.75	-5.0	1657.70	1
GRID	175	1	76.80	5.0	1657.70	1
GRID	176	1	76.80	-5.0	1657.70	1
GRID	177	1	32.50	5.0	1645.00	1
GRID	178	1	32.50	-5.0	1645.00	1
GRID	179	1	45.75	5.0	1628.25	1
GRID	180	1	45.75	-5.0	1628.25	1
GRID	181	1	59.25	5.0	1619.00	1
GRID	182	1	59.25	-5.0	1619.00	1
GRID	183	1	72.75	5.0	1613.65	1
GRID	184	1	72.75	-5.0	1613.65	1
GRID	185	1	76.80	5.0	1613.65	1
GRID	186	1	76.80	-5.0	1613.65	1
GRID	187	1	32.25	5.0	1590.00	1
GRID	188	1	32.25	-5.0	1590.00	1
GRID	189	1	46.00	5.0	1573.75	1
GRID	190	1	46.00	-5.0	1573.75	1
GRID	191	1	59.00	5.0	1562.50	1
GRID	192	1	59.00	-5.0	1562.50	1
GRID	193	1	72.75	5.0	1555.00	1
GRID	194	1	72.75	-5.0	1555.00	1
GRID	195	1	32.10	5.0	1547.50	1
GRID	196	1	32.10	-5.0	1547.50	1
GRID	197	1	46.00	5.0	1533.50	1
GRID	198	1	46.00	-5.0	1533.50	1
GRID	199	1	59.00	5.0	1523.50	1
GRID	200	1	59.00	-5.0	1523.50	1
GRID	201	1	72.75	5.0	1516.80	1
GRID	202	1	72.75	-5.0	1516.80	1
GRID	203	1	81.20	5.0	1516.80	1
GRID	204	1	81.20	-5.0	1516.80	1
GRID	205	1	81.20	5.0	1511.00	1
GRID	206	1	81.20	-5.0	1511.00	1
GRID	207	1	32.00	5.0	1517.50	1
GRID	208	1	32.00	-5.0	1517.50	1
GRID	209	1	46.00	5.0	1512.00	1
GRID	210	1	46.00	-5.0	1512.00	1
GRID	211	1	59.00	5.0	1507.50	1
GRID	212	1	59.00	-5.0	1507.50	1
GRID	213	1	72.75	5.0	1505.30	1
GRID	214	1	72.75	-5.0	1505.30	1
GRID	215	1	81.20	5.0	1505.30	1
GRID	216	1	81.20	-5.0	1505.30	1
GRID	217	1	32.00	5.0	1492.00	1
GRID	218	1	32.00	-5.0	1492.00	1
GRID	219	1	46.00	5.0	1492.00	1
GRID	220	1	46.00	-5.0	1492.00	1
GRID	221	1	59.00	5.0	1492.00	1
GRID	222	1	59.00	-5.0	1492.00	1
GRID	223	1	72.75	5.0	1492.00	1
GRID	224	1	72.75	-5.0	1492.00	1
\$	GRID	POINTS 301 THRU 399 ARE			FUR THE AFT CENTER SECTION	
GRID	303	1	59.00	5.0	1491.00	1
GRID	304	1	59.00	-5.0	1491.00	1
GRID	305	1	46.00	5.0	1491.00	1
GRID	306	1	46.00	-5.0	1491.00	1
GRID	307	1	33.10	5.0	1491.00	1
GRID	308	1	33.10	-5.0	1491.00	1
GRID	309	1	72.75	5.0	1450.00	1
GRID	310	1	72.75	-5.0	1450.00	1
GRID	311	1	59.00	5.0	1450.00	1
GRID	312	1	59.00	-5.0	1450.00	1
GRID	313	1	46.00	5.0	1450.00	1
GRID	314	1	46.00	-5.0	1450.00	1
GRID	315	1	32.88	5.0	1450.00	1
GRID	316	1	32.88	-5.0	1450.00	1

Table I (Continued)

GRID	317	1	72.75	5.0	1410.00	1
GRID	318	1	72.75	-5.0	1410.00	1
GRID	319	1	59.00	5.0	1410.00	1
GRID	320	1	59.00	-5.0	1410.00	1
GRID	321	1	46.00	5.0	1410.00	1
GRID	322	1	46.00	-5.0	1410.00	1
GRID	323	1	32.53	5.0	1410.00	1
GRID	324	1	32.53	-5.0	1410.00	1
GRID	325	1	72.75	5.0	1370.00	1
GRID	326	1	72.75	-5.0	1370.00	1
GRID	327	1	59.00	5.0	1370.00	1
GRID	328	1	59.00	-5.0	1370.00	1
GRID	329	1	46.00	5.0	1370.00	1
GRID	330	1	46.00	-5.0	1370.00	1
GRID	331	1	32.14	5.0	1370.00	1
GRID	332	1	32.14	-5.0	1370.00	1
GRID	333	1	72.75	5.0	1330.00	1
GRID	334	1	72.75	-5.0	1330.00	1
GRID	335	1	59.00	5.0	1330.00	1
GRID	336	1	59.00	-5.0	1330.00	1
GRID	337	1	46.00	5.0	1330.00	1
GRID	338	1	46.00	-5.0	1330.00	1
GRID	339	1	31.74	5.0	1330.00	1
GRID	340	1	31.74	-5.0	1330.00	1
GRID	341	1	72.75	5.0	1290.00	1
GRID	342	1	72.75	-5.0	1290.00	1
GRID	343	1	59.00	5.0	1290.00	1
GRID	344	1	59.00	-5.0	1290.00	1
GRID	345	1	46.00	5.0	1290.00	1
GRID	346	1	46.00	-5.0	1290.00	1
GRID	347	1	31.35	5.0	1290.00	1
GRID	348	1	31.35	-5.0	1290.00	1
GRID	349	1	72.75	5.0	1250.00	1
GRID	350	1	72.75	-5.0	1250.00	1
GRID	351	1	59.00	5.0	1250.00	1
GRID	352	1	59.00	-5.0	1250.00	1
GRID	353	1	46.00	5.0	1250.00	1
GRID	354	1	46.00	-5.0	1250.00	1
GRID	355	1	30.96	5.0	1250.00	1
GRID	356	1	30.96	-5.0	1250.00	1
GRID	357	1	72.75	5.0	1210.00	1
GRID	358	1	72.75	-5.0	1210.00	1
GRID	359	1	59.00	5.0	1210.00	1
GRID	360	1	59.00	-5.0	1210.00	1
GRID	361	1	46.00	5.0	1210.00	1
GRID	362	1	46.00	-5.0	1210.00	1
GRID	363	1	30.57	5.0	1210.00	1
GRID	364	1	30.57	-5.0	1210.00	1
GRID	365	1	72.75	5.0	1171.50	1
GRID	366	1	72.75	-5.0	1171.50	1
GRID	367	1	59.00	5.0	1173.00	1
GRID	368	1	59.00	-5.0	1173.00	1
GRID	369	1	46.00	5.0	1173.00	1
GRID	370	1	46.00	-5.0	1173.00	1
GRID	371	1	30.20	5.0	1173.00	1
GRID	372	1	30.20	-5.0	1173.00	1
↓						
GRID POINTS 401 THRU 499 ARE FOR THE FORWARD CENTER SECTION						
GRID	403	1	59.00	5.0	1171.00	1
GRID	404	1	59.00	-5.0	1171.00	1
GRID	405	1	46.00	5.0	1171.00	1
GRID	406	1	46.00	-5.0	1171.00	1
GRID	407	1	33.10	5.0	1171.00	1
GRID	408	1	33.10	-5.0	1171.00	1
GRID	409	1	72.75	5.0	1130.00	1
GRID	410	1	72.75	-5.0	1130.00	1
GRID	411	1	59.00	5.0	1130.00	1
GRID	412	1	59.00	-5.0	1130.00	1
GRID	413	1	46.00	5.0	1130.00	1
GRID	414	1	46.00	-5.0	1130.00	1
GRID	415	1	32.88	5.0	1130.00	1
GRID	416	1	32.88	-5.0	1130.00	1
GRID	417	1	72.75	5.0	1090.00	1
GRID	418	1	72.75	-5.0	1090.00	1
GRID	419	1	59.00	5.0	1090.00	1
GRID	420	1	59.00	-5.0	1090.00	1
GRID	421	1	46.00	5.0	1090.00	1
GRID	422	1	46.00	-5.0	1090.00	1

Table I (Continued)

GRID	423	1	32.53	5.0	1090.00	1
GRID	424	1	32.53	-5.0	1090.00	1
GRID	425	1	72.75	5.0	1050.00	1
GRID	426	1	72.75	-5.0	1050.00	1
GRID	427	1	59.00	5.0	1050.00	1
GRID	428	1	59.00	-5.0	1050.00	1
GRID	429	1	46.00	5.0	1050.00	1
GRID	430	1	46.00	-5.0	1050.00	1
GRID	431	1	32.14	5.0	1050.00	1
GRID	432	1	32.14	-5.0	1050.00	1
GRID	433	1	72.75	5.0	1010.00	1
GRID	434	1	72.75	-5.0	1010.00	1
GRID	435	1	59.00	5.0	1010.00	1
GRID	436	1	59.00	-5.0	1010.00	1
GRID	437	1	46.00	5.0	1010.00	1
GRID	438	1	46.00	-5.0	1010.00	1
GRID	439	1	31.74	5.0	1010.00	1
GRID	440	1	31.74	-5.0	1010.00	1
GRID	441	1	72.75	5.0	970.00	1
GRID	442	1	72.75	-5.0	970.00	1
GRID	443	1	59.00	5.0	970.00	1
GRID	444	1	59.00	-5.0	970.00	1
GRID	445	1	46.00	5.0	970.00	1
GRID	446	1	46.00	-5.0	970.00	1
GRID	447	1	31.35	5.0	970.00	1
GRID	448	1	31.35	-5.0	970.00	1
GRID	449	1	72.75	5.0	930.00	1
GRID	450	1	72.75	-5.0	930.00	1
GRID	451	1	59.00	5.0	930.00	1
GRID	452	1	59.00	-5.0	930.00	1
GRID	453	1	46.00	5.0	930.00	1
GRID	454	1	46.00	-5.0	930.00	1
GRID	455	1	30.96	5.0	930.00	1
GRID	456	1	30.96	-5.0	930.00	1
GRID	457	1	72.75	5.0	890.00	1
GRID	458	1	72.75	-5.0	890.00	1
GRID	459	1	59.00	5.0	890.00	1
GRID	460	1	59.00	-5.0	890.00	1
GRID	461	1	46.00	5.0	890.00	1
GRID	462	1	46.00	-5.0	890.00	1
GRID	463	1	30.57	5.0	890.00	1
GRID	464	1	30.57	-5.0	890.00	1
GRID	465	1	72.75	5.0	851.50	1
GRID	466	1	72.75	-5.0	851.50	1
GRID	467	1	59.00	5.0	852.50	1
GRID	468	1	59.00	-5.0	852.50	1
GRID	469	1	46.00	5.0	852.50	1
GRID	470	1	46.00	-5.0	852.50	1
GRID	471	1	30.20	5.0	852.50	1
GRID	472	1	30.20	-5.0	852.50	1
\$	GRID POINTS 501 THRU 699 ARE FOR THE FORWARD SECTION					
GRID	503	1	59.00	5.0	850.50	1
GRID	504	1	59.00	-5.0	850.50	1
GRID	505	1	46.00	5.0	850.50	1
GRID	506	1	46.00	-5.0	850.50	1
GRID	507	1	30.40	5.0	850.50	1
GRID	508	1	30.40	-5.0	850.50	1
GRID	509	1	72.75	5.0	808.00	1
GRID	510	1	72.75	-5.0	808.00	1
GRID	511	1	59.00	5.0	808.00	1
GRID	512	1	59.00	-5.0	808.00	1
GRID	513	1	46.00	5.0	808.00	1
GRID	514	1	46.00	-5.0	808.00	1
GRID	515	1	30.20	5.0	808.00	1
GRID	516	1	30.20	-5.0	808.00	1
GRID	517	1	72.75	5.0	766.00	1
GRID	518	1	72.75	-5.0	766.00	1
GRID	519	1	59.00	5.0	766.00	1
GRID	520	1	59.00	-5.0	766.00	1
GRID	521	1	46.00	5.0	766.00	1
GRID	522	1	46.00	-5.0	766.00	1
GRID	523	1	30.05	5.0	766.00	1
GRID	524	1	30.05	-5.0	766.00	1
GRID	525	1	72.75	5.0	724.00	1
GRID	526	1	72.75	-5.0	724.00	1
GRID	527	1	59.00	5.0	724.00	1
GRID	528	1	59.00	-5.0	724.00	1

Table I (Continued)

GRID	529	1	46.00	5.0	724.00	1
GRID	530	1	46.00	-5.0	724.00	1
GRID	531	1	30.00	5.0	724.00	1
GRID	532	1	30.00	-5.0	724.00	1
GRID	533	1	72.75	5.0	681.40	1
GRID	534	1	72.75	-5.0	681.40	1
GRID	535	1	63.40	5.0	681.40	1
GRID	536	1	63.40	-5.0	681.40	1
GRID	537	1	46.00	5.0	681.40	1
GRID	538	1	46.00	-5.0	681.40	1
GRID	539	1	29.75	5.0	681.40	1
GRID	540	1	29.75	-5.0	681.40	1
GRID	541	1	45.00	3.612034065.00	1	1
GRID	542	1	45.00	-5.0	665.00	1
GRID	543	1	23.65	2.356371660.00	1	1
GRID	544	1	23.65	-5.0	660.00	1
GRID	545	1	72.75	5.0	650.00	1
GRID	546	1	72.75	-5.0	650.00	1
GRID	547	1	63.40	5.0	650.00	1
GRID	548	1	63.40	-5.0	650.00	1
GRID	549	1	50.00	3.750653635.00	1	1
GRID	550	1	50.00	-5.0	635.00	1
GRID	551	1	37.50	3.334368645.00	1	1
GRID	552	1	37.50	-5.0	645.00	1
GRID	553	1	18.70	1.658405642.50	1	1
GRID	554	1	18.70	-5.0	642.50	1
GRID	555	1	72.75	5.0	620.00	1
GRID	556	1	72.75	-5.0	620.00	1
GRID	557	1	63.40	5.0	620.00	1
GRID	558	1	63.40	-5.0	620.00	1
GRID	559	1	50.00	3.750653615.00	1	1
GRID	560	1	50.00	-5.0	615.00	1
GRID	561	1	30.00	2.917795620.00	1	1
GRID	562	1	30.00	-5.0	620.00	1
GRID	563	1	13.00	0.190323622.50	1	1
GRID	564	1	13.00	-5.0	622.50	1
GRID	565	1	72.75	5.0	590.00	1
GRID	566	1	72.75	-5.0	590.00	1
GRID	567	1	63.40	5.0	590.00	1
GRID	568	1	63.40	-5.0	590.00	1
GRID	569	1	50.00	3.750653590.00	1	1
GRID	570	1	50.00	-5.0	590.00	1
GRID	571	1	30.00	2.917795592.50	1	1
GRID	572	1	30.00	-5.0	592.50	1
GRID	573	1	13.00	0.190323595.00	1	1
GRID	574	1	13.00	-5.0	595.00	1
GRID	575	1	72.75	5.0	560.00	1
GRID	576	1	72.75	-5.0	560.00	1
GRID	577	1	63.40	5.0	560.00	1
GRID	578	1	63.40	-5.0	560.00	1
GRID	579	1	50.00	3.750653560.00	1	1
GRID	580	1	50.00	-5.0	560.00	1
GRID	581	1	32.50	3.078027565.00	1	1
GRID	582	1	32.50	-5.0	565.00	1
GRID	583	1	13.00	0.190323570.00	1	1
GRID	584	1	13.00	-5.0	570.00	1
GRID	585	1	72.75	5.0	530.00	1
GRID	586	1	72.75	-5.0	530.00	1
GRID	587	1	63.40	5.0	540.00	1
GRID	588	1	63.40	-5.0	540.00	1
GRID	589	1	52.50	3.610345542.50	1	1
GRID	590	1	52.50	-5.0	542.50	1
GRID	591	1	35.00	3.215357548.50	1	1
GRID	592	1	35.00	-5.0	548.50	1
GRID	593	1	13.00	0.190323552.50	1	1
GRID	594	1	13.00	-5.0	552.50	1
GRID	595	1	71.25	5.0	522.80	1
GRID	596	1	71.25	-5.0	522.80	1
GRID	597	1	63.40	5.0	528.20	1
GRID	598	1	63.40	-5.0	528.20	1
GRID	599	1	68.70	5.0	516.90	1
GRID	600	1	68.70	-5.0	516.90	1
GRID	601	1	60.55	5.0	522.45	1
GRID	602	1	60.55	-5.0	522.45	1
GRID	603	1	46.00	3.438497532.50	1	1
GRID	604	1	46.00	-5.0	532.50	1
GRID	605	1	13.00	0.190323540.00	1	1

Table I (Continued)

GRID	606	1	13.00	-5.0	540.00	1
GRID	607	1	13.00	0.190323525	525.00	1
GRID	608	1	13.00	-5.0	525.00	1
GRID	609	1	13.00	0.190323510	510.50	1
GRID	610	1	13.00	-5.0	510.50	1
GRID	611	1	63.20	5.0	509.50	1
GRID	612	1	63.20	-5.0	509.50	1
GRID	613	1	56.00	5.0	510.00	1
GRID	614	1	56.00	-5.0	510.00	1
GRID	615	1	40.00	3.438497525	525.00	1
GRID	616	1	40.00	-5.0	525.00	1
GRID	617	1	24.60	2.396921525	525.00	1
GRID	618	1	24.60	-5.0	525.00	1
GRID	619	1	21.00	2.024739517	517.50	1
GRID	620	1	21.00	-5.0	517.50	1
GRID	621	1	19.00	1.711230510	510.50	1
GRID	622	1	19.00	-5.0	510.50	1
GRID	623	1	53.30	5.0	500.90	1
GRID	624	1	53.30	-5.0	500.90	1
GRID	625	1	47.50	5.0	509.10	1
GRID	626	1	47.50	-5.0	509.10	1
GRID	627	1	40.40	5.0	493.95	1
GRID	628	1	40.40	-5.0	493.95	1
GRID	629	1	35.90	5.0	503.00	1
GRID	630	1	35.90	-5.0	503.00	1
GRID	631	1	26.60	5.0	489.45	1
GRID	632	1	26.60	-5.0	489.45	1
GRID	633	1	24.00	5.0	499.20	1
GRID	634	1	24.00	-5.0	499.20	1
GRID	635	1	13.00	5.0	498.30	1
GRID	636	1	13.00	-5.0	498.30	1
GRID	637	1	13.0	5.0	487.25	1
GRID	638	1	13.0	-5.0	487.25	1
GRID	639	1	10.25	5.0	487.25	1
GRID	640	1	10.25	-5.0	487.25	1
GRID	641	1	0.50	5.0	481.70	1
GRID	642	1	0.50	-5.0	481.70	1
GRID	643	1	10.25	5.0	521.70	1
GRID	644	1	10.25	-5.0	521.70	1
GRID	645	1	0.50	5.0	521.70	1
GRID	646	1	0.50	-5.0	521.70	1
GRID	647	1	72.75	5.0	522.50	1
GRID	648	1	72.75	-5.0	522.50	1
MAT1	100	10.00E+0		0.30	.0003	
MAT1	260	30.00E+0		0.28	.000405	
MAT1	300	410.0		0.49	1.598E-4	0.35
MAT1	400	6000.		0.49	1.000E-4	0.30
PARAM	CTYPL	DIR				
PARAM	COUPMASS1					
PARAM	DECOMUFT2					
PARAM	N	18				
PARAM	G	.04				
PARAM	KMAX	0				
PARAM	NLOAD	10				
PBAR	501	200	1.16	.0087	1.44	
PBAR	502	200	1.16	.0087	1.44	
PBAR	503	200	1.50	.045	0.78	
PQUAD2	10	200	0.25	0.0	39	100 0.50 0.0
PQUAD2	40	100	0.625	0.0		
PQUAD2	42	200	1.00	0.0		
PQUAD2	43	200	1.50	0.0		
PQUAD2	44	200	1.25	0.0		
PQUAD2	45	200	1.00	0.0		
PQUAD2	46	200	.40	.0		
PQUAD2	47	200	.362	.0		
PQUAD2	48	200	0.40	0.0		
PQUAD2	49	200	0.75	0.0		
PQUAD2	50	200	0.375	0.0		
PQUAD2	52	200	.52	.0		
PQUAD2	54	200	0.25	0.0		
PQUAD2	56	200	0.30	0.0		
PQUAD2	58	200	0.60	0.0		
PQUAD2	60	200	.52	.0		
PQUAD2	62	200	.52	.0		
PQUAD2	63	200	.477	.0		
PQUAD2	64	200	.417	.0		
PQUAD2	65	200	.365	.0		

Table I (Continued)

PQUAD2	66	200	.349	.0					
PQUAD2	67	200	.379	.0					
PQUAD2	68	200	.411	.0					
PQUAD2	69	200	1.35	.0					
PQUAD2	70	200	2.30	.0					
PQUAD2	71	200	0.80	0.0					
PQUAD2	72	200	0.72	0.0					
PQUAD2	73	200	0.72	0.0					
PQUAD2	521	200	.62	.0					
RLOAD1	1	801						1000	
RLOAD1	2	802						1000	
RLOAD1	3	803						1000	
RLOAD1	4	804						1000	
RLOAD1	5	805						1000	
RLOAD1	6	806						1000	
RLOAD1	7	807						1000	
RLOAD1	8	808						1000	
RLOAD1	9	809						1000	
RLOAD1	10	810						1000	
SPC1	39	456	103	THRU				106	
SPC1	39	456	109	THRU				112	
SPC1	39	456	115	THRU				118	
SPC1	39	456	121	THRU				124	
SPC1	39	456	131	THRU				136	
SPC1	39	456	143	THRU				148	
SPC1	39	456	155	THRU				160	
SPC1	39	456	167	THRU				172	
SPC1	39	456	177	THRU				182	
SPC1	39	456	187	THRU				192	
SPC1	39	456	195	THRU				200	
SPC1	39	456	207	THRU				212	
SPC1	39	456	217	THRU				222	
SPC1	39	456	303	THRU				308	
SPC1	39	456	311	THRU				316	
SPC1	39	456	319	THRU				324	
SPC1	39	456	327	THRU				332	
SPC1	39	456	335	THRU				340	
SPC1	39	456	343	THRU				348	
SPC1	39	456	351	THRU				356	
SPC1	39	456	359	THRU				364	
SPC1	39	456	367	THRU				372	
SPC1	39	456	403	THRU				408	
SPC1	39	456	411	THRU				416	
SPC1	39	456	419	THRU				424	
SPC1	39	456	427	THRU				432	
SPC1	39	456	435	THRU				440	
SPC1	39	456	443	THRU				448	
SPC1	39	456	451	THRU				456	
SPC1	39	456	459	THRU				464	
SPC1	39	456	467	THRU				472	
SPC1	39	456	503	THRU				508	
SPC1	39	456	511	THRU				516	
SPC1	39	456	519	THRU				524	
SPC1	39	456	527	THRU				532	
SPC1	39	456	535	THRU				544	
SPC1	39	456	547	THRU				554	
SPC1	39	456	557	THRU				564	
SPC1	39	456	567	THRU				574	
SPC1	39	456	577	THRU				584	
SPC1	39	456	587	THRU				594	
SPC1	39	456	601	THRU				610	
SPC1	39	456	613	THRU				622	
SPC1	39	456	633	THRU				636	
SPC1	39	456	127	128		598	625	626	
SPC1	39	456	629	630					
SPC1	39	6	37	38		645	646		
TABLED1	1000								+TU1
+TU1	0.0	1.0	400.0	1.0	ENDT				
TABLED1	2000								+TR1
+TR1	0.0	0.0	10.0	0.6293	15.0	0.9951	20.0	1.3659	+TR2
+TR2	30.0	2.1024	40.0	2.8390	50.0	3.5756	ENDT		
TABLED1	2001								+T11
+T11	0.0	0.0	10.0	0.6420	15.0	0.9737	20.0	1.3005	+T12
+T12	30.0	1.9590	40.0	2.6176	50.0	3.2761	ENDT		
ENDDATA									

**
**

TABLE II - NASTRAN CASE CONTROL DECK FOR OBTAINING UNIT LOAD
SOLUTION FOR THE SRM CYCLIC SYMMETRY MODEL

TITLE # FULL MOTOR MODEL AT F=15.2456 HZ
LINE # 72
MAXLINES # 100000
ECHO # BOTH
FREQ # 1
SDAMP # 2000
SET 5 # 21,101,113,125,149,173,203,205,206,213,309,325,409,457,525,
585,623,641,647,648
DISPLACEMENT # 5
SPC # 39
SUBCASE 1
LABEL # SEGMENT 1-R
DLUAD # 1
SUBCASE 2
LABEL # SEGMENT 1-L
SUBCASE 3
LABEL # SEGMENT 2-R
SUBCASE 4
LABEL # SEGMENT 2-L
SUBCASE 5
LABEL # SEGMENT 3-R
SUBCASE 6
LABEL # SEGMENT 3-L
SUBCASE 7
LABEL # SEGMENT 4-R
SUBCASE 8
LABEL # SEGMENT 4-L
SUBCASE 9
LABEL # SEGMENT 5-R
SUBCASE 10
LABEL # SEGMENT 5-L
SUBCASE 11
LABEL # SEGMENT 6-R
SUBCASE 12
LABEL # SEGMENT 6-L
SUBCASE 13
LABEL # SEGMENT 7-R
SUBCASE 14
LABEL # SEGMENT 7-L
SUBCASE 15
LABEL # SEGMENT 8-R
SUBCASE 16
LABEL # SEGMENT 8-L
SUBCASE 17
LABEL # SEGMENT 9-R
SUBCASE 18
LABEL # SEGMENT 9-L
SUBCASE 19
LABEL # SEGMENT 10-R
SUBCASE 20
LABEL # SEGMENT 10-L
SUBCASE 21
LABEL # SEGMENT 11-R
SUBCASE 22
LABEL # SEGMENT 11-L
SUBCASE 23
LABEL # SEGMENT 12-R
SUBCASE 24
LABEL # SEGMENT 12-L
SUBCASE 25
LABEL # SEGMENT 13-R
SUBCASE 26
LABEL # SEGMENT 13-L
SUBCASE 27
LABEL # SEGMENT 14-R
SUBCASE 28
LABEL # SEGMENT 14-L
SUBCASE 29
LABEL # SEGMENT 15-R

Table II (Continued)

SUBCASE 30
LABEL # SEGMENT 15-L
SUBCASE 31
LABEL # SEGMENT 16-R
SUBCASE 32
LABEL # SEGMENT 16-L
SUBCASE 33
LABEL # SEGMENT 17-R
SUBCASE 34
LABEL # SEGMENT 17-L
SUBCASE 35
LABEL # SEGMENT 18-R
SUBCASE 36
LABEL # SEGMENT 18-L
SUBCASE 37
LABEL # SEGMENT 1-F
DLOAD # 2
SUBCASE 38
LABEL # SEGMENT 1-L

SUBCASES 39 THROUGH 350 ARE REPETITIVE AND WERE
OMITTED FOR BREVITY

SUBCASE 351
LABEL # SEGMENT 14-R
SUBCASE 352
LABEL # SEGMENT 14-L
SUBCASE 353
LABEL # SEGMENT 15-R
SUBCASE 354
LABEL # SEGMENT 15-L
SUBCASE 355
LABEL # SEGMENT 16-R
SUBCASE 356
LABEL # SEGMENT 16-L
SUBCASE 357
LABEL # SEGMENT 17-R
SUBCASE 358
LABEL # SEGMENT 17-L
SUBCASE 359
LABEL # SEGMENT 18-R
SUBCASE 360
LABEL # SEGMENT 18-L
BEGIN BULK

TABLE III - NASTRAN EXECUTIVE CONTROL DECK FOR THE SRM CYCLIC SYMMETRY ANALYSIS


```
NASTRAN CONFIG=9,SYSTEM(31)=4096,SYSTEM(45)=64
ID SHUTTLE SRM
CHKPNT YES
TIME 900
APP DISP
DIAG 5,6
DIAG 8,13,14,21,22
SOL 8,1 $ FREQUENCY RESPONSE
$- CYCLIC TRANSFORMATION - FREQUENCY RESPONSE -----00000010
$ 12/01/73 R I C I D F O R M A T & / SERIES M 00000020
$ / R L H V E R S I O N 00000030
$ CASE CONTROL INPUT 00000040
$ A SUBCASE IS USED FOR EACH SUBSTRUCTURE AND LOADING CONDITION. 00000050
$ ALL MPC AND SPC REQUESTS MUST BE ABOVE THE SUBCASE LEVEL. 00000060
$ 00000070
$ BULK DATA INPUT 00000080
$ PARAMETERS USED ARE... 00000090
$ CTYPE %REQUIRED< ROT # ROTATIONAL 00000100
$ DIH # DIHEDRAL 00000110
$ DSYM # DIH PLUS DEFORMATION SYMMETRY 00000120
$ DANT # DIH PLUS DEFORMATION ANTISYMMETRY 00000130
$ N %REQUIRED< NUMBER OF SEGMENTS 00000140
$ KMIN %DEFAULT 0 < MIN RANGE OF CYCLIC INDEX K 00000150
$ KMAX %DEFAULT -1< MAX RANGE OF CYCLIC INDEX K %-1 IMPLIES ALL< 00000160
$ CYCIO %DEFAULT 0< INPUT/OUTPUT, &1 # PHYSICAL, -1 # SYM CUMP 00000170
$ CYCSEQ%DEFAULT -1< MATRIX ELEMENT SEQUENCE, 1 # SEPARATE 00000180
$ -1 # ALTERNATING 00000190
$ NLOAD %DEFAULT 0< NUMBER OF LOADING CONDITIONS 00000200
$ NOKPRT%DEFAULT -1< IF &1 K WILL BE OUTPUT AT THE TOP OF LOOP 00000210
$ 00000220
$ CYJOIN BULK DATA CARDS ARE REQUIRED. 00000230
$ 00000240
$ THE MODEL MUST CONTAIN K4 STRUCTURAL DAMPING %FOR FREQ DEP MATL< 00000250
$ TWO TABLEX,TR%K AND T1%K, ARE SELECTED IN CASE CONTROL VIA 00000260
$ SDAMP %THE ID OF TR IS SELECTED, THE ID OF T1 MUST BE ONE LARGER< 00000270
$ THE STIFFNESS MATRIX %WITH STRUCTURAL DAMPING< WILL BE 00000280
$ K * % 1. & 1*G < & K4 * % TR%K & 1*T1%K < 00000290
$ WHERE K # STIFFNESS MATRIX, G # PARAM OVERALL DAMPING 00000300
$ 00000310
$ THE ANALYSIS WILL LOOP THRU A RANGE OF THE CYCLIC INDEX K # KMIN,KMAX 00000320
$ 00000330
$ ALTER 2 00000340
$ FILE UXVF#APPEND $ 00000350
$ COND ERRORN,N $ IF USER HAS NOT SPECIFIED N %DEFAULT # -1< 00000360
$ COND FIND,KMAX $ 00000370
$ JUMP KNOWN $ 00000380
$ LABEL FIND $ 00000390
$ PARAM //C,N,DIV/V,Y,KMAX#-1/V,Y,N/C,N,2 $ 00000400
$ LABEL KNOWN $ 00000410
$ PARAM //C,N,NUP/V,Y,CYCIO#1/V,Y,NOKPRT#-1 $ 00000420
$ ALTER 92 00000430
$ GPCYC GLOM4,EQDYN,USED/CYCDU/V,Y,CTYPE/V,N,NOCU $ DATA FOR CYC12 00000440
$ CHPNT CYCDU $ 00000450
$ ALTER 129,129 $ 00000460
$ PURGE K2DD/NOK2PP/M2DD/NUM2PP/D2DD/NOB2PP $ 00000470
$ ALTER 133,133 00000480
$ GKAD USETD,GM,GU,KAA,BAA,MAA, ,K2PP,M2PP,B2PP/KDD,BDD,BDD,GMU, 00000490
$ GDD,K2DD,M2DD,B2DD/C,N,FREQRESP/C,N,DISP/C,N,DIRECT/C,Y,G#0,0/ 00000500
$ C,N,0,0/C,N,G,0/V,N,NOK2PP/V,N,NUM2PP/V,N,NUB2PP/ V,N,MPCF1/ 00000510
$ V,N,SINGLE/V,N,UMIT/V,N,NOUE/C,N,-1 /V,N,NUBGG/V,N,NDEK2/C, 00000520
$ N,-1 $ REMOVE K4 00000530
$ ALTER 139,139 $ ACTUALLY ALTER 139,141 00000540
$ EQUIV K4AA,K4DE/NOUE $ 00000550
$ CHPNT K4DD $ 00000560
$ COND LBLNOUE,NOUE $ 00000570
$ VEC USETD/EPV/C,N,D/C,N,A/C,N,E $ 00000580
$ MERGE K4AA,,,EPV,/K4DD $ 00000590
$ CHPNT K4DD $ 00000600
$ LABEL LBLNOUE $ 00000610
```

Table III (Continued)

FRLG	CASEXX, USETD, DLI, FRL, GMD, GDD, DIT, ZPPF, PSF, PDF, FOL, PHE/	00000620
	C, N, DIRECT \$ COMPUTE LOADS	00000630
CHKPNT	PPF, PSF, PLF, FOL \$	00000640
EQUIV	PPF, PEF/NUSET \$	00000650
CHKPNT	PDF \$	00000660
EQUIV	PDF, PXF/CYCID \$	00000670
CHKPNT	PDF \$	00000680
CND	LCYC1, CYCID \$ IF %CYCID.GE.0< TRANSFORM TO SYMMETRIC COMPONENTS	00000690
CYCT1	HDF/PXF, CCYCF/V, Y, CTYPE/Z, N, FURE/V, Y, N/V, Y, KMAX/V, Y, NLOAD/	00000700
	V, Y, KMIN \$	00000710
CHKPNT	PDF \$	00000720
LABEL	LCYC1 \$	00000730
PARAM	Z/C, N, ADD/V, N, K/Z, N, O/V, Y, KMIN#0 \$ INITIALIZE K # KMIN	00000740
LABEL	TOPCYC \$\$\$\$\$\$\$\$\$ LOOP ON K \$	00000750
CND	NGKPT, NGKPT \$	00000760
PRTPARM	Z/C, N, O/Z, N, K \$	00000770
LABEL	NGKPT \$	00000780
ALTER 140, 140		00000790
CYCT2	CYDD, KDD, MDD, PKF, LDD, K4DD/KKKF, MKKF, PKF, DKKF, K4KKF/Z, ...	00000800
	FOREFREQ/V, Y, N#-1/V, N, K/V, Y, CYCSEQ#-1/V, Y, NLOAD#1/V, N, NCGU/	00000810
	V, Y, KMAX/V, Y, KMIN \$	00000820
CHKPNT	KKKF, MKKF, PKF, DKKF, K4KKF \$	00000830
FRRDI	CASEXX, DIT, KKKF, BKKF, MKKF, K4KKF, PKF, FRL, FOL/UKVF/Z, N, DIRECT/	00000840
	V, N, NGINCU/Z, Y, DICUMPT#1 \$	00000850
CHKPNT	UKVF \$	00000860
ALTER 141, 141		00000870
CYCT2	CYDD, ..., UKVF, ..., UXVF, ..., Z, N, BACKFREQ/V, Y, N/V, N, K/V, Y, CYCSEQ/V,	00000880
	Y, NLOAD/V, N, NCGU/V, Y, KMAX/V, Y, KMIN \$	00000890
CHKPNT	UXVF \$	00000900
PARAM	Z/C, N, ADD/V, N, K/V, N, K/Z, N, 1 \$ K # K & 1	00000910
PARAM	Z/C, N, SUB/V, N, DONE/V, Y, KMAX/V, N, K \$	00000920
CND	LCYC2, DONE \$ IF K.GT. KMAX< EXIT LOOP	00000930
REPT	TOPCYC, 100 \$	00000940
JUMP	ERROR1 \$	00000950
LABEL	LCYC2 \$	00000960
EQUIV	UXVF, UDVF/CYCID \$	00000970
CHKPNT	UDVF \$	00000980
CND	LCYC3, CYC1L \$ IF %CYCID.GE.0< TRANSFORM TO PHYSICAL VARIABLES	00000990
CYCT1	UXVF/UDVF, CCYCF/V, Y, CTYPE/Z, N, BACK/V, Y, N/V, Y, KMAX/V, Y, NLOAD/	00010000
	V, Y, KMIN \$	00010010
CHKPNT	UDVF \$	00010020
\$		
OUTPUT2	UDVF, ..., Z/C, N, -1/Z, N, 17/Z, N, #WANG \$	00001030
LABEL	LCYC3 \$	00001040
\$		00001050
ALTER 199		00001060
LABEL	ERRORN \$ FAILED TO SPECIFY PARAM N.GT.0	00001070
PRTPARM	Z/C, N, O/Z, N, N \$ END OF ALTER	00001080
ENDALTER		
CEND		

A relatively long computer run time was anticipated for the unit load solutions. Therefore, an effort was made to reduce the anticipated run time. The method investigated for a reduction in run time was the use of a cyclic index, K , less than K_{\max} . When the Mac-Neal-Schwendler Company presented the modified NASTRAN program to Hercules, they stated that some problems could probably be solved with sufficient accuracy with a cyclic index less than the maximum value. During the Component Vibration Program, Hercules investigated the possibility of reducing the cyclic index by running real eigenvalue solutions. The conclusion was that all K indices were required for the particular motor being studied to obtain all natural frequencies up to at least 500 Hz and probably for higher frequencies as well. Based on that study, all cyclic indices were used for the analyses performed during the component vibration program.

For frequency response type solutions, a more applicable way to study the need for high values of the K index is to conduct frequency response type solutions with various K values. One section of the SRM model consisting of 15 propellant elements and 9 case elements was analyzed for $K = 3$, $K = 6$, and $K = 9$. The value $K = 9$ is the maximum value for the 36 slice SRM finite element grid. Some results from these three analyses are shown in Table IV. Based on the results of the comparison analyses, the decision was made to use a $K = 6$ in the main analysis. The $K = 6$ results were judged to be sufficiently accurate representations of the $K = 9$ solutions. Using fewer than the maximum number of cyclic indices in a solution is similar to omitting some of the higher frequency modes to reduce degrees of freedom of the system when modal coordinates are used to solve a problem.

As mentioned above, only 10 unit loads were applied for the SRM receptance matrix, $[R_{SRM}]$, calculation run. To obtain the R_{SRM} matrix more directly, three loads would have been applied, one at a time, to each of the 36 nodes at the SRM/Nose cone interface. Instead of obtaining $3 \times 36 = 108$ solutions, the results from six unit loads at two nodes were used to obtain all required information. The results of applying loads at node 1 (Fig. 3) could be rotated to apply to loads at any other odd numbered node. For example, the radial response at node six due to a unit axial load at node three would be the same as the radial response at node 4 with the unit axial load applied at node 1. The responses due to loads applied at nodes 1 and 2 were rotated as required by using PARTITION and MERGE operations in a DMAP program. The UDVF data block was operated on in the DMAP program to obtain the desired receptance matrix. The DMAP program used consisted of about 300 DMAP statements and the program required three separate runs to complete due to NASTRAN program limitations. The matrix $[R_{SRM}]$ is a complex matrix of order 112. The large $[R_{SRM}]$ matrix is not included in this report.

A separate computer run was made to calculate the $\{U_0\}_{SRM}$ vector. Since applied loads were symmetric, the run was made with cyclic index $K = 0$. Using a 500K core, the CPU time was 70 minutes and the total run time was about 83 minutes. As in the previous case, a DMAP alter was used to write the UDVF data block on tape. A separate DMAP program was used to form $\{U_0\}_{SRM}$ from the

TABLE IV-FREQUENCY RESPONSE DISPLACEMENTS FOR THREE DIFFERENT VALUES FOR THE CYCLIC INDEX K, (K = 3, K = 6, AND K_{MAX} = 9)

SEGMENT 1-R		COMPLEX DISPLACEMENT VECTOR						
FREQUENCY = 1.524560E 01		(REAL/IMAGINARY)						
POINT ID.	TYPE	T1	T2	T3	R1	R2	R3	
<u>TEST MODEL FOR KMAX#3</u>								
205	G	7.166108E-08	-7.477267E-07	-3.045188E-06	-3.146822E-09	6.616563E-08	-8.316366E-09	
		-1.306287E-07	-1.625193E-06	-1.515271E-06	-8.543155E-10	3.116781E-08	-1.589042E-08	
206	G	9.237641E-08	-7.323066E-07	-2.907410E-06	-1.800614E-08	6.285683E-08	-7.016652E-09	
		-7.244475E-08	-1.644541E-06	-1.458909E-06	-8.028529E-09	2.969269E-08	-1.610388E-08	
317	G	-7.428835E-06	-1.071028E-06	-2.803330E-06	6.430363E-08	6.888052E-08	-1.120411E-08	
		-3.488169E-06	-1.618133E-06	-1.503684E-06	-1.931287E-08	-2.581336E-09	-2.903942E-08	
318	G	-4.959053E-06	-2.173022E-06	-2.640450E-06	2.681718E-08	-8.368306E-08	3.848291E-08	
		-3.612518E-06	-2.235774E-06	-1.454430E-06	1.490769E-08	2.290529E-08	8.460351E-09	
<u>TEST MODEL FOR KMAX#6</u>								
205	G	4.288140E-08	-7.449726E-07	-3.100956E-06	-4.022279E-09	7.893107E-08	-8.192075E-09	
		-2.379936E-07	-1.617913E-06	-1.651073E-06	1.742043E-08	8.101688E-08	-1.929699E-08	
206	G	6.652181E-08	-7.338899E-07	-2.964317E-06	-1.957518E-08	7.377542E-08	-6.769447E-09	
		-1.932053E-07	-1.648361E-06	-1.610436E-06	-1.576734E-08	8.616877E-08	-1.462936E-08	
317	G	-7.009246E-06	-1.460219E-06	-2.801001E-06	5.644200E-07	6.749013E-08	2.928855E-07	
		-1.312000E-05	-3.028721E-07	-1.896462E-06	-2.810990E-07	5.797357E-08	-3.945129E-07	
318	G	-1.046917E-06	-2.186842E-06	-2.557690E-06	-1.230503E-08	-2.031337E-07	6.756871E-09	
		-1.520100E-05	-2.777544E-06	-1.909249E-06	8.389344E-08	1.128189E-07	1.414596E-07	
<u>TEST MODEL FOR KMAX#9</u>								
205	G	4.461379E-08	-7.450626E-07	-3.100310E-06	-7.165010E-09	7.810797E-08	-7.693721E-09	
		-2.383449E-07	-1.617902E-06	-1.651259E-06	1.809167E-08	8.125050E-08	-1.935144E-08	
206	G	7.22275E-08	-7.338783E-07	-2.962454E-06	-1.921828E-08	7.118535E-08	-6.827523E-09	
		-1.939914E-07	-1.648363E-06	-1.610894E-06	-1.584095E-08	8.676346E-08	-1.462126E-08	
317	G	-6.108984E-06	-1.922941E-06	-2.779801E-06	1.397480E-06	5.631955E-08	7.257868E-07	
		-1.338366E-05	-1.869335E-07	-1.901995E-06	-4.949932E-07	6.118654E-08	-4.990727E-07	
318	G	3.934812E-06	-2.132125E-06	-2.451431E-06	-8.226220E-08	-3.050474E-07	-3.640308E-08	
		-1.641781E-05	-2.790764E-06	-1.932970E-06	1.025290E-07	1.345186E-07	1.522931E-07	

UDVF data block. The DMAP program listing is given in Table V. The calculated $\{U_o\}_{SRM}$ vector is shown in Table VI. The complex displacements shown in Table VI represent the response of the SRM cyclic symmetry model to the 15.25 Hz first longitudinal acoustic mode, (see equations 31a and 31b).

Calculation of $[R_{SRB}]$ and $\{U_o\}_{SRB}$

The equations for the calculation of $[R_{SRB}]$ and $\{U_o\}_{SRB}$ are given in Section III of this report, (refer to equations 28 and 37). The DMAP program used for these calculations is shown in Table VII. The resulting data are given in Table VIII.

During the time when computer runs were being made to set up the calculation of $[R_{SRB}]$, the series multiply and add module (SMPYAD) was found to contain an error. The SMPYAD module does not work correctly with complex matrices. Therefore, the DMAP programs all use only the MPYAD multiply and add module.

The Nose Cone receptance matrix was required in the calculation of $[R_{SRB}]$. The Nose Cone receptance matrix was obtained from the 64 degree-of-freedom SRB model furnished by Rockwell. The DMAP program used to calculate the Nose Cone receptance matrix is shown in Table IX. The Nose Cone receptance matrix, $[R_{NCONE}]$ is presented in Table X.

Analysis of the Rockwell ET and Orbiter Models

The Rockwell finite element models are characterized by mass and stiffness matrices. The mass and stiffness matrices for each model were transmitted to Hercules on a computer tape. A FORTRAN program was written to read the Rockwell tape and write a NASTRAN compatible tape.

The NASTRAN tape was used as input to the DMAP sequence shown in Table XI. The DMAP program calculates receptance matrices by applying unit loads to the applicable attachment coordinates. The equations of motion as defined in equation 3 are solved to determine displacement response to the unit loads. A structural damping factor of $g = 0.06$ has been used in the calculations. The receptance matrices obtained from the DMAP program are given in Table XII.

Calculation of the Force and Displacement Response

The displacements and forces at the attach points were calculated by the DMAP program shown in Table XIII, (Refer to equations 13, 14, 42, and 43b). The output from the program shown in Table XIII, is given in Table XIV. The following terminology is used in Table XIV:

TABLE V - DMAP PROGRAM LISTING FOR CALCULATION OF UZRO


```
BEGIN$
$ UZRO EXTRACTOR
INPUT I2 /UDVF,.,.,./C,N,-7/C,N,17/C,N,WANG $
PARTN UDVF,C1R,./,U21,/C,N,1/C,N,3 $
PARTN UDVF,C2R,./,U22,/C,N,1/C,N,3 $
PARTN ULVF,C3R,./,U23,/C,N,1/C,N,3 $
PARTN UDVF,C4R,./,U24,/C,N,1/C,N,3 $
PARTN UDVF,C5R,./,U25,/C,N,1/C,N,3 $
PARTN ULVF,C6R,./,U26,/C,N,1/C,N,3 $
PARTN ULVF,C7R,./,U27,/C,N,1/C,N,3 $
PARTN UDVF,C8R,./,U28,/C,N,1/C,N,3 $
PARTN UDVF,C9R,./,U29,/C,N,1/C,N,3 $
PARTN ULVF,C10R,./,U210,/C,N,1/C,N,3 $
PARTN ULVF,C11R,./,U211,/C,N,1/C,N,3 $
PARTN UDVF,C12R,./,U212,/C,N,1/C,N,3 $
PARTN UDVF,C13R,./,U213,/C,N,1/C,N,3 $
PARTN UDVF,C14R,./,U214,/C,N,1/C,N,3 $
PARTN ULVF,C15R,./,U215,/C,N,1/C,N,3 $
PARTN UDVF,C16R,./,U216,/C,N,1/C,N,3 $
PARTN UDVF,C17R,./,U217,/C,N,1/C,N,3 $
PARTN UDVF,C18R,./,U218,/C,N,1/C,N,3 $
PARTN UZ1,RP1/U11,./C,N,1/C,N,3 $
PARTN UZ2,RP1/U21,./C,N,1/C,N,3 $
PARTN UZ3,RP1/U31,./C,N,1/C,N,3 $
PARTN UZ4,RP1/U41,./C,N,1/C,N,3 $
PARTN UZ5,RP1/U51,./C,N,1/C,N,3 $
PARTN UZ6,RP1/U61,./C,N,1/C,N,3 $
PARTN UZ7,RP1/U71,./C,N,1/C,N,3 $
PARTN UZ8,RP1/U81,./C,N,1/C,N,3 $
PARTN UZ9,RP1/U91,./C,N,1/C,N,3 $
PARTN UZ10,RP1/U101,./C,N,1/C,N,3 $
PARTN UZ11,RP1/U111,./C,N,1/C,N,3 $
PARTN UZ12,RP1/U121,./C,N,1/C,N,3 $
PARTN UZ13,RP1/U131,./C,N,1/C,N,3 $
PARTN UZ14,RP1/U141,./C,N,1/C,N,3 $
PARTN UZ15,RP1/U151,./C,N,1/C,N,3 $
PARTN UZ16,RP1/U161,./C,N,1/C,N,3 $
PARTN UZ17,RP1/U171,./C,N,1/C,N,3 $
PARTN UZ18,RP1/U181,./C,N,1/C,N,3 $
PARTN UZ1,RP2/U12,./C,N,1/C,N,3 $
PARTN UZ2,RP2/U22,./C,N,1/C,N,3 $
PARTN UZ3,RP2/U32,./C,N,1/C,N,3 $
PARTN UZ4,RP2/U42,./C,N,1/C,N,3 $
PARTN UZ5,RP2/U52,./C,N,1/C,N,3 $
PARTN UZ6,RP2/U62,./C,N,1/C,N,3 $
PARTN UZ7,RP2/U72,./C,N,1/C,N,3 $
PARTN UZ8,RP2/U82,./C,N,1/C,N,3 $
PARTN UZ9,RP2/U92,./C,N,1/C,N,3 $
PARTN UZ10,RP2/U102,./C,N,1/C,N,3 $
PARTN UZ11,RP2/U112,./C,N,1/C,N,3 $
PARTN UZ12,RP2/U122,./C,N,1/C,N,3 $
PARTN UZ13,RP2/U132,./C,N,1/C,N,3 $
PARTN UZ14,RP2/U142,./C,N,1/C,N,3 $
PARTN UZ15,RP2/U152,./C,N,1/C,N,3 $
PARTN UZ16,RP2/U162,./C,N,1/C,N,3 $
PARTN UZ17,RP2/U172,./C,N,1/C,N,3 $
PARTN UZ18,RP2/U182,./C,N,1/C,N,3 $
PARTN UZ4,RP3/U2061,./C,N,1/C,N,3 $
PARTN UZ7,RP3/U2062,./C,N,1/C,N,3 $
MERGE U11,U12,.,.,RP4/UZ1R/C,N,1/C,N,4/C,N,2 $
MERGE U21,U22,.,.,RP4/UZ2R/C,N,1/C,N,4/C,N,2 $
MERGE U31,U32,.,.,RP4/UZ3R/C,N,1/C,N,4/C,N,2 $
MERGE U41,U42,.,.,RP4/UZ4R/C,N,1/C,N,4/C,N,2 $
MERGE U51,U52,.,.,RP4/UZ5R/C,N,1/C,N,4/C,N,2 $
MERGE U61,U62,.,.,RP4/UZ6R/C,N,1/C,N,4/C,N,2 $
MERGE U71,U72,.,.,RP4/UZ7R/C,N,1/C,N,4/C,N,2 $
MERGE U81,U82,.,.,RP4/UZ8R/C,N,1/C,N,4/C,N,2 $
MERGE U91,U92,.,.,RP4/UZ9R/C,N,1/C,N,4/C,N,2 $
MERGE U101,U102,.,.,RP4/UZ10R/C,N,1/C,N,4/C,N,2 $
MERGE U111,U112,.,.,RP4/UZ11R/C,N,1/C,N,4/C,N,2 $
```

Table V (Continued)

```

MERGE U121,U122,...,RP4/UZ12R/C,N,1/C,N,4/C,N,2 $
MERGE U131,U132,...,RP4/UZ13R/C,N,1/C,N,4/C,N,2 $
MERGE U141,U142,...,RP4/UZ14R/C,N,1/C,N,4/C,N,2 $
MERGE U151,U152,...,RP4/UZ15R/C,N,1/C,N,4/C,N,2 $
MERGE U161,U162,...,RP4/UZ16R/C,N,1/C,N,4/C,N,2 $
MERGE U171,U172,...,RP4/UZ17R/C,N,1/C,N,4/C,N,2 $
MERGE U181,U182,...,RP4/UZ18R/C,N,1/C,N,4/C,N,2 $
MERGE U2061,U2062,...,RP5/UZ19R/C,N,1/C,N,4/C,N,2 $
MERGE UZ1R,UZ2R,...,RP5/UZA/C,N,1/C,N,4/C,N,2 $
MERGE UZA,UZ3R,...,RP7/UZB/C,N,1/C,N,4/C,N,2 $
MERGE UZB,UZ4R,...,RP8/UZC/C,N,1/C,N,4/C,N,2 $
MERGE UZC,UZ5R,...,RP4/UZD/C,N,1/C,N,4/C,N,2 $
MERGE UZD,UZ6R,...,RP10/UZE/C,N,1/C,N,4/C,N,2 $
MERGE UZF,UZ7R,...,RP11/UZF/C,N,1/C,N,4/C,N,2 $
MERGE UZF,UZ8R,...,RP12/UZG/C,N,1/C,N,4/C,N,2 $
MERGE UZG,UZ9R,...,RP13/UZH/C,N,1/C,N,4/C,N,2 $
MERGE UZH,UZ10R,...,RP14/UZI/C,N,1/C,N,4/C,N,2 $
MLRGE UZ1,UZ11R,...,RP15/UZJ/C,N,1/C,N,4/C,N,2 $
MERGE UZJ,UZ12R,...,RP16/UZK/C,N,1/C,N,4/C,N,2 $
MERGE UZK,UZ13R,...,RP17/UZL/C,N,1/C,N,4/C,N,2 $
MERGE UZL,UZ14R,...,RP18/UZM/C,N,1/C,N,4/C,N,2 $
MERGE UZN,UZ15R,...,RP19/UZN/C,N,1/C,N,4/C,N,2 $
MERGE UZN,UZ16R,...,RP20/UZO/C,N,1/C,N,4/C,N,2 $
MERGE UZO,UZ17R,...,RP21/UZP/C,N,1/C,N,4/C,N,2 $
MERGE UZP,UZ18R,...,RP22/UZO/C,N,1/C,N,4/C,N,2 $
MERGE UZO,UZ19R,...,RP23/UZO/C,N,1/C,N,4/C,N,2 $
MATFRN UZRU,.,./ $
OUTPUT2 UZRU,.,./C,N,-1/C,N,15/C,N,UZROTP $
ENDS

```


TABLE VII - DMAP PROGRAM FOR THE CALCULATION OF R(SRB) AND U_z(SRB)


```
INPUTT2 /RMAT,....,/C,N,-7/C,N,17/C,N,RMATTP $
INPUT I2 /RNOSE,....,/C,N,-7/C,N,15/C,N,NOSELTP $
PARTN RMAT,RSFV,/RS11,RS21,RS12,RS22/C,N,-1/C,N,4/C,N,2/C,N,2 $
PARTN RNOSE,RNPV,/RN11,RN21,RN12,RN22/C,N,-1/C,N,4/C,N,2/C,N,2 $
$
FORM ALPHA
MPYAD TFI,RN22,/TRNP1/C,N,0/C,N,1 $
MPYAD RS11,TFI,TRNP1/APR1/C,N,0/C,N,1 $
MPYAD TFI,APR1,/ALPHA/C,N,1/C,N,1 $
$
INVERT ALPHA
SOLVE ALPHA,/ALFINV/C,N,0/C,N,1/C,N,2 /C,N,4 $
$
CHECK INVERSE
MPYAD ALFINV,ALPHA,/UCHK/C,N,0/C,N,1 $
MATPRN UCHK,....,/$
TRNSP TFI/TFI1 $
MPYAD ALFINV,TFI1,/XP1/C,N,0/C,N,1/C,N,0/C,N,2 $
MPYAD TFI,RN21,/XP2/C,N,0/C,N,1/C,N,0/C,N,2 $
MPYAD XP1,XP2,/CT1/C,N,0/C,N,1/C,N,0/C,N,2 $
MPYAD RS12,TEAR,/XP3/C,N,0/C,N,1/C,N,0/C,N,2 $
MPYAD XP1,XP3,/CT2/C,N,0/C,N,1/C,N,0/C,N,2 $
MPYAD RN12,CT1,RN11/R11/C,N,0/C,N,-1/C,N,1/C,N,2 $
MPYAD TEAR,RS21,/XPA/C,N,1/C,N,1/C,N,0/C,N,2 $
MPYAD TFI,CT1,/XP5/C,N,0/C,N,1/C,N,0/C,N,2 $
MPYAD XP4,XP5,/R21/C,N,0/C,N,1/C,N,0/C,N,2 $
MPYAD RN12,CT2,/R12/C,N,0/C,N,1 $
MPYAD TEAR,RS22,/XP6/C,N,1/C,N,1/C,N,0/C,N,2 $
MPYAD XP6,TEAR,/TRT/C,N,0/C,N,1/C,N,0/C,N,2 $
MPYAD TFI,CT2,/XP7/C,N,0/C,N,1/C,N,0/C,N,2 $
MPYAD XP4,XP7,TRT/R22/C,N,0/C,N,-1/C,N,1/C,N,2 $
MERGE R11,R21,R12,R22,RNV,/RSRB/C,N,-1/C,N,4/C,N,2 $
MATPRN RSRB,....,/$
$
CALCULATE UZR0(SRB)
INPUTT2 /UZRU,....,/C,N,-7/C,N,19/C,N,UZRUPT $
TRNSP TEAR/TEART $
MPYAD ALFINV,TFI1,/CT3/C,N,0/C,N,1 $
MPYAD RN12,CT3,/R11/C,N,0/C,N,1 $
MPYAD TEART,RS21,/BS21/C,N,0/C,N,1 $
MATPRN RN12,CT3,R11,BS21,/$
MPYAD BS21,TFI1,/XP8/C,N,0/C,N,1/C,N,0/C,N,2 $
MPYAD XPE,CT3,/RT21/C,N,0/C,N,-1/C,N,0/C,N,2 $
MERGE R11,RT21,TEART,M1VC,M1VR/UZTFM/C,N,1/C,N,4/C,N,2 $
MPYAD UZTFM,UZR0,/UZSRB/C,N,0/C,N,1 $
MATPRN RSRB,UZSRB,....,/$
OUTPUT2 RSRB,UZSRB,....,/C,N,-1/C,N,20/C,N,SRBTAPE $
END$
```


TABLE VII (CONTINUED)

BEGIN	HULK									
DMI	M1VC	0	2	1	1		112	1		
DMI	M1VC	1	109	1.0	1.0	1.0	1.0			
DMI	M1VR	0	2	1	1		6	1		
DMI	M1VR	1	4	1.0	1.0	1.0				
DMI	RMV	0	2	1	1		6	1		
DMI	RMV	1	4	1.0	1.0	1.0				
DMI	RNPV	0	2	1	1		9	1		
DMI	RNPV	1	4	1.0	1.0	1.0	1.0	1.0	+VT1	
+VT1										
LMI	RSPV	0	2	1	1		112	1		
DMI	RSPV	1	109	1.0	1.0	1.0	1.0			
DMI	TBAR	0	2	1	2		4	3		
DMI	TBAR	1	1	-0.866025	-0.50					
DMI	TBAR	2	1	0.5	-0.866025					
DMI	TBAR	3	3	-0.866025	0.5					
DMI	TFT	0	2	1	2		108	6		
DMI	TFT	1	3	1.0	6	1.0	9	1.0	+R11	
+R11	12	1.0	15	1.0	18	1.0	21	1.0	+R12	
+R12	24	1.0	27	1.0	30	1.0	33	1.0	+R13	
+R13	36	1.0	39	1.0	42	1.0	45	1.0	+R14	
+R14	48	1.0	51	1.0	54	1.0	57	1.0	+R15	
+R15	60	1.0	63	1.0	66	1.0	69	1.0	+R16	
+R16	72	1.0	75	1.0	78	1.0	81	1.0	+R17	
+R17	84	1.0	87	1.0	90	1.0	93	1.0	+R16	
+R18	96	1.0	99	1.0	102	1.0	105	1.0	+R19	
+R19	108	1.0								
DMI	TFT	2	1	0.0	-1.0	4	-0.173648	-0.984808	+R21	
+R21	7	-0.342020	-0.939693	10	-0.50	-0.866025	13	-0.642788	+R22	
+R22		-0.766044	-0.766044	-0.642788	19	-0.866025	-0.50	22	+R23	
+R23		-0.939693	-0.342020	-0.954808	-0.173648	28	-1.0	0.0	+R24	
+R24	31	-0.984808	0.173648	34	-0.939693	30	0.342020	37	-0.866025	+R25
+R25	0.50	40	-0.766044	0.642788	43	-0.642788	0.766044	46	+R26	
+R26	-0.50	0.166025	49	-0.342020	0.939693	52	-0.173648	0.984808	+R27	
+R27	55	0.0	1.0	58	0.173648	0.984808	61	0.342020	+R28	
+R28	0.939693	64	0.50	0.866025	67	0.642788	0.766044	70	+R29	
+R29	0.766044	0.642788	73	0.866025	0.50	76	0.939693	0.342020	+R210	
+R210	79	0.984808	0.173648	82	1.0	0.0	85	0.984808	+R211	
+R211	-0.173648	88	0.939693	-0.342020	91	0.866025	-0.50	94	+R212	
+R212	0.766044	-0.642788	97	0.642788	-0.766044	100	0.50	-0.866025	+R213	
+R213	103	0.342020	-0.939693	106	0.173648	-0.984808				
DMI	TFT	3	1	1.0	0.0	4	0.984808	-0.173648	+R31	
+R31	7	0.939693	-0.342020	10	0.866025	-0.50	13	0.766044	+R32	
+R32	-0.642788	16	0.642788	-0.766044	19	0.50	-0.866025	22	+R33	
+R33	0.342020	-0.939693	25	0.173648	-0.984808	28	0.0	-1.0	+R34	
+R34	31	-0.173648	-0.984808	34	-0.342020	-0.939693	37	-0.50	+R35	
+R35	-0.866025	40	-0.642788	-0.766044	43	-0.766044	-0.642788	46	+R36	
+R36	-0.866025	-0.50	49	-0.939693	-0.342020	52	-0.984808	-0.173648	+R37	
+R37	55	-1.0	0.0	58	-0.984808	0.173648	61	-0.939693	+R38	
+R38	0.342020	64	-0.866025	0.50	67	-0.766044	0.642788	70	+R39	
+R39	-0.642788	0.766044	73	-0.50	0.866025	76	-0.342020	0.939693	+R310	
+R310	79	-0.173648	0.984808	82	0.0	1.0	85	0.173648	+R311	
+R311	0.984808	88	0.342020	0.939693	91	0.50	0.866025	94	+R312	
+R312	0.642788	0.766044	97	0.766044	0.642788	100	0.866025	0.50	+R313	
+R313	103	0.939693	0.342020	106	0.984808	0.173648				
DMI	TFT	4	2	72.75	5	72.75	8	72.75	+R41	
+R41	11	72.75	14	72.75	17	72.75	20	72.75	+R42	
+R42	23	72.75	26	72.75	29	72.75	32	72.75	+R43	
+R43	35	72.75	38	72.75	41	72.75	44	72.75	+R44	
+R44	47	72.75	50	72.75	53	72.75	56	72.75	+R45	
+R45	59	72.75	62	72.75	65	72.75	68	72.75	+R46	
+R46	71	72.75	74	72.75	77	72.75	80	72.75	+R47	
+R47	83	72.75	86	72.75	89	72.75	92	72.75	+R48	
+R48	95	72.75	98	72.75	101	72.75	104	72.75	+R49	
+R49	107	72.75								
DMI	TFT	5	3	72.75	6	71.6448	9	68.3626	+R51	
+R51	12	63.0033	15	55.7297	18	46.7628	21	36.3750	+R52	
+R52	24	24.8820	27	12.6329	30	0.0	33	-12.6329	+R53	
+R53	36	-24.8820	39	-36.3750	42	-46.7628	45	-55.7297	+R54	
+R54	48	-63.0033	51	-68.3626	54	-71.6448	57	-72.7500	+R55	

Table VII (Continued)

+R55	60	-71.644863	-68.362666	-63.003369	-55.7297	+R56
+R56	72	-46.762875	-36.375075	-24.882081		-12.6329
+R57	84	0.0	12.6329	24.8820	93	36.3750
+R58	96	46.7628	55.7297	63.0033	105	68.3626
+R59	108	71.6448				+R59
DMI	1F1	6	0.0	12.6329	9	24.8820
+R61	12	36.3750	46.7628	55.7297	21	63.0033
+R62	24	68.3626	71.6448	72.7500	33	71.6448
+R63	36	68.3626	63.0033	55.7297	45	46.7628
+R64	48	36.3750	24.8820	12.6329	57	0.0
+R65	60	-12.632963	-24.882066	-36.375069		-46.7628
+R66	72	-55.729775	-63.003378	-68.362681		-71.6448
+R67	84	-71.644887	-71.644890	-68.362693		-63.0033
+R68	96	-55.729799	-46.7628102	-36.3750105		-24.8820
+R69	108	-12.6329				+R69
ENDDATA						

TABLE VIII - MATRIX $[R_{SRB}]$ AND VECTOR $\{U_0\}_{SRB}$

SRB R-MATRIX CALCULATIONS BASED ON SRM R-MATRIX
 MATRIX RSRB COMPLEX 6 COLUMN X 6 ROW MATRIX
COLUMN 1 ROWS 1 THRU 6

-1.0721E-06+ -2.8316E-07I 2.7638E-07+ -3.8851E-08I 1.0368E-08+ -2.9145E-10I -4.4086E-07+ -8.7521E-08I -3.0532E-09+ -5.0467E-09I
 -4.4093E-07+ -8.6312E-08I

COLUMN 2 ROWS 1 THRU 6

3.2365E-07+ -4.3479E-09I -5.5775E-07+ -5.6597E-08I -8.4758E-09+ 5.1744E-10I -2.0685E-07+ -4.9241E-09I -4.3587E-10+ 1.2155E-09I
 -2.0689E-07+ -6.3766E-09I

COLUMN 3 ROWS 1 THRU 6

1.0584E-08+ -1.3178E-10I -8.3235E-09+ 6.1490E-10I -1.9801E-06+ -5.8202E-08I -2.0559E-08+ 5.2088E-07I -2.5983E-07+ 8.9303E-07I
 2.3942E-08+ -5.2024E-07I

COLUMN 4 ROWS 1 THRU 6

-2.8757E-09+ -2.2556E-10I -1.3411E-08+ -1.8032E-09I -8.7513E-11+ -1.8600E-11I 7.7950E-07+ -2.7705E-07I -4.0438E-07+ -5.3795E-08I
 -1.1821E-07+ 1.6415E-08I

54

COLUMN 5 ROWS 1 THRU 6

-6.2070E-12+ -8.2369E-11I -7.9054E-11+ -2.0327E-11I -1.3300E-08+ -1.8104E-09I -4.0438E-07+ -5.3791E-08I 3.1251E-07+ -3.3918E-07I
 -1.5389E-08+ 6.2032E-08I

COLUMN 6 ROWS 1 THRU 6

-2.8758E-09+ -2.2559E-10I -1.3411E-08+ -1.8032E-09I 5.1428E-11+ 1.5829E-11I -1.1821E-07+ 1.6417E-08I -1.5392E-08+ 6.2040E-08I
 7.7951E-07+ -2.7705E-07I

SRB R-MATRIX CALCULATIONS BASED ON SRM R-MATRIX
 MATRIX USRB COMPLEX 1 COLUMN X 6 ROW MATRIX

COLUMN 1 ROWS 1 THRU 6

7.4050E-04+ -3.9892E-05I -2.4277E-06+ 4.1615E-07I -1.2038E-06+ 1.6081E-07I 5.5987E-05+ -5.3144E-06I -3.0959E-05+ 3.6283E-06I
 5.5958E-05+ -5.6357E-06I

TABLE IX - DMAP PROGRAM FOR R(NOSECONE) CALCULATIONS

```
***  
***  
BEGIN$  
INPUTT2 /KSRBTOT,MSRBTOT,,,/C,N,-7/C,N,15/C,N,ROCKWELL $  
PARTN KSRBTOT,PSV,/,,,,KSRBF/C,N,-1/C,N,2/C,N,2/C,N,2/C,N,2/C,N,2 $  
PARTN MSRBTOT,PVM,/,,,,MSRBF/C,N,-1/C,N,2/C,N,2/C,N,2/C,N,2/C,N,2 $  
MATPRN KSRBF,MSRBF,/,/,/ $  
MPYAD KSRBF,TRN,/KPCONE/C,N,0/C,N,1 $  
MPYAD TRN,KPCONE,/KNCONE/C,N,1/C,N,1 $  
PARTN MSRBF,SMP,/M11,M21,M12,M22/C,N,-1/C,N,2/C,N,2/C,N,2/C,N,2/C,N,2$  
ADD M21,/M321/C,Y,ALPHA=(0.33333,0.0) $  
ADD M12,/M312/C,Y,ALPHA=(0.33333,0.0) $  
ADD M22,/M322/C,Y,ALPHA=(0.33333,0.0) $  
MERGE M11,M321,M312,M322,SMP,/MNCONE/C,N,-1/C,N,2/C,N,2 $  
MATPRN KNCONE,MNCONE,/,/,/ $  
ADD MNCONE,/WMNC/C,Y,ALPHA=(-9.175,9023,0.0) $  
ADD KNCONE,/KNWD/C,Y,ALPHA=(1.0,0.06) $  
ADD WMNC,KNWD/DNUSE/C,Y,ALPHA=(1.0,0.0)/C,Y,BETA=(1.0,0.0) $  
SOLVE DNUSE,FNUSE/DSPN/C,N,1/C,N,1/C,N,2/C,N,4 $  
PARTN DSPN,DPV/,RNUSE,/,/C,N,1/C,N,4/C,N,2/C,N,2 $  
MATPRN RNUSE,/,/,/ $  
OUTPUT2 RNUSE,/,/,/C,N,-1/C,N,17/C,N,NUSETP $  
END$
```


TABLE IX (CONTINUED)

BEGIN BULK									
DMI	DPV	0	2	1	1		17	1	
DMI	DPV	1	9	1.0	1.0	1.0	1.0	1.0	+DP1
+DP1	1.0	1.0	1.0	1.0					
DMI	FNOSE	0	2	1	1		17	9	
DMI	FNOSE	1	9	1.0					
DMI	FNOSE	2	10	1.0					
DMI	FNOSE	3	11	1.0					
DMI	FNOSE	4	12	1.0					
DMI	FNOSE	5	13	1.0					
DMI	FNOSE	6	14	1.0					
DMI	FNOSE	7	15	1.0					
DMI	FNOSE	8	16	1.0					
DMI	FNOSE	9	17	1.0					
DMI	PSV	0	2	1	1		64	1	
DMI	PSV	1	1	1.0	1.0	1.0	1.0	1.0	+PVV
+PVV	1.0	1.0	1.0	1.0	1.0	1.0			
DMI	PVM	0	2	1	1		64	1	
DMI	FVM	1	1	1.0	1.0	1.0	1.0	1.0	+PMM1
+PMM1	1.0	1.0	1.0	1.0	1.0	1.0	1.0	1.0	+PMM2
+PMM2	1.0	1.0	1.0	1.0					
DMI	SMP	0	2	1	1		17	1	
DMI	SMP	1	12	1.0	1.0	1.0	1.0	1.0	+SM1
+SM1	1.0								
DMI	TRN	0	2	1	1		11	17	
DMI	TRN	1	1	1.0					
DMI	TRN	2	2	1.0					
DMI	TRN	3	3	1.0					
DMI	TRN	4	4	1.0					
DMI	TRN	5	5	1.0					
DMI	TRN	6	6	1.0					
DMI	TRN	7	7	1.0					
DMI	TRN	8	8	1.0					
DMI	TRN	9	9	1.0					
DMI	TRN	10	10	1.0					
DMI	TRN	11	11	1.0					
DMI	TRN	12	1	-1.0	5	-1.0	9	-1.0	
DMI	TRN	13	2	-1.0	6	-1.0	10	-1.0	
DMI	TRN	14	3	-1.0	7	-1.0	11	-1.0	
DMI	TRN	15	4	-1.0	8	-1.0	11	78.0	
DMI	TRN	16	3	-323.3387		-202.50011		-84.825	
DMI	TRN	17	2	323.338 6		202.500 9		-78.0	+TM1
+TM1	10	84.825							

ENDDATA

TABLE X - NOSE CONE RECEPTANCE MATRIX

R-MATRIX CALCULATIONS FOR THE NOSE CONE MODEL (APPROX. MASS)
 MATRIX RNOSE COMPLEX 9 COLUMN X 9 ROW MATRIX
COLUMN 1 ROWS 1 THRU 9

-1.2560E-06+ -7.0220E-09I 3.1091E-07+ 4.5565E-10I 1.0863E-08+ -6.5270E-10I -9.4655E-07+ 3.1893E-10I -1.6343E-07+ 7.5151E-10I
 6.5561E-10+ -3.9227E-11I -2.2639E-11+ 1.4847E-12I 1.7871E-11+ -1.0679E-12I -5.1515E-09+ -2.3092E-11I

COLUMN 2 ROWS 1 THRU 9

3.1091E-07+ 4.5565E-10I -6.2048E-07+ -2.9739E-08I -8.6866E-09+ 5.2470E-10I 3.5691E-09+ -2.1891E-10I -7.6465E-07+ -2.6886E-10I
 -5.1701E-10+ 3.1063E-11I 2.5624E-11+ -1.7090E-12I -1.3498E-11+ 8.0814E-13I 3.8589E-09+ 1.3589E-11I

COLUMN 3 ROWS 1 THRU 9

1.0863E-08+ -6.5270E-10I -8.6866E-09+ 5.2470E-10I -2.0388E-06+ -3.0786E-08I 1.6228E-09+ -9.9075E-11I -1.0447E-09+ 6.3159E-11I
 -7.5332E-07+ -9.5495E-10I 1.8343E-08+ 4.0813E-12I -3.5293E-09+ -3.3578E-11I 3.4748E-11+ -2.1161E-12I

COLUMN 4 ROWS 1 THRU 9

-9.4655E-07+ 3.1893E-10I 3.5691E-09+ -2.1891E-10I 1.6228E-09+ -9.9075E-11I -9.3667E-07+ -2.8380E-10I 1.5246E-09+ -9.3537E-11I
 2.8421E-10+ -1.7382E-11I -7.2048E-12+ 4.7317E-13I 8.1479E-12+ -4.9862E-13I -4.7144E-11+ 2.8967E-12I

COLUMN 5 ROWS 1 THRU 9

-1.6343E-07+ 7.5151E-10I -7.6465E-07+ -2.6886E-10I -1.0447E-09+ 6.3159E-11I 1.5246E-09+ -9.3537E-11I -9.1733E-07+ -9.6455E-10I
 -9.0372E-11+ 5.4182E-12I 1.8249E-12+ -1.2178E-13I -2.6899E-12+ 1.6150E-13I -2.4089E-09+ 2.8585E-11I

COLUMN 6 ROWS 1 THRU 9

6.5561E-10+ -3.9227E-11I -5.1701E-10+ 3.1063E-11I -7.5332E-07+ -9.5495E-10I 2.8421E-10+ -1.7382E-11I -9.0372E-11+ 5.4182E-12I
 -9.1500E-07+ -1.0702E-09I 1.2999E-11+ -8.3427E-13I 2.4625E-09+ -3.1848E-11I 3.0177E-12+ -1.8128E-13I

COLUMN 7 ROWS 1 THRU 9

-2.2639E-11+ 1.4847E-12I 2.5624E-11+ -1.7090E-12I 1.8343E-08+ 4.0813E-12I -7.2048E-12+ 4.7317E-13I 1.8249E-12+ -1.2178E-13I
 1.2999E-11+ -8.3427E-13I -2.2714E-10+ -5.7101E-13I 3.2920E-13+ -2.0440E-14I -9.9749E-14+ 6.7867E-15I

COLUMN 8 ROWS 1 THRU 9

1.7871E-11+ -1.0679E-12I -1.3498E-11+ 8.0814E-13I -3.5293E-09+ -3.3578E-11I 8.1479E-12+ -4.9862E-13I -2.6899E-12+ 1.6150E-13I
 2.4625E-09+ -3.1848E-11I 3.2920E-13+ -2.0440E-14I -5.5030E-11+ -9.6259E-13I 8.7384E-14+ -5.2479E-15I

COLUMN 9 ROWS 1 THRU 9

-5.1515E-09+ -2.3092E-11I 3.8589E-09+ 1.3589E-11I 3.4748E-11+ -2.1161E-12I -4.7144E-11+ 2.8967E-12I -2.4089E-09+ 2.8585E-11I
 3.0177E-12+ -1.8128E-13I -9.9749E-14+ 6.7867E-15I 8.7384E-14+ -5.2479E-15I -5.6659E-11+ -8.6345E-13I

TABLE XI - (Continued)

R-MATRIX CALCULATIONS

CARD COUNT	1	2	3	4	5	6	7	8	9	10
1-	DMT	FFI	3	4	5	6	7	8	9	10
2-	DMT	FET	1	1.0	1.0	1.0	1.0	1.0	1.0	1.0
3-	DMT	FET	2	1.0	1.0	1.0	1.0	1.0	1.0	1.0
4-	DMT	FET	3	1.0	1.0	1.0	1.0	1.0	1.0	1.0
5-	DMT	FET	4	1.0	1.0	1.0	1.0	1.0	1.0	1.0
6-	DMT	FET	5	1.0	1.0	1.0	1.0	1.0	1.0	1.0
7-	DMT	FET	6	1.0	1.0	1.0	1.0	1.0	1.0	1.0
8-	DMT	FET	7	1.0	1.0	1.0	1.0	1.0	1.0	1.0
9-	DMT	FET	8	1.0	1.0	1.0	1.0	1.0	1.0	1.0
10-	DMT	FET	9	1.0	1.0	1.0	1.0	1.0	1.0	1.0
11-	DMT	FET	10	1.0	1.0	1.0	1.0	1.0	1.0	1.0
12-	DMT	FETA	11	1.0	1.0	1.0	1.0	1.0	1.0	1.0
13-	DMT	FETA	1	1.0	1.0	1.0	1.0	1.0	1.0	1.0
14-	DMT	FETA	2	1.0	1.0	1.0	1.0	1.0	1.0	1.0
15-	DMT	FETA	3	1.0	1.0	1.0	1.0	1.0	1.0	1.0
16-	DMT	FETA	4	1.0	1.0	1.0	1.0	1.0	1.0	1.0
17-	DMT	FETA	5	1.0	1.0	1.0	1.0	1.0	1.0	1.0
18-	DMT	FETA	6	1.0	1.0	1.0	1.0	1.0	1.0	1.0
19-	DMT	FETA	7	1.0	1.0	1.0	1.0	1.0	1.0	1.0
20-	DMT	FETA	8	1.0	1.0	1.0	1.0	1.0	1.0	1.0
21-	DMT	FETA	9	1.0	1.0	1.0	1.0	1.0	1.0	1.0
22-	DMT	FETA	10	1.0	1.0	1.0	1.0	1.0	1.0	1.0
23-	DMT	FIN	1	1.0	1.0	1.0	1.0	1.0	1.0	1.0
24-	DMT	FIN	2	1.0	1.0	1.0	1.0	1.0	1.0	1.0
25-	DMT	FIN	3	1.0	1.0	1.0	1.0	1.0	1.0	1.0
26-	DMT	FIN	4	1.0	1.0	1.0	1.0	1.0	1.0	1.0
27-	DMT	FIN	5	1.0	1.0	1.0	1.0	1.0	1.0	1.0
28-	DMT	FIN	6	1.0	1.0	1.0	1.0	1.0	1.0	1.0
29-	DMT	FIN	7	1.0	1.0	1.0	1.0	1.0	1.0	1.0
30-	DMT	FOBA	1	1.0	1.0	1.0	1.0	1.0	1.0	1.0
31-	DMT	FOBA	2	1.0	1.0	1.0	1.0	1.0	1.0	1.0
32-	DMT	FOBA	3	1.0	1.0	1.0	1.0	1.0	1.0	1.0
33-	DMT	FOBA	4	1.0	1.0	1.0	1.0	1.0	1.0	1.0
34-	DMT	FORB	1	1.0	1.0	1.0	1.0	1.0	1.0	1.0
35-	DMT	FORB	2	1.0	1.0	1.0	1.0	1.0	1.0	1.0
36-	DMT	FORB	3	1.0	1.0	1.0	1.0	1.0	1.0	1.0
37-	DMT	FORB	4	1.0	1.0	1.0	1.0	1.0	1.0	1.0
38-	DMT	FORB	5	1.0	1.0	1.0	1.0	1.0	1.0	1.0
39-	DMT	PARB	1	1.0	1.0	1.0	1.0	1.0	1.0	1.0
40-	DMT	PARB	2	1.0	1.0	1.0	1.0	1.0	1.0	1.0
41-	DMT	PARB	3	1.0	1.0	1.0	1.0	1.0	1.0	1.0
42-	DMT	PARB	4	1.0	1.0	1.0	1.0	1.0	1.0	1.0
43-	DMT	PET	1	1.0	1.0	1.0	1.0	1.0	1.0	1.0
44-	DMT	PET	2	1.0	1.0	1.0	1.0	1.0	1.0	1.0
45-	DMT	PET	3	1.0	1.0	1.0	1.0	1.0	1.0	1.0
46-	DMT	PETA	1	1.0	1.0	1.0	1.0	1.0	1.0	1.0
47-	DMT	PETA	2	1.0	1.0	1.0	1.0	1.0	1.0	1.0
48-	DMT	PETA	3	1.0	1.0	1.0	1.0	1.0	1.0	1.0
49-	DMT	PETA	4	1.0	1.0	1.0	1.0	1.0	1.0	1.0
50-	DMT	PORB	1	1.0	1.0	1.0	1.0	1.0	1.0	1.0
51-	DMT	PORB	2	1.0	1.0	1.0	1.0	1.0	1.0	1.0
52-	DMT	PVC	1	1.0	1.0	1.0	1.0	1.0	1.0	1.0
53-	DMT	PVC	2	1.0	1.0	1.0	1.0	1.0	1.0	1.0
54-	DMT	PVC	3	1.0	1.0	1.0	1.0	1.0	1.0	1.0
	ENDDATA									

TABLE XII - RECEPTANCE MATRICES CALCULATED FOR THE ROCKWELL MODELS

R-MATRIX CALCULATIONS

MATRIX SRBMAT		%GIND NAME 101 < IS A COMPLEX		6 COLUMN X		6 ROW RECTANG MATRIX.			
COLUMN	ROWS	1 THRU	6	1 THRU	6	1 THRU	6		
7.3798E-086	-7.3629E-061	4.1351E-076	1.1433E-071	7.7816E-096	8.4139E-101	1.6931E-076	3.5097E-081	2.7445E-096	1.6070E-111
1.8980E-076	3.5636E-081								
COLUMN 2		ROWS 6		1 THRU 6		1 THRU 6			
4.1351E-076	1.1433E-071	-7.9966E-076	-2.9395E-071	-9.3798E-071	-2.5707E-091	-4.1962E-076	-8.5878E-081	-5.0806E-096	-1.9124E-101
-4.2094E-076	-6.7221E-081								
COLUMN 3		ROWS 6		1 THRU 6		1 THRU 6			
7.7816E-096	8.4139E-101	-9.3798E-096	-2.5707E-091	-1.7879E-061	-1.1616E-061	4.5752E-076	4.1076E-071	3.2164E-076	5.6025E-071
-4.6139E-076	-4.1209E-071								
COLUMN 4		ROWS 6		1 THRU 6		1 THRU 6			
1.6931E-076	3.5097E-081	-4.1962E-076	-8.5878E-081	4.5752E-076	4.1076E-071	4.0698E-076	-2.5089E-071	-2.5779E-076	-3.0973E-071
4.9451E-086	1.5740E-071								
COLUMN 5		ROWS 6		1 THRU 6		1 THRU 6			
2.7445E-096	1.6070E-111	-5.0806E-096	-1.9124E-101	3.2164E-076	5.6025E-071	-2.5779E-076	-3.0973E-071	1.2774E-076	-5.5882E-071
4.6938E-076	2.9621E-071								
COLUMN 6		ROWS 6		1 THRU 6		1 THRU 6			
1.8980E-076	3.5636E-081	-4.2094E-076	-8.7221E-081	-4.6139E-076	-4.1209E-071	4.9451E-086	1.5740E-071	4.6938E-076	2.9621E-071
4.0762E-076	-2.8134E-071								

THE NUMBER OF NON-ZERO WORDS IN THE LONGEST RECORD # 24

THE DENSITY OF THIS MATRIX IS 100.00 PERCENT.

MATRIX ORBSMAT		%GIND NAME 102 < IS A COMPLEX		5 COLUMN X		5 ROW RECTANG MATRIX.			
COLUMN	ROWS	1 THRU	5	1 THRU	5	1 THRU	5		
7.7453E-066	-2.3629E-061	2.6967E-066	6.5232E-071	-2.7592E-066	-1.0818E-061	5.6631E-086	-6.0888E-091	2.0397E-066	8.2225E-071
COLUMN 2	ROWS 5	1 THRU 5	1 THRU 5	1 THRU 5	1 THRU 5	1 THRU 5	1 THRU 5	1 THRU 5	1 THRU 5
2.6967E-066	6.5232E-071	1.4531E-066	-1.0647E-061	7.2662E-076	5.5218E-071	-1.6749E-086	-5.0276E-091	-5.0977E-076	-1.0267E-071
COLUMN 3		ROWS 5		1 THRU 5		1 THRU 5			
-2.7592E-066	-1.0818E-061	7.2662E-076	5.5218E-071	-9.8510E-076	-9.3572E-071	1.3995E-086	2.2861E-091	9.8428E-076	5.2296E-071
COLUMN 4		ROWS 5		1 THRU 5		1 THRU 5			
5.6631E-086	-6.0888E-091	-1.6749E-086	-5.0276E-091	1.3995E-086	2.2861E-091	2.1695E-076	-1.5321E-081	-6.2017E-086	1.1834E-081
COLUMN 5		ROWS 5		1 THRU 5		1 THRU 5			
2.0397E-066	8.2225E-071	-5.0977E-076	-1.0267E-071	9.8428E-076	5.2296E-071	-6.2017E-086	1.1834E-081	-5.7270E-076	-1.0027E-061

THE NUMBER OF NON-ZERO WORDS IN THE LONGEST RECORD # 20

THE DENSITY OF THIS MATRIX IS 100.00 PERCENT.

TABLE XII - (Continued)

R-MATRIX CALCULATIONS

MATRIX ETSMAT %GIND NAME 103 < IS A COMPLEX 11 COLUMN X 11 ROW RECTANG MATRIX.

COLUMN	1	THRU	ROWS	1	THRU	ROWS				
COLUMN 1	4.7112E-09E	1.1890E-091	4.3989E-10E	3.3737E-08E	8.3327E-091	-1.5412E-03E	-3.7635E-091	-1.2807E-04E	4.5473E-081	7.3665E-091
COLUMN 2	1.0216E-07E	-1.4885E-081	-1.3794E-08E	-7.9818E-08E	9.1853E-091	-1.6357E-10E	-1.2658E-121	-7.0481E-08E	4.5473E-081	7.3665E-091
COLUMN 3	1.1955E-09E	-3.9763E-101								
COLUMN 4	5.6924E-08E	1.4366E-081	-5.3151E-09E	4.0763E-07E	-1.0068E-071	-1.2807E-04E	4.5473E-081	-4.3467E-06E	-5.4944E-071	-8.8995E-081
COLUMN 5	1.2943E-08E	1.7585E-071	1.6667E-07E	9.6442E-07E	-1.1098E-071	1.9763E-09E	1.5294E-111	8.5160E-07E	8.5160E-07E	8.5160E-07E
COLUMN 6	2.2044E-07E	-4.7561E-081	3.6948E-10E	-2.3940E-101	4.5277E-07E	7.9237E-081	1.0216E-07E	-1.4885E-081	-1.2343E-06E	1.7966E-071
COLUMN 7	1.2984E-07E	-1.4293E-081	-8.0107E-08E	5.1407E-081	-6.3172E-07E	2.0132E-071	7.2727E-09E	-2.4779E-091	-7.4020E-08E	1.3646E-071
COLUMN 8	1.9213E-08E	5.7312E-091	-9.7693E-12E	2.1799E-111	6.3782E-08E	-1.4469E-081	-1.3794E-08E	2.7463E-091	1.6667E-07E	-6.2737E-091
COLUMN 9	-6.6731E-08E	7.3232E-091	4.9587E-06E	-3.6078E-071	1.3322E-06E	-1.2509E-071	-2.5163E-07E	1.9366E-081	-1.7456E-07E	-6.2737E-091
COLUMN 10	1.7454E-08E	9.4569E-091	-2.4177E-11E	4.0748E-111	3.7071E-07E	-5.2587E-081	-7.9818E-08E	9.1853E-091	9.6442E-07E	-1.1098E-071
COLUMN 11	-8.0175E-07E	2.0132E-071	1.3322E-06E	-1.2509E-071	5.3831E-07E	-2.0644E-071	-6.0912E-08E	5.4475E-091	-7.5806E-07E	-1.0243E-071
COLUMN 12	8.1803E-07E	-6.9280E-081	-9.0928E-08E	5.6534E-091	-2.1836E-08E	5.8733E-091	4.7112E-09E	-1.1890E-091	-5.6924E-08E	1.4366E-081
COLUMN 13	3.6844E-09E	-8.2372E-101	-1.9213E-08E	5.7312E-091	-1.7454E-08E	9.4569E-091	5.3117E-09E	-8.2213E-101	-6.0946E-09E	5.6709E-091
COLUMN 14	9.0928E-08E	5.6534E-091	4.3666E-07E	-2.6872E-081	5.0318E-11E	3.1834E-111	4.3989E-10E	-3.5264E-111	-5.3151E-09E	4.2609E-101
COLUMN 15	3.6938E-10E	-2.3940E-101	-9.7693E-12E	2.1799E-111	-2.4177E-11E	4.0748E-111	6.8449E-12E	-4.3815E-121	-1.5376E-11E	2.6522E-111
COLUMN 16	5.2356E-12E	-3.9489E-121								
COLUMN 17	-2.1836E-08E	5.8733E-091	5.0318E-11E	3.1834E-111	8.1607E-07E	-9.5282E-081	-3.3737E-08E	8.3327E-091	4.0763E-07E	-1.0068E-071
COLUMN 18	-9.6599E-09E	2.0892E-091	6.3782E-08E	-1.4469E-081	3.7071E-07E	-5.2587E-081	8.8979E-10E	-2.5339E-111	3.2777E-07E	-4.3031E-081
COLUMN 19	5.3117E-09E	-8.2213E-101	6.8449E-12E	-4.3815E-121	8.8979E-10E	-2.5339E-111	-1.6357E-10E	-1.2658E-121	1.9763E-09E	1.5294E-111
COLUMN 20	7.2727E-09E	-2.4779E-091	-2.5163E-07E	1.9366E-081	-6.0912E-08E	5.4475E-091	1.1278E-06E	-6.9367E-081	3.5229E-07E	-2.1687E-081
COLUMN 21	3.4047E-07E	-2.1320E-081								
COLUMN 22	-6.0946E-09E	5.6709E-091	-1.5376E-11E	2.6522E-111	3.2777E-07E	-4.3031E-081	-7.0481E-08E	7.3665E-091	8.5160E-07E	-1.0884E-071
COLUMN 23	7.4020E-08E	1.3646E-071	-1.7456E-07E	-6.2737E-091	-7.5806E-07E	-1.0243E-071	3.5229E-07E	-2.1687E-081	-4.5743E-07E	-1.0884E-071
COLUMN 24	1.7846E-08E	1.5136E-091								
COLUMN 25	3.6464E-09E	-8.2372E-101	5.2356E-12E	-3.9489E-121	-9.6599E-09E	2.0892E-091	2.1195E-09E	-3.9763E-101	-2.5609E-08E	4.8045E-091
COLUMN 26	1.2984E-07E	-1.4293E-081	-8.0107E-08E	5.1407E-081	-6.3172E-07E	1.7585E-071	3.4047E-07E	-2.1320E-081	1.7846E-08E	1.5136E-091
COLUMN 27	1.2196E-06E	-7.4779E-081								

44

THE NUMBER OF NON-ZERO WORDS IN THE LONGEST RECORD *

THE DENSITY OF THIS MATRIX IS 100.00 PERCENT.

TABLE XII - (Continued)

R-MATRIX CALCULATIONS

MATRIX ORRHMAT	%INO NAME	101 < 15 A	COMPLEX	4 COLUMN X	4 ROW	RECTANG	MATRIX.
COLUMN 1	ROWS 1 THRU 4						
-5.7674E-07E	-3.5533E-06I	-6.7636E-07E	-8.4681E-06I	-1.5038E-06E	-4.9102E-07I	-7.8509E-08E	-1.4657E-07I
COLUMN 2	ROWS 1 THRU 4						
-6.7636E-07E	-8.4681E-06I	4.3980E-07E	-2.4439E-07I	-2.1022E-07E	-3.1231E-07I	-3.0786E-07E	-1.0077E-07I
COLUMN 3	ROWS 1 THRU 4						
-1.5038E-06E	-4.9102E-07I	-2.1022E-07E	-3.1231E-07I	-1.1779E-06E	-1.1159E-06I	-7.1764E-07E	-3.5710E-07I
COLUMN 4	ROWS 1 THRU 4						
-7.8509E-08E	-1.4657E-07I	-3.0786E-07E	-1.0077E-07I	-7.1764E-07E	-3.5710E-07I	8.3340E-07E	-3.1540E-07I

THE NUMBER OF NON-ZERO WORDS IN THE LONGEST RECORD # 16

THE DENSITY OF THIS MATRIX IS 100.00 PERCENT.

TABLE XII - (Continued)

R-MATRIX CALCULATIONS

MATRIX ETAMAT %GIND NAME 132 X 15 A COMPLEX 10 COLUMN X 10 ROW RECTANG MATRIX.

COLUMN	1	ROWS	1	THRU	10																
5.9637E-06E	-5.6453E-09I	6.2391E-07E	-1.7526E-07I	6.4607E-07E	1.0099E-07I	7.4643E-06E	-8.3115E-07I	-5.2666E-07E	6.0456E-08I	2.2636E-06E	-1.9643E-07I	2.6541E-06E	-1.4193E-07I	3.5266E-08I	1.6607E-06E	-1.2320E-07I	1.0958E-07E	3.7508E-08I	5.0456E-08I	2.2636E-06E	-1.9643E-07I
-2.2262E-06E	4.7244E-08I	1.5789E-06E	-8.8164E-08I	4.4122E-07E	-1.0483E-07I	2.6541E-06E	-1.4193E-07I	3.5266E-08I	1.6607E-06E	-1.2320E-07I	1.0958E-07E	3.7508E-08I	5.0456E-08I	2.2636E-06E	-1.9643E-07I	3.5266E-08I	1.6607E-06E	-1.2320E-07I	1.0958E-07E	3.7508E-08I	5.0456E-08I
2.7962E-08E	-1.5325E-09I	1.9762E-07E	2.8370E-08I	1.4017E-07E	-1.5765E-08I	5.2656E-07E	6.0456E-08I	3.7508E-08I	1.6607E-06E	-1.2320E-07I	1.0958E-07E	3.7508E-08I	5.0456E-08I	2.2636E-06E	-1.9643E-07I	3.5266E-08I	1.6607E-06E	-1.2320E-07I	1.0958E-07E	3.7508E-08I	5.0456E-08I
5.3834E-07E	-1.1109E-08I	-7.2928E-07E	5.6437E-08I	3.3969E-08I	3.3969E-08I	3.3969E-08I	3.3969E-08I	3.3969E-08I	3.3969E-08I	3.3969E-08I	3.3969E-08I	3.3969E-08I	3.3969E-08I	3.3969E-08I	3.3969E-08I	3.3969E-08I	3.3969E-08I	3.3969E-08I	3.3969E-08I	3.3969E-08I	3.3969E-08I
-1.1281E-08E	-2.6082E-09I	6.3166E-07E	-9.4561E-08I	9.4561E-08I	-2.3287E-07I	-2.2262E-06E	4.7244E-08I	2.2636E-06E	-1.9643E-07I	3.5266E-08I	1.6607E-06E	-1.2320E-07I	1.0958E-07E	3.7508E-08I	5.0456E-08I	2.2636E-06E	-1.9643E-07I	3.5266E-08I	1.6607E-06E	-1.2320E-07I	1.0958E-07E
4.5854E-06E	-7.4456E-07I	7.9625E-07E	3.5676E-07E	3.5676E-07E	3.5676E-07E	3.5676E-07E	3.5676E-07E	3.5676E-07E	3.5676E-07E	3.5676E-07E	3.5676E-07E	3.5676E-07E	3.5676E-07E	3.5676E-07E	3.5676E-07E	3.5676E-07E	3.5676E-07E	3.5676E-07E	3.5676E-07E	3.5676E-07E	3.5676E-07E
5.1928E-09E	-2.5455E-10I	5.7074E-07E	-1.3042E-08I	1.3042E-08I	-1.4045E-06E	4.6889E-06E	-1.7811E-10I	5.9637E-06E	-1.5325E-09I	1.9762E-07E	2.8370E-08I	1.4017E-07E	-1.5765E-08I	5.2656E-07E	6.0456E-08I	3.7508E-08I	1.6607E-06E	-1.2320E-07I	1.0958E-07E	3.7508E-08I	5.0456E-08I
7.9625E-07E	3.5676E-08I	1.6790E-06E	-1.5619E-07I	1.5619E-07I	1.3661E-07E	2.9692E-10I	6.0142E-07E	-1.1926E-07I	1.0687E-06E	6.1542E-06E	-4.0709E-08I	-5.6276E-07E	-1.0802E-07I	1.0687E-06E	6.1542E-06E	-4.0709E-08I	-5.6276E-07E	-1.0802E-07I	1.0687E-06E	6.1542E-06E	-4.0709E-08I
4.6098E-07E	-4.1366E-08I	-5.1436E-06E	-4.2914E-09I	4.6889E-06E	-1.7811E-10I	5.9637E-06E	-1.5325E-09I	1.9762E-07E	2.8370E-08I	1.4017E-07E	-1.5765E-08I	5.2656E-07E	6.0456E-08I	3.7508E-08I	1.6607E-06E	-1.2320E-07I	1.0958E-07E	3.7508E-08I	5.0456E-08I	2.2636E-06E	-1.9643E-07I
-1.1281E-08E	-2.6082E-09I	5.1928E-09E	-2.5455E-10I	-3.0950E-09E	-2.4068E-09I	9.7014E-09E	-2.7835E-10I	4.2325E-09E	-2.5785E-09I	2.7962E-08E	-1.5325E-09I	1.9762E-07E	2.8370E-08I	1.4017E-07E	-1.5765E-08I	5.2656E-07E	6.0456E-08I	3.7508E-08I	1.6607E-06E	-1.2320E-07I	1.0958E-07E
-5.1436E-06E	-4.2914E-09I	3.3046E-06E	-3.163E-07I	3.4099E-08E	-6.6039E-09I	6.0456E-08I	3.8441E-06E	-9.5513E-09I	6.8301E-07E	-1.7526E-07I	-1.9762E-07E	2.8370E-08I	1.4017E-07E	-1.5765E-08I	5.2656E-07E	6.0456E-08I	3.7508E-08I	1.6607E-06E	-1.2320E-07I	1.0958E-07E	3.7508E-08I
6.3166E-07E	-9.4561E-08I	5.7074E-07E	-1.3042E-08I	1.3042E-08I	1.3661E-07E	2.9692E-10I	6.0142E-07E	-1.1926E-07I	1.0687E-06E	6.1542E-06E	-4.0709E-08I	-5.6276E-07E	-1.0802E-07I	1.0687E-06E	6.1542E-06E	-4.0709E-08I	-5.6276E-07E	-1.0802E-07I	1.0687E-06E	6.1542E-06E	-4.0709E-08I
4.6889E-06E	-1.7811E-10I	3.4099E-08E	-6.6039E-09I	8.2376E-08I	6.6039E-09I	6.6039E-09I	6.6039E-09I	6.6039E-09I	6.6039E-09I	6.6039E-09I	6.6039E-09I	6.6039E-09I	6.6039E-09I	6.6039E-09I	6.6039E-09I	6.6039E-09I	6.6039E-09I	6.6039E-09I	6.6039E-09I	6.6039E-09I	6.6039E-09I
3.2524E-06E	-3.287E-07I	-1.4045E-06E	8.2376E-08I	8.2376E-08I	8.2376E-08I	8.2376E-08I	8.2376E-08I	8.2376E-08I	8.2376E-08I	8.2376E-08I	8.2376E-08I	8.2376E-08I	8.2376E-08I	8.2376E-08I	8.2376E-08I	8.2376E-08I	8.2376E-08I	8.2376E-08I	8.2376E-08I	8.2376E-08I	8.2376E-08I
3.0950E-09E	-2.4068E-09I	1.3661E-07E	-2.9692E-10I	2.9692E-10I	2.9692E-10I	2.9692E-10I	2.9692E-10I	2.9692E-10I	2.9692E-10I	2.9692E-10I	2.9692E-10I	2.9692E-10I	2.9692E-10I	2.9692E-10I	2.9692E-10I	2.9692E-10I	2.9692E-10I	2.9692E-10I	2.9692E-10I	2.9692E-10I	2.9692E-10I
-4.4455E-07E	-1.8819E-07I	1.3661E-07E	-2.9692E-10I	2.9692E-10I	2.9692E-10I	2.9692E-10I	2.9692E-10I	2.9692E-10I	2.9692E-10I	2.9692E-10I	2.9692E-10I	2.9692E-10I	2.9692E-10I	2.9692E-10I	2.9692E-10I	2.9692E-10I	2.9692E-10I	2.9692E-10I	2.9692E-10I	2.9692E-10I	2.9692E-10I
9.7014E-09E	-2.7835E-10I	3.8441E-06E	-9.5513E-09I	6.8301E-07E	-1.7526E-07I	-1.9762E-07E	2.8370E-08I	1.4017E-07E	-1.5765E-08I	5.2656E-07E	6.0456E-08I	3.7508E-08I	1.6607E-06E	-1.2320E-07I	1.0958E-07E	3.7508E-08I	5.0456E-08I	2.2636E-06E	-1.9643E-07I	3.5266E-08I	1.6607E-06E
-6.8614E-07E	2.2644E-07I	6.0142E-07E	-1.1926E-07I	2.9974E-07E	1.1319E-08I	1.1319E-08I	1.1319E-08I	1.1319E-08I	1.1319E-08I	1.1319E-08I	1.1319E-08I	1.1319E-08I	1.1319E-08I	1.1319E-08I	1.1319E-08I	1.1319E-08I	1.1319E-08I	1.1319E-08I	1.1319E-08I	1.1319E-08I	1.1319E-08I
4.2325E-09E	-2.4575E-09I	6.1081E-07E	-9.2404E-08I	-1.0687E-06E	6.1542E-06E	-4.0709E-08I	-5.6276E-07E	-1.0802E-07I	1.0687E-06E	6.1542E-06E	-4.0709E-08I	-5.6276E-07E	-1.0802E-07I	1.0687E-06E	6.1542E-06E	-4.0709E-08I	-5.6276E-07E	-1.0802E-07I	1.0687E-06E	6.1542E-06E	-4.0709E-08I
-1.0747E-06E	-1.2411E-08I	-7.2928E-07E	5.6437E-08I	-4.0709E-08I	-5.6276E-07E	-1.0802E-07I	1.0687E-06E	6.1542E-06E	-4.0709E-08I	-5.6276E-07E	-1.0802E-07I	1.0687E-06E	6.1542E-06E	-4.0709E-08I	-5.6276E-07E	-1.0802E-07I	1.0687E-06E	6.1542E-06E	-4.0709E-08I	-5.6276E-07E	-1.0802E-07I

THE NUMBER OF NON-ZERO WORDS IN THE LONGEST RECORD # 40
 THE DENSITY OF THIS MATRIX IS 100.00 PERCENT.

*** USER INFORMATION MESSAGE 4114.
 DATA BLOCK SRBMAT WRITTEN ON FORTRAN UNIT 17, TRL # 6
 101 2 4 24 10000

*** USER INFORMATION MESSAGE 4114.
 DATA BLOCK ORBSMAT WRITTEN ON FORTRAN UNIT 17, TRL # 5
 102 2 4 20 10000

*** USER INFORMATION MESSAGE 4114.
 DATA BLOCK ETSMAT WRITTEN ON FORTRAN UNIT 17, TRL # 11
 103 2 4 44 10000

*** USER INFORMATION MESSAGE 4114.
 DATA BLOCK ORBMAT WRITTEN ON FORTRAN UNIT 17, TRL # 4
 104 2 4 16 10000

TABLE XIII (CONTINUED)

BEGIN BULK

DMI	CP1	0	2	1	1		11	1	
DMI	CP1	1	6	1.0	1.0	1.0	1.0	1.0	+CPP1
+CPP1	1.0								
DMI	CP2	0	2	1	1		10	1	
DMI	CP2	1	5	1.0	1.0	1.0	1.0	1.0	+CPP2
+CPP2	1.0								
DMI	IM1	0	2	1	4		6	6	
DMI	IM1	1	1	1.0					
DMI	IM1	2	2	1.0					
DMI	IM1	3	3	1.0					
DMI	IM1	4	4	1.0					
DMI	IM1	5	5	1.0					
DMI	IM1	6	6	1.0					
DMI	IM2	0	2	1	4		5	5	
DMI	IM2	1	1	1.0					
DMI	IM2	2	2	1.0					
DMI	IM2	3	3	1.0					
DMI	IM2	4	4	1.0					
DMI	IM2	5	5	1.0					
DMI	IM3	0	2	1	4		4	4	
DMI	IM3	1	1	1.0					
DMI	IM3	2	2	1.0					
DMI	IM3	3	3	1.0					
DMI	IM3	4	4	1.0					
DMI	RP1	0	2	1	1		11	1	
DMI	RP1	1	4	1.0	1.0	1.0	1.0	1.0	+RPP1
+RPP1	1.0	1.0	1.0						
DMI	RP2	0	2	1	1		8	1	
DMI	RP2	1	6	1.0	1.0	1.0			
DMI	RP3	0	2	1	1		11	1	
DMI	RP3	1	9	1.0	1.0	1.0			
DMI	RP4	0	2	1	1		16	1	
DMI	RP4	1	4	1.0	1.0	1.0	1.0	1.0	+RPP4
+RPP4	1.0	1.0							
DMI	RP5	0	2	1	1		7	1	
DMI	RP5	1	5	1.0	1.0	1.0			
DMI	RP6	0	2	1	1		10	1	
DMI	RPC	1	8	1.0	1.0	1.0			

ENDDATA

TABLE XIV - SHUTTLE RESPONSE TO THE FIRST LONGITUDINAL ACOUSTIC MODE AT 15.25HZ

DISPLACEMENT AND FORCE CALCULATIONS FOR THE TOTAL SHUTTLE WITHOUT SMPYD
 MATRIX UDOT COMPLEX 1 COLUMN X 6 ROW RECTANG MATRIX

COLUMN 1 ROWS 1 THRU 6
 3.6313E-04+ 2.3733E-03I 1.1266E-03+ 1.4977E-03I -5.9348E-05+ 7.6705E-05I 5.3709E-04+ 1.3451E-03I -2.2166E-05+ 4.8622E-04I
 4.5511E-04+ 1.4513E-03I

COLUMN 1 ROWS 1 THRU 6 - MATRIX FTOI COMPLEX 1 COLUMN X 6 ROW RECTANG MATRIX

4.0739E 02+ 3.7105E 03I 2.4448E 03+ 4.3484E 03I -3.9097E 01+ 4.1883E 01I 2.5013E 02+ 9.8654E 02I 3.0957E 02+ -2.0172E 02I
 1.9141E 02+ 9.6946E 02I

COLUMN 1 ROWS 1 THRU 5 - MATRIX UBAR COMPLEX 1 COLUMN X 5 ROW RECTANG MATRIX

1.1608E-03+ -8.1320E-04I -3.1455E-04+ 1.1921E-04I 6.6520E-04+ -1.6371E-04I -2.4104E-05+ -7.5373E-06I -4.2688E-04+ 2.0476E-04I

COLUMN 1 ROWS 1 THRU 5 - MATRIX FBAR COMPLEX 1 COLUMN X 5 ROW RECTANG MATRIX

3.9312E 00+ -2.4923E-01I -5.6334E 01+ 9.2662E 00I 1.4225E 02+ -3.9950E 02I 5.6922E 01+ 6.3904E 01I -1.0445E 02+ -1.5441E 01I

COLUMN 1 ROWS 1 THRU 6 MATRIX RRSS COMPLEX 6 COLUMN X 6 ROW SQUARE MATRIX

7.9596E-07+ -7.1221E-08I -9.0980E-08+ 5.6547E-09I 4.0879E-09+ 1.7062E-08I 3.9682E-09+ -5.8302E-10I 4.9630E-08+ 9.9915E-10I
 2.2243E-09+ -4.9918E-09I

COLUMN 2 ROWS 1 THRU 6

-9.0980E-08+ 5.6347E-09I 4.3665E-07+ -2.6872E-08I 3.2908E-10+ -2.6073E-11I 1.2689E-11+ -4.2644E-12I 6.5883E-10+ 2.5378E-10I
 3.4720E-12+ 2.9182E-11I

COLUMN 3 ROWS 1 THRU 6

4.0879E-09+ 1.7062E-08I 3.2908E-10+ -2.6073E-11I 7.8242E-07+ -2.0165E-07I 3.9927E-09+ -5.9158E-10I 1.6923E-07+ 1.4696E-07I
 -1.4343E-08+ 5.9155E-08I

COLUMN 4 ROWS 1 THRU 6

3.9682E-09+ -5.8302E-10I 1.2689E-11+ -4.2644E-12I 3.9927E-09+ -5.9158E-10I 1.1156E-06+ -6.8369E-08I 3.4374E-07+ -2.1528E-08I
 3.3723E-07+ -2.0926E-08I

COLUMN 5 ROWS 1 THRU 6

4.9630E-08+ 9.9915E-10I 6.5883E-10+ 2.5378E-10I 1.6923E-07+ 1.4696E-07I 3.4374E-07+ -2.1528E-08I -4.6079E-07+ -5.3178E-07I
 5.7320E-08+ -1.0863E-07I

COLUMN 6 ROWS 1 THRU 6

2.2243E-09+ -4.9918E-09I 3.4720E-12+ 2.9182E-11I -1.4343E-08+ 5.9155E-08I 3.3723E-07+ -2.0926E-08I 5.7320E-08+ -1.0863E-07I
 1.2233E-06+ -1.0597E-07I

TABLE XIV - (Continued)

DISPLACEMENT AND FORCE CALCULATIONS FOR THE TOTAL SHUTTLE

MATRIX UTOA COMPLEX 1 COLUMN X 6 ROW RECTANG MATRIX

COLUMN 1 ROWS 1 THRU 6

-5.2789E-04+ 2.5206E-04I 3.5068E-04+ 8.7975E-05I 1.4799E-04I 1.4799E-04I 5.7148E-04I 5.6614E-05+ -2.2030E-04I
 -4.6542E-04+ 7.9334E-04I

COLUMN 1 ROWS 1 THRU 6 MATRIX FTOA COMPLEX 1 COLUMN X 6 ROW RECTANG MATRIX

-1.1588E 03+ 4.0357E 02I 7.5285E 01+ 3.9158E 02I 5.3497E 01+ 7.8910E 01I 5.6346E 01+ -8.1477E 02I 1.4388E 02+ -3.8602E-02E
 1.0535E 02+ -8.7018E 02I

COLUMN 1 ROWS 1 THRU 4 MATRIX UBAA COMPLEX 1 COLUMN X 4 ROW RECTANG MATRIX

-5.0018E-04+ -5.2101E-04I -6.7139E-07+ 6.4700E-06I 1.4738E-04+ 1.3544E-04I 9.9546E-05+ -2.7345E-04I

COLUMN 1 ROWS 1 THRU 4 MATRIX FBAA COMPLEX 1 COLUMN X 4 ROW RECTANG MATRIX

-9.9454E 01+ 2.0604E 02I -6.9084E 01+ 2.8010E 02I 1.3690E 02+ -3.6465E 02I -1.2748E 01+ 1.6498E 02I

COLUMN 1 ROWS 1 THRU 6 MATRIX RRSA COMPLEX 6 COLUMN X 6 ROW SQUARE MATRIX

4.6010E-07+ -4.1699E-08I -3.3665E-09+ -1.0737E-08I 2.1537E-08+ -2.4242E-08I -1.0282E-08+ -3.6367E-09I -5.0250E-10+ -7.7617E-09I
 -1.2581E-08+ -9.5482E-09I

COLUMN 2 ROWS 1 THRU 6

-3.3665E-09+ -1.0737E-08I 3.0938E-06+ -5.1416E-07I -6.6800E-07+ -8.9387E-07I 6.1371E-07+ -1.4000E-08I 8.8826E-09+ -2.5133E-07I
 6.0634E-07+ -2.1764E-07I

COLUMN 3 ROWS 1 THRU 6

2.1537E-08+ -2.4242E-08I -6.6800E-07+ -8.9387E-07I -2.9735E-06+ -3.8822E-06I 8.3063E-07+ 2.6823E-07I -1.7636E-06+ -9.0404E-07I
 -7.2421E-07+ -4.9573E-07I

COLUMN 4 ROWS 1 THRU 6

-1.0282E-08+ -3.6367E-09I 6.1371E-07+ -1.4000E-08I 8.3063E-07+ 2.6823E-07I 3.8098E-07+ -2.3501E-07I 8.9526E-08+ 1.8486E-08I
 -7.4871E-07+ -1.4252E-07I

COLUMN 5 ROWS 1 THRU 6

-5.0250E-10+ -7.7617E-09I 8.8826E-09+ -2.5133E-07I -1.7636E-06+ -9.0404E-07I 8.9526E-08+ 1.8486E-08I 5.2921E-07+ -3.9967E-07I
 -2.7543E-07+ -2.7356E-07I

COLUMN 6 ROWS 1 THRU 6

-1.2581E-08+ -9.5482E-09I 6.0634E-07+ -2.1764E-07I -7.2421E-07+ -4.9573E-07I -7.4871E-07+ -1.4252E-07I -2.7543E-07+ -2.7356E-07I
 2.8228E-08+ -4.5051E-07I

TABLE XIV - (Continued)

DISPLACEMENT AND FORCE CALCULATIONS FOR THE TOTAL SHUTTLE

COLUMN 1 ROWS 1 THRU 6 MATRIX USIG COMPLEX 1 COLUMN X 6 ROW RECTANG MATRIX

-1.6476E-04+ 2.7894E-03I 1.4773E-03+ 1.5857E-03I -1.5442E-04+ 2.2469E-04I 1.8366E-04+ 1.9166E-03I -7.8780E-05+ 2.6592E-04I

COLUMN 1 ROWS 1 THRU 6 MATRIX FSIG COMPLEX 1 COLUMN X 6 ROW RECTANG MATRIX

-7.5146E 02+ 4.1141E 03I 2.5200E 03+ 4.7400E 03I -9.2594E 01+ 1.2079E 02I 3.0648E 02+ 1.7177E 02I 4.5345E 02+ -5.8774E 02I

COLUMN 1 ROWS 1 THRU 5 MATRIX UBSC COMPLEX 1 COLUMN X 5 ROW RECTANG MATRIX

6.6062E-04+ -1.3342E-03I -3.1522E-04+ 1.2568E-04I 8.1259E-04+ -2.8268E-05I 7.5442E-05+ -2.8098E-04I -4.2688E-04+ 2.0476E-04I

COLUMN 1 ROWS 1 THRU 5 MATRIX FBSC COMPLEX 1 COLUMN X 5 ROW RECTANG MATRIX

-9.5523E 01+ 2.0579E 02I -1.2542E 02+ 2.8937E 02I 2.7915E 02+ -7.6415E 02I 4.4174E 01+ 2.2889E 02I -1.0445E 02+ -1.5441E 01I

<u>Matrix Name in Table</u>	<u>Matrix</u>	<u>Boundary Conditions</u>
UTOT	$\{U_T\}$	Symmetric
FTOT	$\{F_T\}$	Symmetric
UBAR	$\{\bar{U}\}$	Symmetric
FBAR	$\{\bar{F}\}$	Symmetric
RRSS	$[R_{RSS}]$	Symmetric
UTOA	$\{U_T\}$	Antisymmetric
FTOA	$\{F_T\}$	Antisymmetric
UBAA	$\{\bar{U}\}$	Antisymmetric
FBAA	$\{\bar{F}\}$	Antisymmetric
RRSA	$[R_{RSS}]$	Antisymmetric
USIG	$\{U_T\}_{SYM} + \{U_T\}_{ASYM}$	Not Applicable
FSIG	$\{F_T\}_{SYM} + \{F_T\}_{ASYM}$	Not Applicable
UBSG	$\{\bar{U}\}_{SYM} + \{\bar{U}\}_{ASYM}$	Not Applicable
FBSG	$\{\bar{F}\}_{SYM} + \{\bar{F}\}_{ASYM}$	Not Applicable

SECTION V

DISCUSSION OF RESULTS

Response of the Space Shuttle Vehicle to the first longitudinal acoustic mode has been calculated. A sketch of the vehicle, indicating nodes at the interconnection points, is shown in Figure 1. As shown in Figure 1, Node 303 represents the forward SRB/ET attach point. Nodes 310 and 311 are the aft SRB/ET attach points. Nodes 90 and 91 represent the connections between the ET and the Orbiter. The X, Y, Z coordinate system shown in Figure 1 is the system used with the Rockwell/NASA models of the ET, SRB, and Orbiter.

Based on symmetry about the X-Z plane, the problem was solved with both symmetric and anti-symmetric boundary conditions. The solution based on symmetry boundary conditions represents the situation where both SRM's are under going unstable, in-phase pressure oscillations. The solution based on the anti-symmetry boundary conditions represents the corresponding out-of-phase situation. The sum of the symmetric and asymmetric solutions represents the situation where only one SRM undergoes unstable pressure oscillations.

The forces and displacements from the in-phase analysis are given in Tables XV and XVI. The largest force for the ± 1 psi pressure oscillation level is 1,610 pounds at Node 303 in the Y direction. For a pressure oscillation level of ± 10 psi, the maximum force would increase to 16,100 pounds. The corresponding displacements and forces from the out-of-phase analysis are shown in Tables XVII and XVIII. The maximum force from the "out-of-phase" solution is 1,012 pounds at Node 303 in the X direction.

When the in-phase and out-of-phase solutions are added to obtain the results for the situation where only one booster is undergoing unstable pressure oscillations, a maximum interface force of 2,127 pounds is obtained at Node 303 in the X direction. However, such addition of the solutions represents a pressure oscillation level of ± 2 psi. The normalized maximum force for a ± 1 psi pressure level would, therefore, be 1,064 pounds. The "in-phase" condition, therefore, produces the greatest forces.

Although reasonable care was taken during construction and checkout of the finite element models used in this analysis, and in the set-up of the analysis procedure, the results could be in error. Because of the relatively involved procedure that was used to calculate attach point forces, an error could be difficult to detect. Some kind of a check on results would be desirable. Since time and budget would not allow for analysis of a very simple model by the detailed procedure for checkout purposes, an attempt has been made to obtain at least a rough order-of-magnitude checkout by performing some simple hand calculations.

TABLE XV

Displacements at the Attach Points
Due to Symmetric Oscillation in the First
Acoustic Mode at 15.25 Hz. (± 1 psi pressure oscillation level)

<u>DISPLACEMENT COMPONENT</u>	<u>DISPLACEMENT AMPLITUDE (IN.)</u>	<u>DISPLACEMENT PHASE (DEG.)</u>
U _{303X}	.00094	96
U _{303Y}	.00063	38
U _{303Z}	.00005	-179
U _{310Y}	.00054	87
U _{310Z}	.00024	97
U _{311Y}	.00056	88
U _{90X}	.00039	-32
U _{90Z}	.00012	172
U _{91X}	.00019	-6
U _{91Y}	.00001	-117
U _{91Z}	.00011	144

TABLE XVI

Forces at the Attach Points Due to
Symmetric Oscillation in the First Acoustic
Mode at 15.25 Hz. (\pm 1 psi pressure oscillation level)

<u>FORCE COMPONENT</u>	<u>FORCE AMPLITUDE (LB.)</u>	<u>FORCE PHASE (DEG.)</u>
F _{303X}	1306	95
F _{303Y}	1610	49
F _{303Z}	28	174
F _{310Y}	391	91
F _{310Z}	89	-64
F _{311Y}	356	93
F _{90X}	1	-32
F _{90Z}	14	148
F _{91X}	152	-67
F _{91Y}	38	82
F _{91Z}	59	-104

TABLE XVII

Displacements at the Attach Points Due
to Asymmetric (out-of-phase) Oscillation in
the First Acoustic Mode at 15.25 Hz.
(± 1 psi pressure oscillation level)

<u>DISPLACEMENT COMPONENT</u>	<u>DISPLACEMENT AMPLITUDE (IN.)</u>	<u>DISPLACEMENT PHASE (DEC.)</u>
U _{303X}	.00048	136
U _{303Y}	.00029	-20
U _{303Z}	.00012	117
U _{310Y}	.00044	95
U _{310Z}	.00008	-98
U _{311Y}	.00056	99
U _{90Y}	.00045	-159
U _{91X}	.00001	139
U _{91Y}	.00012	29
U _{91Z}	.00017	-82

TABLE XVIII

Forces at the Attach Points Due to
Asymmetric (out-of-phase) Oscillation in
the First Acoustic Mode at 15.25 Hz.
(± 1 psi pressure oscillation level)

<u>FORCE COMPONENT</u>	<u>FORCE AMPLITUDE (LB.)</u>	<u>FORCE PHASE (DEG.)</u>
F _{303X}	1012	142
F _{303Y}	249	51
F _{303Z}	64	117
F _{310Y}	507	-108
F _{310Z}	219	-77
F _{311Y}	599	-108
F _{90Y}	150	93
F _{91X}	184	81
F _{91Y}	235	89
F _{91Z}	83	85

Estimation of Longitudinal Mode Attach Forces by Hand Calculation

To make a crude estimate of the attach forces, the SRB was considered to be a rigid body. When forces representing the chamber pressure are applied to the SRM finite element model, a net axial force on the model is produced. The net force occurs because the nozzle opening in the aft dome does not carry any load to offset the force produced on a corresponding area in the forward dome. If the pressure applied to the finite element model were an oscillatory pressure, then the net force would be oscillatory. The net force thus applied would cause oscillatory axial accelerations of the total SRB considered as a rigid body.

A uniform internal static pressure was applied to the SRM finite element model. The model was constrained in the axial direction at the SRM/Nose Cone attach points. For the 10 degree slice model with symmetry boundary conditions applied at the slice sides, (i.e., radial-axial planes), axial constraint forces of 49.58 lbs were calculated for each side of the grid, a total of 99.16 lbs for the 10 degree slice. For a complete 360 degree motor the 1 psi thrust would therefore be $36 \times 99.16 = 3569.76$ lbs. For a chamber pressure of 850 psi the thrust of $850 \times 3569.76 = 3.03 \times 10^6$ lbs compares well with the 3.1×10^6 lbs estimated by Space Shuttle engineers. This good agreement gives us confidence that the SRM model is yielding reasonable rigid body results.

For the static analysis discussed above a uniform positive 1.0 psi pressure was applied to the SRM model throughout the combustion cavity. When the first longitudinal acoustic mode is active in the combustion cavity, the pressure mode shape calls for a positive pressure in the head end at the same time the pressure is negative in the aft end. Thus, because of the pressure mode shape, a net positive thrust can be produced by the aft end pressure acting over the aft dome area, (less the nozzle opening), and acting simultaneously with the positive thrust caused by the integral of the pressure over the forward dome.

To estimate the forward dome thrust load, the 1.0 psi pressure is multiplied by the motor cross sectional area:

$$F_{\text{fwd}} = (1.0) \pi (72)^2 = 16286 \text{ lbs}$$

The net thrust as determined above for a uniform pressure load was:

$$F_{\text{fwd}} - F_{\text{aft}} = 3570 \text{ lbs}$$

Therefore, $F_{\text{aft}} = 12716$ lbs

Adding F_{fwd} to F_{aft} to account for the pressure mode shape gives a total net thrust of

$$F_N = 16286 + 12716 = 29,002 \text{ lbs}$$

The pressure mode shape is assumed to have an amplitude of ± 1.0 psi in the forward end and a -1.0 psi in the aft end.

The total thrust of 29,000 lbs acting on the mass of the SRB would cause a rigid body acceleration of $(29,000 \text{ lbs/W})$, where W is the SRB weight. If the SRB weighs 1.26×10^6 lbs, then a 15.25 Hz oscillation would occur with acceleration amplitude of

$$a = \frac{29 \times 10^3}{1.26 \times 10^6} = 23 \times 10^{-3} \text{ g's}$$

For harmonic motion the corresponding displacement would be:

$$X = \frac{a}{(\omega^2)} = \frac{23 \times 10^{-3} \times 386.4}{(2 \pi 15.24)^2} = 9.69 \times 10^{-4} \text{ in.}$$

The above results show that the SRB could be expected to move back and forth as a rigid body at 15.25 cycles per second with a displacement amplitude of 9.7×10^{-4} inches in response to the first longitudinal acoustic mode.

In operation, the SRB is attached to the ET in the axial direction at a single point (node 303). If a rigid SRB were attached to a rigid ground, the total net oscillatory thrust of 29,000 lbs could be transmitted through the attach point. At the other extreme, if the ET attach point were very soft, the SRB would oscillate near the rigid body displacement of 9.7×10^{-4} inches and attach point forces would be small. Based on this simplified rigid body analysis, attach point forces in the range of 0 to 29,000 lbs would be expected. The corresponding expected displacements would be in the range from 9.7×10^{-4} to 0.0 inches with the larger forces corresponding with the smaller displacements.

To obtain a better estimate for the upper limit force that might be expected, consider the receptance matrix for the combined ET and Orbiter, R_{RSS} . For a crude estimate of the axial force, assume that only F_{303x} is non zero in the equation:

$$\{U\} = [R_{RSS}] \{F\}$$

(Refer to equation 44 for the components of $\{U\}$ and $\{F\}$). Then the first equation from the above matrix equation would be:

$$U_{303x} = r_{11} F_{303x}$$

The matrices $[R_{RSS}]_{SYM} = RRSS$ and $[R_{RSS}]_{ASYM} = RRSA$ are given in Table XIV. From the table,

$$(r_{11})_{SYM} = 7.9596E-07 - 7.1221 E-08 i = 7.99 E-7 \angle -5.1$$

$$(r_{11})_{ASYM} = 4.6010E-07 - 4.1699 E-08 i = 4.62 E-7 \angle -5.2$$

Now, suppose the maximum free body displacement of 9.7×10^{-4} inches is applied to the ET/Orbiter combination at attach node 303 in the axial (X) direction:

$$(F_{303X})_{SYM} = \frac{1}{(r_{11})_{SYM}} (U_{303X}) = \frac{9.7 \times 10^{-4}}{7.99 \times 10^{-7}} = 1214 \text{ lbs}$$

$$(F_{303X})_{ASYM} = \frac{1}{(r_{11})_{ASYM}} (U_{303X}) = \frac{9.7 \times 10^{-4}}{4.62 \times 10^{-7}} = 2100 \text{ lbs}$$

For comparison with the numbers calculated in these rough estimates, the corresponding values from the computer analysis are recalled:

$$(U_{303X})_{SYM} = 9.4 \times 10^{-4} \text{ in.}$$

$$(U_{303X})_{ASYM} = 4.8 \times 10^{-4} \text{ in.}$$

$$(F_{303X})_{SYM} = 1306 \text{ lb}$$

$$(F_{303X})_{ASYM} = 1012 \text{ lb}$$

Based on the relatively good agreement between the rough estimates and the computer solutions, we can justify added confidence in the accuracy and applicability of the computer solutions.

SECTION VI

CONCLUSIONS AND RECOMMENDATIONS

This analysis program has resulted in estimates for the attach point forces between the solid rocket motors and the external tank and has therefore met the program objectives. Good agreement between hand calculations and computer analysis results show at least that the computer results are of a reasonable order of magnitude. The significance of the maximum attach point force of 1610 lbs for a ± 1.0 psi pressure oscillation level, (or 16,100 lbs for a ± 10 psi level) must be determined by Space Shuttle engineers.

Due to time and budget limitations, this analysis only covered the first longitudinal acoustic mode at a zero burn time. Future work could include other modes and other burn times. Some simplified hand calculations could be made for a transverse mode. The desirability of additional analysis work could best be determined by Shuttle engineers who are familiar with space shuttle structure capabilities and requirements.

LIST OF REFERENCES

1. Jensen, F. R., Analytical Prediction of Motor Component Vibrations Driven by Acoustic Combustion Instability, Final Report AFRPL-TR-76-11, Hercules Incorporated, for the Air Force Rocket Propulsion Laboratory, Edwards, CA, February 1976.
2. The NASTRAN Theoretical Manual, (Level 15), R. H. MacNeal, Ed., April 1972, NAS SP-221(01), NASA, Washington, D.C., p. 12.1-3.
3. Ibid, p. 9.3-8.
4. The NASTRAN User's Manual, (Level 15), C. W. McCormick, Ed., June 1972, NAS SP-222(01), NASA, Washington, D.C., p. 3.9-11.
5. Bishop, R. E. D., and Johnson, D. C., The Mechanics of Vibration, Cambridge at the University Press, 1960, London, England.
6. Index to the Shock and Vibration Bulletins, February 1968, The Shock and Vibration Information Center, Naval Research Laboratory, Washington, D.C.
7. Harris, C. M., and Crede, C. E., Shock and Vibration Handbook, Vol 1, Chapter 10, McGraw-Hill Book Co., New York, 1961.
8. Bishop, R. E. D., Gladwell, G. M. L., and Michaelson, S., The Matrix Analysis of Vibration, Section 5.5, Cambridge at the University Press, London, 1965.
9. Bishop, R. E. D., and Johnson, D. C., The Mechanics of Vibration, Cambridge at the University Press, London, 1960.
10. Crafton, P. A., Shock and Vibration in Linear Systems, Harper and Brothers, New York, 1961.
11. MacNeal, R. H., Electric Circuit Analogies for Elastic Structures, Vol 2, John Wiley and Sons, New York, 1962.
12. Rubin, S., Review of Mechanical Immittance and Transmission Concepts, Presented at the 71st Meeting of the Acoustical Society of America, Boston, Mass., June 1966.
13. Rubin, S., Class Notes distributed at UCLA Short Course on Structural Dynamics Analysis, Los Angeles, California, 1967.
14. Rubin, S., On the Use of Eight-Pole Parameters for Analysis of Beam Systems, Soc. of Automotive Engineers, Reprint 925F, October 1964.
15. Analytical Prediction of Motor Component Vibrations Driven by Acoustic Combustion Instability, op. cit.

16. NASTRAN Theoretical Manual, op. cit.
17. Analytical Prediction of Motor Component Vibrations Driven by Acoustic Combustion Instability, op. cit.
18. Ibid.